The role of the (hem)ITAM-coupled receptors

C-type lectin-like receptor 2 (CLEC-2) and Glycoprotein (GP) VI

for platelet function:

in vitro and _in vivo_ studies in mice

***

Die Rolle der (hem)ITAM-gekoppelten Rezeptoren

C-type lectin-like receptor 2 (CLEC-2) und Glycoprotein (GP) VI

in der Thrombozytenfunktion:

in vitro- und _in vivo_-Studien in Mäusen

Doctoral thesis for a doctoral degree
at the Graduate School of Life Sciences,
Julius-Maximilians-Universität Würzburg,
Section Biomedicine

submitted by

Frauke May

from

Koblenz

Würzburg, 2011

Submitted on:

Members of the *Promotionskomitee*:

Chairperson: **Prof. Dr. Manfred Gessler**

Primary Supervisor: **Prof. Dr. Bernhard Nieswandt**

Supervisor (Second):   **Prof. Dr. Ulrich Walter**

Supervisor (Third):   **PD Dr. Heike Hermanns**

Date of Public Defense:

Date of Receipt of Certificate:

This thesis is dedicated to my father, Günter May.

TABLE OF CONTENTS

SUMMARY

Platelet activation and adhesion results in thrombus formation that is essential for normal hemostasis, but can also cause irreversible vessel occlusion leading to myocardial infarction or stroke. The C-type lectin-like receptor 2 (CLEC-2) was recently identified to be expressed on the platelet surface, however, a role for this receptor in hemostasis and thrombosis had not been demonstrated. In the current study, the involvement of CLEC-2 in platelet function and thrombus formation was investigated using mice as a model system.

In the first part of the thesis, it was found that treatment of mice with a newly generated monoclonal antibody against murine CLEC-2 (INU1) led to the complete and highly specific loss of the receptor in circulating platelets (a process termed "immunodepletion"). CLEC-2-deficient platelets were completely unresponsive to the CLEC-2-specific agonist rhodocytin, whereas activation induced by all other tested agonists was unaltered. This selective defect translated into severely decreased platelet aggregate formation under flow *ex vivo*; and *in vivo* thrombosis models revealed impaired stabilization of formed thrombi with enhanced embolization. Consequently, CLEC-2 deficiency profoundly protected mice from occlusive arterial thrombus formation. Furthermore, variable bleeding times in INU1-treated mice indicated a moderate hemostatic defect. This reveals for the first time that CLEC-2 significantly contributes to thrombus stability *in vitro* and *in vivo* and plays a crucial role in hemostasis and arterial thrombosis. Thus, CLEC-2 represents a potential novel anti-thrombotic target that can be functionally inactivated *in vivo*. This *in vivo* down-regulation of platelet surface receptors might be a promising approach for future anti-thrombotic therapy.

The second part of the work investigated the effect of double-immunodepletion of the *immunoreceptor tyrosine-based activation motif* (ITAM)- and hemITAM-coupled receptors, platelet glycoprotein (GP) VI and CLEC-2, on hemostasis and thrombosis using a combination of the GPVI- and CLEC-2-specific antibodies, JAQ1 and INU1, respectively. Isolated targeting of either GPVI or CLEC-2 *in vivo* did not affect expression or function of the respective other receptor. However, simultaneous treatment with both antibodies resulted in the sustained loss of GPVI and CLEC-2 signaling in platelets, while leaving other activation pathways intact. In contrast to single deficiency of either receptor, GPVI/CLEC-2 double-deficient mice displayed a dramatic hemostatic defect. Furthermore, this treatment resulted in profound impairment of arterial thrombus formation that far exceeded the effects seen in single-depleted animals. Importantly, similar results were obtained in $Gp6^{-/-}$ mice that were depleted of CLEC-2 by INU1-treatment, demonstrating that this severe bleeding phenotype was not caused by secondary effects of combined antibody treatment. These data suggest that GPVI and CLEC-2 can be independently or simultaneously down-regulated in platelets *in vivo* and reveal an unexpected functional redundancy of the two receptors in hemostasis and thrombosis. Since GPVI and CLEC-2 have intensively been discussed as potential anti-

thrombotic targets, these results may have important implications for the development of novel, yet save anti-GPVI or anti-CLEC-2-based therapies.

ZUSAMMENFASSUNG

Die Thrombozytenaktivierung und –adhäsion sowie die nachfolgende Thrombusbildung ist ein essentieller Prozess in der primären Hämostase, der aber auch irreversible Gefäßverschlüsse und damit Herzinfarkt oder Schlaganfall verursachen kann. Erst kürzlich wurde beschrieben, dass der *C-type lectin-like receptor 2* (CLEC-2) auf der Thrombozytenoberfläche exprimiert wird, jedoch wurde für diesen Rezeptor noch keine Funktion in den Prozessen der Hämostase und Thrombose gezeigt. In der vorliegenden Arbeit wurde die Rolle von CLEC-2 in der Thrombozytenfunktion und Thrombusbildung im Mausmodel untersucht.

In dem ersten Teil dieser Arbeit konnte gezeigt werden, dass die Behandlung von Mäusen mit dem neu generierten monoklonalen Antikörper INU1, der gegen murines CLEC-2 gerichtet ist, zu dem vollständigen und hochspezifischen Verlust des Rezeptors in zirkulierenden Thrombozyten führte, ein Prozess, der als „Immundepletion" bezeichnet wird. Die CLEC-2-defizienten Thrombozyten waren nicht mehr durch den CLEC-2-spezifischen Agonisten Rhodozytin aktivierbar, während die Aktivierung durch alle anderen getesteten Agonisten nicht beeinträchtigt war. Dieser selektive Defekt führte unter Flussbedingungen *ex vivo* zu stark verminderter Aggregatbildung der Thrombozyten. Außerdem zeigten *in vivo*-Thrombosestudien, dass die gebildeten Thromben instabil waren und vermehrt embolisierten. Infolgedessen war die CLEC-2 Defizienz mit einem deutlichen Schutz vor arterieller Thrombose verbunden. Außerdem ließ die in INU1-behandelten Mäusen beobachtete variable Verlängerung der Blutungszeit auf einen moderaten hämostatischen Defekt schließen. Diese Ergebnisse zeigen zum ersten Mal, dass CLEC-2 *in vitro* und *in vivo* signifikant zur Thrombusstabilität beiträgt und eine essentielle Rolle in der Hämostase und arteriellen Thrombose spielt. Daher stellt CLEC-2 eine potentiell neue antithrombotische Zielstruktur dar, die *in vivo* inaktiviert werden kann. Diese *in vivo*-Herabregulierung von Thrombozytenoberflächenrezeptoren könnte einen vielversprechenden Ansatz für zukünftige antithrombotische Therapien darstellen.

Der zweite Teil dieser Arbeit behandelte den Effekt einer Doppelimmundepletion der *immunoreceptor tyrosine-based activation motiv* (ITAM)- und hemITAM-gekoppelten Rezeptoren Glykoprotein (GP) VI und CLEC-2 auf Hämostase und Thrombose mittels einer Kombination der GPVI- beziehungsweise CLEC-2-spezifischen Antikörper JAQ1 und INU1. Eine Einzeldepletion von GPVI oder CLEC-2 *in vivo* beeinträchtigte nicht die Expression und Funktion des jeweils anderen Rezeptors. Eine gleichzeitige Behandlung mit beiden Antikörpern führte jedoch zu dem nachhaltigen Verlust der GPVI- und CLEC-2-vermittelten Signale in Thrombozyten, während andere Signalwege nicht betroffen waren. Im Gegensatz zu den Einzeldefizienzen, wiesen die GPVI/CLEC-2 doppeldefizienten Mäuse einen schwerwiegenden Blutungsphänotyp auf. Außerdem führte die Behandlung zu einer starken

Beeinträchtigung der arteriellen Thrombusbildung, die die Effekte der Einzeldefizienzen weit übertraf. Von Bedeutung ist auch, dass gleiche Ergebnisse in *Gp6*$^{-/-}$ Mäusen gefunden wurden, die mittels INU1-Behandlung CLEC-2-depletiert wurden. Dies veranschaulicht, dass der Blutungsphänotyp nicht durch Sekundäreffekte der kombinierten Antikörperbehandlung hervorgerufen wurde. Diese Daten deuten darauf hin, dass GPVI und CLEC-2 sowohl unabhängig voneinander als auch gleichzeitig *in vivo* von der Thrombozytenoberfläche herabreguliert werden können und lassen unerwartete redundante Funktionen der beiden Rezeptoren in Hämostase und Thrombose erkennen. Da beide Rezeptoren, GPVI und CLEC-2, als neue antithrombotische Zielstrukturen diskutiert werden, könnten diese Ergebnisse wichtige Auswirkungen auf die Entwicklung von anti-GPVI oder anti-CLEC-2-basierenden Antithrombotika haben.

1 Introduction

In the hematopoietic system, anuclear and discoid-shaped platelets represent the smallest cells with a size of 3-4 μm in humans and 1-2 μm in mice, respectively. Platelets are produced by fragmentation of their precursor cells, the megakaryocytes, in the bone marrow and are constantly released into the blood stream where the resulting physiological platelet count is very high, namely 150,000-300,000/μl in humans and approximately 1,000,000/μl in mice. The average life span of human platelets is restricted to ~10 days, whereas murine platelets circulate for approximately 5 days in the blood before they are cleared by the reticulo-endothelial system in spleen and liver. Platelets are a crucial component of the blood system as platelet aggregation after vessel wall injury is a key mechanism in normal hemostasis that rapidly leads to the formation of a platelet plug. This process is essential to seal vascular injuries and prevent posttraumatic blood loss. Under pathological conditions, however, e.g. at sites of atherosclerotic plaque rupture in stenosed vessels, platelet aggregation may also lead to uncontrolled thrombus formation causing arterial occlusion or embolism and thus resulting in severe diseases such as myocardial infarction or stroke. These pathologies are the leading causes of death in industrialized societies[1]. Therefore, a selective inhibition of platelet activation has become a major anti-thrombotic strategy to prevent or treat ischemic cardio- and cerebrovascular events.

The above described central (patho)physiological role of platelet activation requires tight regulation to ensure efficient plug formation on the one hand and to prevent excessive thrombus growth and vessel occlusion on the other hand. The presence of many different adhesion receptors on the platelet surface in combination with the various signaling pathways triggered during platelet activation enable this sophisticated regulation under physiological as well as under pathophysiological conditions.

1.1 Platelet activation and thrombus formation

Platelet aggregate formation at sites of vascular injury is a multistep process that is initially triggered by exposure of the extracellular matrix (ECM) at the wound site, which contains a number of adhesive macromolecules, such as laminin, collagens and von Willebrand factor (vWF). This leads to the activation of platelet membrane receptors and the corresponding intracellular signaling pathways. The subsequent process of platelet aggregation and thrombus formation can be divided into three major steps:

First, the initial contact of platelets to the ECM is mediated by the interaction between the platelet glycoprotein (GP) Ib-V-IX complex and vWF immobilized on collagen. While this interaction is mandatory at high shear[2], such as found in arterioles or stenosed arteries, it may not be relevant under conditions of low shear as found in veins and large arteries. The

interaction of GPIb-V-IX and vWF is, however, not stable and therefore insufficient to mediate stable adhesion of the platelet to the injured vessel surface. Rather, it leads to a rapid deceleration and "rolling" of the circulating platelets on the vessel wall, a process termed "tethering" (see Fig 1.1).

Following the deceleration, in the second step of thrombus formation, platelets establish contacts with collagen fibers of the ECM via the platelet-specific immunoglobulin superfamily receptor GPVI[3-5]. While GPVI binds to collagen with low affinity and is thus unable to mediate firm adhesion by itself, it triggers intracellular signals that result in integrin activation (see below) and the release of the "second wave" mediators adenosine diphosphate (ADP) and thromboxane A_2 (TxA$_2$). These agonists together with locally produced thrombin contribute to platelet activation by stimulating receptors that couple to heterotrimeric G proteins (G_q, G_{12}/G_{13}, G_i) to activate downstream effectors and subsequently induce full platelet activation[1,6-7].
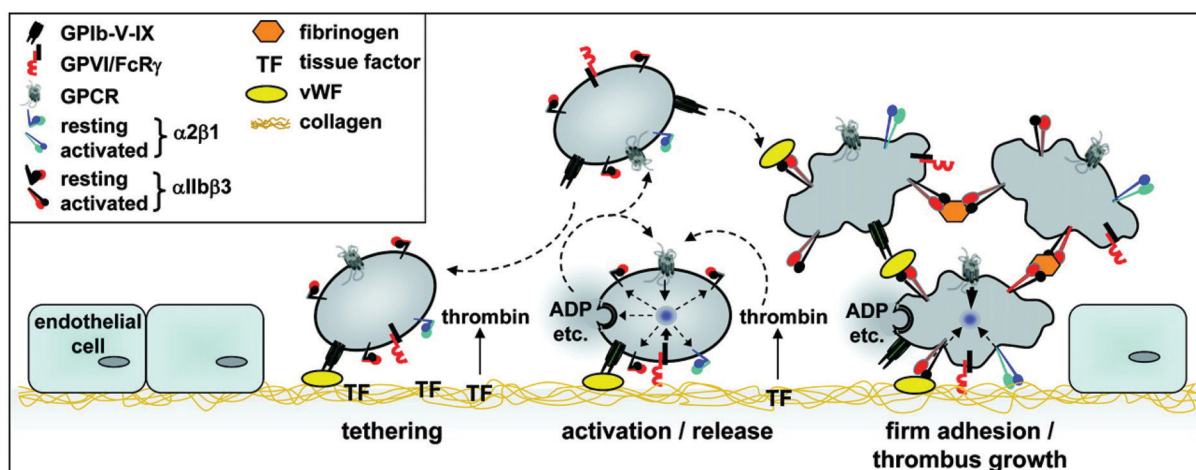
Fig 1.1 Current model of platelet adhesion and aggregation on the extracellular matrix (ECM). Platelet tethering on the ECM is mediated by the GPIbα-vWF interaction. Subsequently, interaction of GPVI with collagen takes place, which triggers the shift of integrins to a high-affinity state and release of ADP and TxA$_2$. In parallel, tissue factor (TF) locally triggers thrombin formation, also contributing to platelet activation. Taken from: Varga-Szabo D, Pleines I and Nieswandt B, *Arterioscler Thromb Vasc Biol*, 2008[8].

In the third step, in response to platelet activation, firm adhesion of the cells to the ECM is mediated by conversion of integrins from a low-affinity to a high-affinity (active) state. This "inside-out"-signaling allows the interaction of the activated integrins with their ligands[9-10]. In this process, high-affinity β1 integrins bind to the following ligands: α2β1 (also termed GPIa/IIa) binds to collagen, α5β1 to fibronectin and α6β1 to laminin, whereas the major platelet integrin αIIbβ3 (GPIIb/IIIa) binds to fibrinogen and collagen-bound vWF on the ECM[8]. Finally, thrombus growth is induced by recruitment and activation of additional platelets from the blood stream by the released "second wave" mediators ADP and TxA$_2$ and subsequent clustering of platelets via plasma fibrinogen and vWF bound to αIIbβ3.

However, as the "second wave" mediators are rather weak platelet agonists, it is speculated that further yet undefined receptors on the platelet surface play a role in thrombus formation and stabilization[11]. There has been ample evidence that even after platelets have aggregated signaling events occur in these platelets to further stabilize the growing platelet plug[11]. However, little is known about which receptors or ligands could play a role in this process. Interestingly, the importance of the platelet C-type lectin-like receptor (CLEC)-2 for platelet activation and thrombus formation during hemostasis and in the course of thrombotic events had not been defined at the beginning of the study presented in this thesis[12].

1.2 Signaling events in the process of platelet activation

Two major classes of activatory receptors drive the process of platelet activation. First, soluble agonists such as ADP, TxA$_2$, epinephrine and serotonin, as well as thrombin stimulate G protein coupled-receptors (GPCRs; G$_q$, G$_{12/13}$, G$_{i/z}$) (see Fig 1.2) leading to activation of phospholipase Cβ (PLCβ) downstream of G$_q$ signaling. The second pathway of platelet activation involves receptors such as integrins, GPVI and CLEC-2, and culminates in activation of PLCγ2. Signaling downstream of GPVI and CLEC-2 is similar to that used by immunoreceptors. It involves sequential activation of Src and Syk family tyrosine kinases that orchestrate a signaling cascade downstream of the receptor-associated *immunoreceptor tyrosine-based activation motif* (ITAM) of the platelet collagen receptor, GPVI[5,13], or -in the case of CLEC-2- signaling is initiated by tyrosine phosphorylation of a single YXXL motif in its cytoplasmic tail termed hemITAM[14]. In both cases, the signaling cascade is regulated through the interaction of several adaptor proteins, including linker for activation of T-cells (LAT) and SH2-domain containing leukocyte protein of 76 kDa (SLP-76). This leads to activation of effector enzymes including phosphatidylinositol-3-kinases (PI-3-K) and PLCγ2. Subsequently, both isoforms of activated PLCs produce inositol 1,4,5-trisphosphate (IP$_3$) and diacylglycerol (DAG) by cleavage of phosphatidylinositol-4,5-bisphosphate (PIP$_2$). IP$_3$ in turn triggers Ca^{2+} mobilization from intracellular stores and subsequent opening of Ca^{2+} channels in the plasma membrane, leading to a process termed *store operated Ca^{2+} entry* (SOCE)[8,15]. DAG activates proteinkinase C (PKC) and probably contributes to Ca^{2+} entry by non-SOCE mechanisms[16]. Elevations in intracellular calcium concentration [Ca^{2+}]$_i$ are an essential step in the process of platelet activation and a prerequisite for final firm adhesion, granule secretion and aggregation of the cells.

Fig 1.2 Major signaling pathways in platelets. Soluble agonists stimulate platelet receptors leading to intracellular signaling via the indicated proteins. Signaling via G protein-coupled receptors involves the corresponding G proteins. Cross-linking of the platelet activating receptors GPVI or CLEC-2 by ligand engagement results in activation of phospholipase (PL) Cγ2. Abbreviations: TF= tissue factor, TxA$_2$= thromboxane A$_2$, TP= TxA$_2$ receptor, PAR= protease-activated receptor, RhoGEF= Rho-specific guanine nucleotide exchange factor, PI3K= phosphatidylinositol 3-kinase, AC= adenylyl cyclase, PIP$_2$= phosphatidylinositol-4,5-bisphosphate, PIP$_3$= phosphatidylinositol-3,4,5-trisphosphate, IP$_3$= inositol-1,4,5-trisphosphate, DAG= diacylglycerol. Taken from: Stegner D and Nieswandt B, *J Mol Med*, 2010[17].

1.3   The C-type lectin-like receptor 2 (CLEC-2)

The C-type lectin-like receptor 2 (CLEC-2) is a type II transmembrane receptor that was originally identified in immune cells and only recently revealed to also be expressed in platelets[18-19]. CLEC-2 serves as the receptor for the snake venom toxin rhodocytin (also termed aggretin) a very potent platelet activating protein isolated from the Malayan pit viper *Calloselasma rhodostoma*[14]. Early work suggested that rhodocytin-induced platelet activation shares some similarities with the responses elicited by collagen, and therefore integrin $\alpha2\beta1$ and GPIbα were initially proposed to be the target structures of rhodocytin on platelets[20-22]. However, this was shortly later disproven by a work of Nieswandt and co-workers demonstrating that platelets become fully activated by rhodocytin in the absence of these receptors[23]. Finally, CLEC-2 could be identified by a mass spectrometry approach as the receptor for rhodocytin[14].

1.3.1   Chromosomal location, expression profile and protein structure of CLEC-2

The gene encoding CLEC-2 is located within a cluster of related genes termed "dectin-1 cluster" in the natural killer gene complex (NKC), including DECTIN-1 and LOX-1 on human chromosome 12 and on mouse chromosome 6, respectively[18,24]. Human CLEC-2 was first identified by Colonna *et al.* by reverse transcriptase (RT) PCR at the transcript level in peripheral blood mononuclear cells (PBMCs), bone marrow, myeloid cells (monocytes, dendritic cells and granulocytes), natural killer cells and liver[18]. Mouse CLEC-2 protein was identified in the same study and shown to share approximately 60% homology with its human homolog (Fig 1.3). CLEC-2 was later found to be also expressed in platelets, liver sinusoidal endothelial cells (LSECs) and megakaryocytes (MKs). Furthermore, it was demonstrated that CLEC-2 has the second highest level of mRNA of megakaryocyte-restricted genes encoding membrane proteins in a Serial Analysis of Gene Expression (SAGE) library made from mouse MKs, indicating that it is primarily localized to the megakaryocyte/platelet lineage, where it is present at high levels[25]. Additionally, CLEC-2 was found to be expressed at low level on peripheral blood neutrophils in mice[26]. Recently, two novel splice variants of *mCLEC-2* were identified with different expression profiles compared to the above described full length transcript of the protein. However, these two new isoforms were shown to be subcellularly expressed and are therefore most probably not operating as receptors *in vivo*. Moreover, the physiological functions of these isoforms have not yet been determined[27].

The protein structure of CLEC-2 is defined by the characteristic assembly of a type II transmembrane receptor, thus the protein exhibits an extracellular carboxyl-terminal domain and an intracellular NH_2-terminal domain. The receptor CLEC-2 belongs to the C-type lectin family, which is divided into two subgroups: the classical and non-classical C-type lectins. The classical or so-called "true" C-type lectins display a carbohydrate recognition domain

(CRD) necessary to bind Ca^{2+} and carbohydrates. In contrast, non-classical C-type lectins, such as CLEC-2, contain a C-type lectin-like domain (CTLD, see Fig 1.3) which is homologous to a CRD but lacks the sequence responsible for Ca^{2+}- and carbohydrate-binding[28-30]. Therefore, it was already early speculated that CLEC-2 may have a different ligand[18]. In general, binding of specific carbohydrate structures is a property of many C-type lectins and important in different processes like cell-cell adhesion or innate immune responses to pathogens[30-31].

Human as well as murine CLEC-2 consists of 229 amino acids (aa, Fig 1.3) with a predicted molecular mass of approximately 27 kDa and an apparent molecular mass of 32-33 kDa under reducing conditions[14,18]. The N-terminal cytoplasmic tail of both human and mouse CLEC-2 consists of 31 aa and displays an YXXL motif with a single tyrosine residue (Fig 1.3, depicted in yellow), forming one-half of an *immunoreceptor tyrosine-based activation motif* (ITAM)[14,18]. This tyrosine residue becomes phosphorylated upon receptor activation and transduces the signal into the cytoplasm. The transmembrane domain (TM, red) comprises 26 aa, integrates the receptor into the phospholipid bilayer of the cell-membrane and is followed by the extracellular neck domain (41 aa, orange), which stabilizes the following C-terminal CTLD domain[18,32].

```
                      Cytoplasmic domain                          TM domain
                         YXXL
CLEC2_homo   MQDEDGYITLNIKTRKPALISVGSASSSWWRVMALILLILCVGMVVGLVALGIWSVMQRN 60
CLEC2_mus    MQDEDGYITLNIKPRKQALSSAEPASS-WWRVMALVLLISSMGLVVGLVALGIMSVTQQK 59
             *************.** ** *. .*** ******:*** .:*:********* ** *::

                      NECK domain                              CTLD domain
CLEC2_homo   YLQGENENRTGTLQQLAKRFCQYVVKQSELKG--TFKGHKCSPCDTNWRYYGDSCYGFFR 118
CLEC2_mus    YLLAEKENLSATLQQLAKKFCQELIRQSEIKTKSTFE-HKCSPCATKWRYHGDSCYGFFR 118
             ** .*:** :.*******:*** ::::***:*   **: ****** *:***:********

CLEC2_homo   HNLTWEESKQYCTDMNATLLKIDNRNIVEYIKARTHLIRWVGLSRQKSNEVWKWEDGSVI 178
CLEC2_mus    RNLTWEESKQYCTEQNATLVKTASQSTLDYIAERITSVRWIGLSRQNSKKDWMWEDSSVL 178
             :************: ****:*   .:. ::** *   :**:*****:*:: * ***.**:

CLEC2_homo   SENMFEFLEDGKGNMNCAYFHNGKMHPTFCENKHYLMCERKAGMTKVDQLP 229
CLEC2_mus    RKNGINLSGNTEENMNCAYLHNGKIHPASCKERHYLICERNAGMTRVDQLL 229
              :* ::: : : ******:****:**: *:::***:***:****:****
```

Fig 1.3 Amino acid sequences of murine and human CLEC-2. The N-terminal cytoplasmic domain (gray) contains the YXXL motif indicated by a yellow box. The transmembrane (TM) domain is labeled in red and the neck domain in orange. The C-terminal CTLD domain (dark gray) is linked by the neck domain to the TM domain. Potential N-glycosylation sites are marked in green. Identical amino acids between human (CLEC-2_hum, accession no. NM_016509) and murine CLEC-2 (CLEC-2_mus, accession no. BC064054) are depicted by asterisks whereas diverged amino acids are labeled with dots. Modified from: Colonna M *et al.*, *J Eur Immunol*, 2000[18] see also[33].

The aa sequences of murine and human CLEC-2 show two identical potential N-glycosylation sites[18,30] (marked in green). The predicted protein structures of human and mouse CLEC-2 show high identity with approximately 60-62% homologous aa (see Fig 1.3)[18]. Important conserved features between human and murine CLEC-2 are six conserved cysteine residues in the CTLD domain, representing three putative interchain disulfide bonds, the YXXL motif in the cytoplasmic domain of the receptor and the lack of a Ca^{2+}-dependent sugar-binding site[18,24]. Furthermore, recently the structure of CLEC-2 was solved by X-ray crystallography and it was shown that the snake venom toxin rhodocytin interacts to a significant extent with the extracellular hypervariable loop of the receptor (green, Fig 1.4)[34-35].

Fig 1.4 Structural features of CLEC-2. The hypervariable long loop region (green) contains a helical segment that has the potential to move upon ligand binding. Site-directed mutagenesis demonstrated that the residues labeled in pink play a role in ligand binding. Taken from: O'Callaghan CA, *Curr Opin Pharmacol*, 2009[12].

1.3.2 CLEC-2-induced intracellular signaling

The cytoplasmic domain of CLEC-2 bears a single YXXL motif which resembles the ITAM motif. However, unlike an ITAM with tandem tyrosine residues, CLEC-2 carries only a single tyrosine residue in its YXXL motif termed hemITAM, which becomes phosphorylated by Src kinases upon binding of the ligand rhodocytin to the extracellular domain of the receptor (Fig 1.5)[14,32,36]. Subsequent to ligand engagement, the tyrosine kinase Syk (Spleen Tyrosine Kinase) binds to the phosphorylated tyrosine residue of the CLEC-2 receptor via its tandem Src homology 2 (SH2) domains (Fig 1.5). Several studies have shown that CLEC-2 is present as a dimer on resting platelets supporting a model in which Syk binds to two phosphorylated hemITAM motifs in two CLEC-2 receptors (see also Fig 1.8), thus inducing more powerful stimulation of the platelets by receptor clustering[32,37-38].

Signaling via CLEC-2 was shown to be blocked by Src kinase inhibitors or by mutation of the tyrosine in this motif to a phenylalanine, which cannot be phosphorylated[14,32]. The activation of Syk leads to subsequent multiple downstream signaling events including tyrosine phosphorylation of LAT, SLP-76, Vav3, Btk, and PLCγ2[14]. Both SH2 domains of Syk are

required for the interaction with CLEC-2 and the inactivation of either domain will block signaling of CLEC-2[32]. Furthermore, it was demonstrated that the adapter protein LAT is essential for CLEC-2-mediated signaling[39]. CLEC-2 can induce partial activation of PLCγ2 in the absence of SLP-76, whereas this adapter is essential for phospholipase activation by GPVI[14,40]. Additionally, the response to rhodocytin is diminished, but not abolished in the absence of the adapter protein B-cell linker protein (BLNK)[32]. Signaling via CLEC-2 can be reduced by inhibitory signaling through Platelet Endothelial Cell Adhesion Molecule (PECAM-1) and G6b-B, both of which have *immunoreceptor tyrosine-based inhibitory motifs* (ITIMs) in their cytoplasmic domains[41-42]. Interestingly, it was demonstrated that upon ligand engagement the receptor CLEC-2 translocates to lipid rafts and that this process is essential for hemITAM phosphorylation and subsequent signal transduction[43]. Furthermore, the same study could show that activation of the small GTPase Rac1 is critically involved in hemITAM phosphorylation. These results explain in parts the already earlier observed diminished responsiveness of Rac1^{-/-} platelets towards rhodocytin in a study from our group and others[43-44].
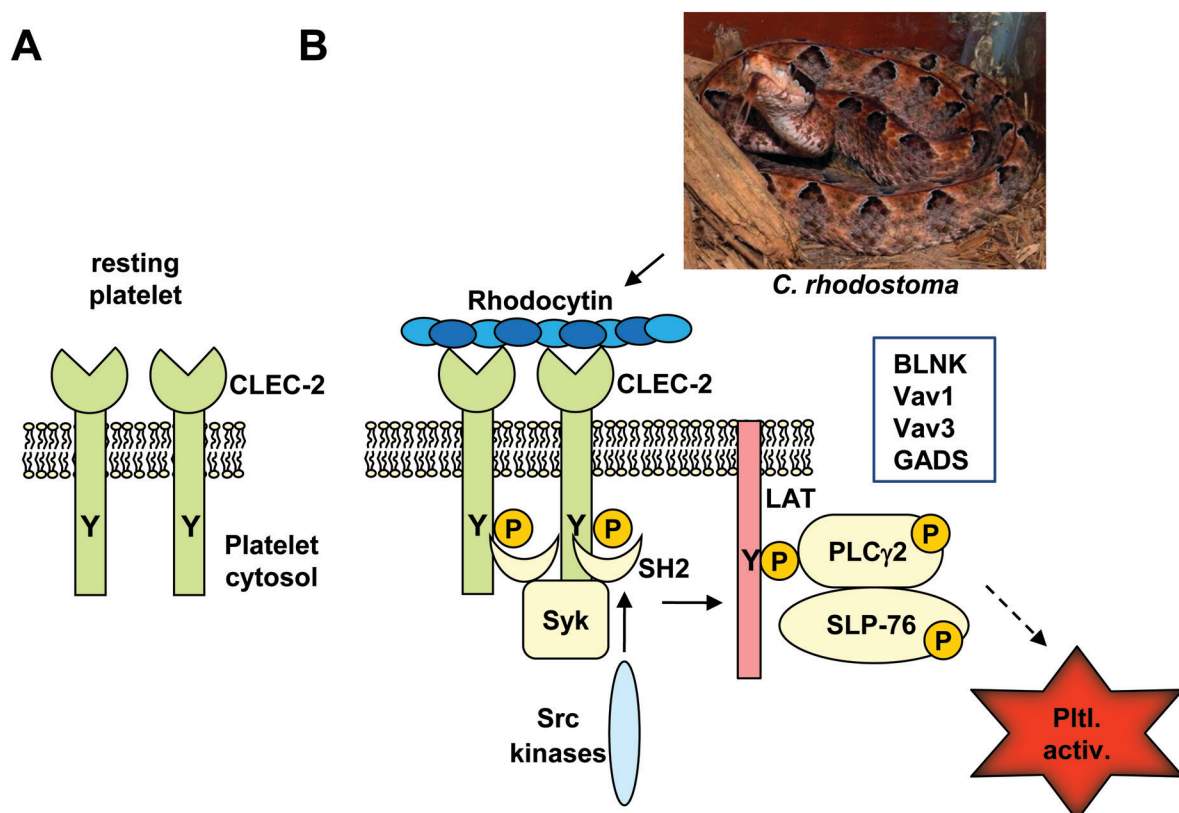
Fig 1.5 Signaling by CLEC-2. A. CLEC-2 is present as a dimer in resting platelets. B. Ligand engagement (rhodocytin) by CLEC-2 causes phosphorylation (P) of a tyrosine residue (Y) by Src kinases on the cytoplasmic domain of CLEC-2. This triggers the interaction with the SH2-domains of Syk and leads to a downstream signaling cascade, involving the proteins indicated and finally culminating in platelet activation (pltl. activ.). Photo: Wikimedia Commons, copyright A. Coritz.

1.3.3 Extracellular ligands and physiological functions of CLEC-2

The venom of the Malayan pit viper *Calloselasma rhodostoma* is known to contain a protein, rhodocytin, which triggers potent platelet activation and aggregation. However, the mechanism of this effect on platelets was longtime unclear until Suzuki-Inoue *et al.* demonstrated in a mass spectrometry approach that the platelet receptor CLEC-2 is the target of rhodocytin[14,45]. This was also the first report to indicate that CLEC-2 is expressed on the platelet surface as the only previous study had not included platelets in the expression analysis of the receptor[18]. Binding of rhodocytin to CLEC-2 promotes downstream signaling events that trigger profound platelet activation and aggregation[14,32]. Nevertheless, it was anticipated that the receptor had potentially other ligand(s)[12].

In addition to a possible role in platelet activation, several other functions for CLEC-2 have been postulated. For example, it was demonstrated that CLEC-2 is also expressed in murine peripheral blood neutrophils where it could possibly serve as an activation receptor mediating phagocytosis and release of pro-inflammatory cytokines, including tumor necrosis factor-alpha (TNF-α)[26]. Furthermore, CLEC-2 was also identified as an attachment factor for human immunodeficiency virus type 1 (HIV-1) on platelets in cell-culture studies using transfected 293T cells. The authors suggested CLEC-2 and the related receptor lectin dendritic cell-specific intercellular adhesion molecule 3-grabbing nonintegrin (DC-SIGN) to mediate the capture and transfer of infectious HIV-1 by platelets in the blood stream. However, they also demonstrated that CLEC-2 does not bind to the HIV-1 envelope protein directly[46]. Later it was hypothesized that the receptor bound to a membrane protein derived from the HIV-producing (renal) 293T cells utilized in the assay of the previous study and that these cells express an endogenous ligand for CLEC-2[47]. Consequently, this study identified the type I transmembrane sialomucin-like glycoprotein podoplanin as an endogenous ligand of CLEC-2. The CLEC-2 ligand podoplanin (also termed aggrus) is a 38 kDa type I transmembrane glycoprotein consisting of 162 aa with an extracellular domain that is highly O-glycosylated. Podoplanin is expressed at high levels in several tissues, including type 1 lung alveolar cells, lymphatic endothelial cells, kidney podocytes and various tumor cells, however, importantly, podoplanin is absent from vascular endothelial cells and platelets[12,36,48-49]. It was shown that CLEC-2 binds to podoplanin on podocytes as well as on 293T cells and suggested that podoplanin is captured by the HI-virus during viral budding on the cells. Binding of podoplanin to CLEC-2 is then used by the virus to be passively transported via platelets in the blood stream[47,50]. Thus, CLEC-2 on platelets could be a potentially important target to inhibit HIV spread in infected humans. Moreover, an earlier study had already demonstrated that CLEC-2 serves as a receptor for podoplanin also expressed on tumor cells and that CLEC-2 is involved in podoplanin-induced platelet aggregation and hematogenous tumor metastasis[48]. This process was shown to significantly

promote tumor cell spreading due to the interaction of CLEC-2 on platelets with podoplanin on the tumor cell surface[51-52]. Thus, the receptor CLEC-2 also has potential as a potent target protein for antimetastatic drug development.

Further insight into the physiological function of the receptor CLEC-2 was gained from different mutant mouse models with interesting phenotypes in the lymphatic-blood vascular separation that were at the time of investigation not attributed to the function of CLEC-2. During embryonic development, the lymphatic vascular system has to be separated from blood vessels but subsequently -after completion of this development in adults- the remaining connections with the blood vessel lumen are only unidirectional at sites where lymph drains into blood at the subclavian veins. However, the mechanisms behind this separation and the reason for the leakage of blood into lymphatic vessels in several mouse mutants were unexplained[53-55]. Recently, evidence has been provided by Uhrin *et al.* showing that during development platelets aggregate and form clots at sites where paired lymph sacs connect with their parental anterior cardinal veins[56]. These platelet aggregates enable the subsequent sprouting of lymphatic vessels and thereby facilitate the correct separation of blood and lymphatic vessels in developing embryos. This much unexpected function of platelets during development was uncovered using podoplanin knock-out embryos exhibiting the described "non-separation" phenotype of blood and lymphatic vessels[54,56]. The authors could demonstrate that platelet aggregation at sites of paired lymph sacs in embryos is triggered by two players, first podoplanin, which is specifically expressed in lymphatic, but not in blood vascular endothelial cells, and second CLEC-2 expressed in platelets. Furthermore, they showed that the aggregation of platelets is crucial for closure of the junction between the lymphatic vascular system and the cardinal veins leading to the separation of the two systems[56]. Additionally, the authors connected the earlier described "non-separating" phenotypes observed in knock-out mice of proteins present in CLEC-2 signaling, namely Syk and SLP-76[40,53,57], and PLCγ2[58] to their findings. All of these mice also showed failure of lymphatic-blood vascular separation. In parallel, another study by Bertozzi *et al.* also demonstrated that CLEC-2 and its downstream protein Syk in platelets are critical to ensure lymphatic-blood vascular separation in embryos[59]. Consistent with these findings, mice lacking the glycosyltransferase T-synthase (encoded by the *C1galt1* gene, termed EHC T-syn$^{-/-}$) in hematopoietic and endothelial cells also exhibit incomplete separation of blood and lymphatic vessels as levels of O-glycosylated podoplanin are reduced in these mice[60]. Interestingly, other phenotypes where blood is found inside lymphatic vessels include mice lacking platelets (myeloid ectotropic viral integration site (Meis) 1 gene deletion[61]) or platelet-derived growth factor-B[54].

1.3.4   The role of CLEC-2 in hemostasis and thrombosis

Due to the impressive activatory potential of CLEC-2 in platelets, it is tempting to speculate that additionally to the described functions in lymphangiogenesis and tumor metastasis CLEC-2 could also play a role in hemostasis and thrombosis in adult organisms.

However, the importance of CLEC-2 for platelet activation during hemostasis and in the course of thrombotic events had not been defined at the starting time of the present thesis and was eagerly awaited. Also, an endogenous ligand of CLEC-2 that directly plays a role in thrombosis and hemostasis has not been identified. The only known endogenous ligand of CLEC-2 -podoplanin- does not come into direct contact with the receptor under physiological conditions in blood vessels. Furthermore, no inhibitory compound or mechanism of the receptor has been described.

Furthermore, during the course of this study three independent publications demonstrated that knock-out of the CLEC-2 protein leads to embryonic and perinatal lethality in mice[59,62-63]. Therefore, it became clear that other strategies would be needed to effectively delete the receptor in platelets, e.g. α-CLEC-2 antibody treatment leading to "immunodepletion" and resulting in a "knock-out like" phenotype.

1.4 The major collagen receptor glycoprotein (GP) VI

The major collagen receptor glycoprotein (GP) VI belongs to the immunoglobulin (Ig) superfamily and is closely related to the Fcα receptor (FcαR) and the natural killer cell receptor[64]. Interestingly, the expression of GPVI is restricted to platelets and megakaryocytes in humans and mice[65] making it a potentially valuable target for anti-thrombotic therapy[66].

1.4.1 Signal transduction of GPVI

GPVI is a type I transmembrane glycoprotein of approximately 62-65 kDa that is non-covalently associated with the intracellular Fc receptor γ-chain (FcRγ-chain) (Fig 1.6)[67]. The FcRγ-chain is the signaling subunit of the complex and is expressed as a disulphide-linked homodimer, each monomer containing two tyrosine residues in the ITAM motif[5,9,68-69].
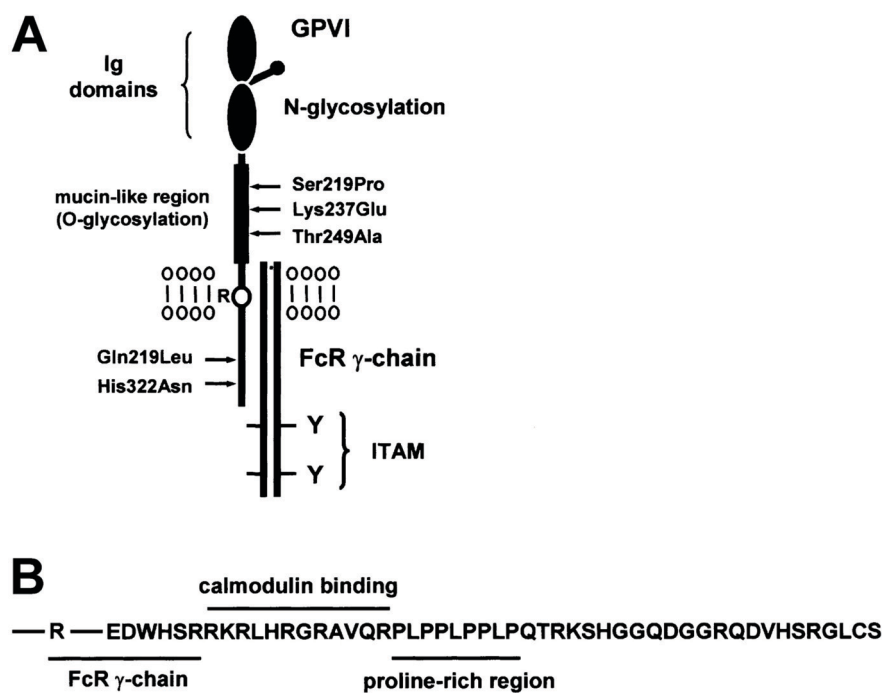
Fig 1.6 Structure of the GPVI-FcRγ-chain complex. A. The extracellular part of GPVI consists of two Ig domains linked to a mucin-rich region and the transmembrane domain carrying an arginine residue (R) required for the association with the FcRγ-chain. The FcRγ-chain is present as a disulphide-linked homodimer and has two tyrosines (Y) in a conserved signaling sequence known as ITAM. B. Amino acid sequence of the cytosolic tail of GPVI. The site of interaction of GPVI with the FcRγ-chain and the binding site of calmodulin are indicated. The proline-rich region serves as a binding site for the SH3-domain of Src kinases. Note: The amino acids following the proline-rich region are present in human but absent in murine GPVI sequence. Taken from: Nieswandt B and Watson SP, *Blood*, 2003[5].

Upon binding to its major ligand collagen, GPVI becomes clustered followed by phosphorylation of the two ITAM-tyrosine residues of the FcRγ-chain[69-71] via the Src kinases Fyn and Lyn[72-73] which bind selectively with their Src homology 3 (SH3) domains to the proline-rich motif of the GPVI cytosolic domain[5] (see also Fig 1.2 and Fig 1.8).

Subsequently, the phosphorylated ITAM serves as a binding site for SH2-domains of the tyrosine kinase Syk[74-75] which is in turn activated and orchestrates a downstream tyrosine phosphorylation cascade including several adapter proteins, such as LAT[76] and SLP-76[77], effector enzymes, such as PI3K, PLCγ2 and small GTPases. This triggers DAG- and IP$_3$-production, leading to activation of PKC and finally culminating in elevation of $[Ca^{2+}]_i$ which enables platelet activation and is associated with integrin activation ("outside-in" activation), effective platelet adhesion, degranulation, and aggregation of the cells[5,36].

1.4.2 Down-regulation of GPVI on the platelet surface using monoclonal antibodies

Earlier studies from our group have demonstrated that *in vivo* (but not *in vitro*) administration of rat monoclonal α-GPVI antibodies (termed JAQ1, 2, 3) leads to "immunodepletion" or down-regulation of the GPVI receptor in circulating platelets resulting in a "knock-out like" phenotype in mice[66,78]. Therefore, the antibody JAQ1 is considered as a useful tool for the analysis of the biological function of GPVI applicable in murine *in vitro*, as well as *in vivo* studies. It was shown that JAQ1 binds to the collagen binding site of the Ig-like domain of GPVI, thus inhibiting platelet aggregation induced by low and intermediate concentrations of collagen *in vitro*[67]. Interestingly, increasing collagen concentrations could overcome this JAQ1-mediated inhibitory effect[79]. However, in the same study it was shown that platelets from FcRγ-chain-deficient mice, which lack the signaling subunit of the GPVI receptor (FcRγ-chain), completely lacked a response to high concentrations of collagen[67].

In contrast to human α-GPVI auto-antibodies isolated from autoimmune patients[64,80-81], JAQ1 alone did not induce platelet aggregation *in vitro*. However, upon cross-linking of JAQ1 with polyclonal α-rat IgG antibodies, aggregation was observed[67]. Whereas *in vitro* treatment of platelets with JAQ1 only led to blockage of GPVI without further effects, surprisingly, a transient but strong thrombocytopenia was observed upon *in vivo* administration of the antibody in mice[66]. Interestingly, this was accompanied by a rapid and irreversible down-regulation of the GPVI receptor from circulating platelets. However, platelet counts recovered back to normal within 48 h and the obtained platelets were GPVI-deficient but otherwise fully functional. The induced GPVI deficiency lasted for at least 14 days and was accompanied by a long-term protection from mortality in a model of collagen-dependent lethal pulmonary thromboembolism[66]. Furthermore, JAQ1-treated animals were long-term protected in models of arterial thrombosis and ischemic stroke. Remarkably, this was associated with only mildly prolonged tail bleeding times[66,82-84]. Due to these intriguing findings, GPVI has extensively been discussed as a potentially valuable anti-thrombotic target in several studies[66,78,85-86].

By treatment with JAQ1, Nieswandt *et al.* demonstrated for the first time that specific depletion of an activating receptor was irreversibly induced from circulating platelets[66]. The underlying mechanism of antibody-induced "immunodepletion" or down-regulation of GPVI

from the platelet surface is still only partially understood. However, recent studies show that JAQ-induced down-regulation can occur via two different mechanisms, either through receptor internalization[66,78] or metalloproteinase-dependent ectodomain shedding[87-89]. Similarly, the antibodies JAQ2 and JAQ3 which bind to two distinct epitopes on the GPVI receptor different from that targeted by JAQ1 also induce down-regulation of GPVI in platelets in mice. Thus, the antibody-induced down-regulation of the receptor is independent of the exact binding of the antibody to the epitope on GPVI[78]. Interestingly, an elegant study using mice deficient in the signaling molecules downstream of GPVI, PLCγ2 and LAT, demonstrated that JAQ1 antibody-induced GPVI shedding was abolished in these animals, while the receptor was irreversibly down-regulated through internalization and intracellular clearing[89]. Importantly, the latter mechanism was not associated with the observed thrombocytopenia in wild-type mice. This finding revealed the possibility to uncouple GPVI down-regulation from undesired side effects with obvious therapeutic implications[89]. In another study, JAQ1-induced shedding of GPVI was further analyzed. Here it was demonstrated that incubation of mouse platelets with carbonyl cyanide m-chlorophenyl-hydrazone (CCCP) lead to induction of mitochondrial injury and subsequently activated metalloproteinases, thus inducing rapid proteolytic cleavage or shedding of GPVI from the platelet surface[87]. Furthermore, it was known that calmodulin is associated to the cytoplasmic tail of GPVI[90] (Fig 1.6) and that upon blockage of this association with the calmodulin inhibitor W7, metalloproteinase-mediated GPVI shedding is provoked *in vitro*[88]. It was further demonstrated that GPVI cleavage *in vitro* can occur through two different sheddases, a disintegrin and metalloproteinase (ADAM) 10 and ADAM17, depending on the shedding-stimulating experimental conditions. However, recent evidence suggests that either both or a third not yet identified sheddase in platelets are responsible for GPVI-cleavage under *in vivo* conditions[85].

Additionally to GPVI, human platelets express a second ITAM-bearing receptor, Fc-γ receptor IIa (FcγRIIa), which is not present on the surface of mouse platelets[91]. Similar to GPVI, the FcγRIIa receptor contains two extracellular Ig domains and signals using an ITAM-dependent pathway. However, unlike GPVI but rather similar to the hemITAM of CLEC-2, human FcγRIIa possesses an ITAM motif within its cytoplasmic tail[92-93]. Interestingly, Gardiner *et al.* demonstrated that individual activation of both ITAM-coupled human pathways, GPVI or FcγRIIa, induced proteolytic down-regulation of both receptors simultaneously; a process termed trans-inhibition (Fig 1.7). At present, it has not been studied whether a similar pathway or mechanism exists for GPVI and CLEC-2 either on human or mouse platelets[94]. For the development of potential α-GPVI or α-CLEC-2 anti-thrombotic agents the clarification of this question would be of high interest.
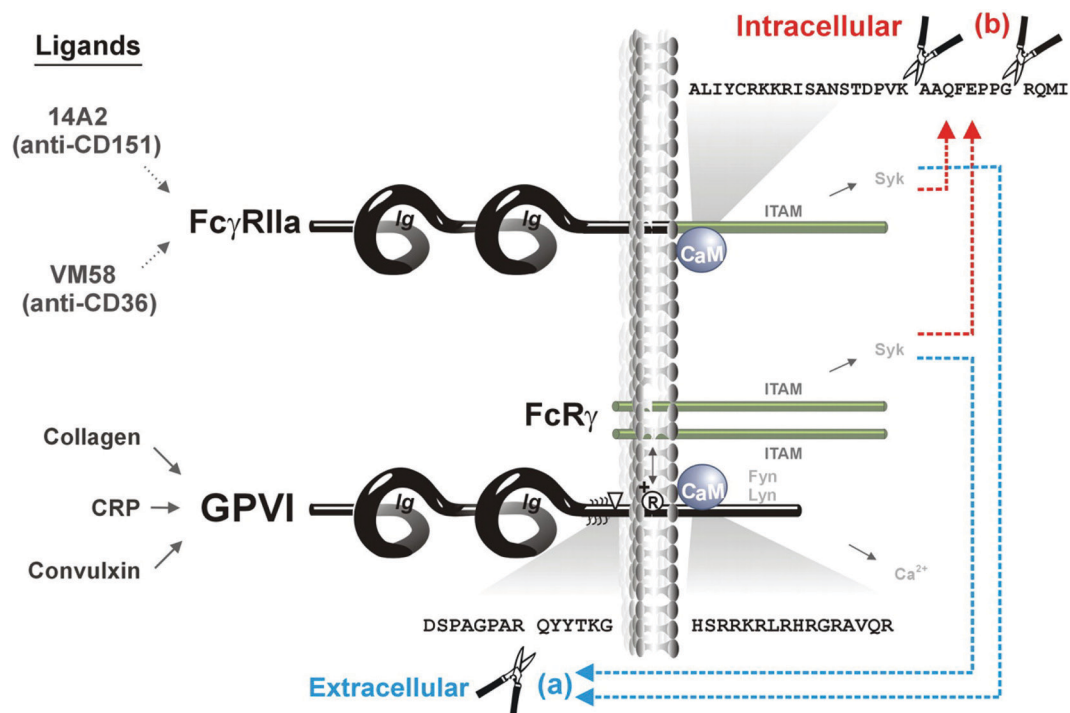
Fig 1.7 Proteolytic pathways for irreversible inactivation of ITAM-bearing receptors in human platelets. Binding of ligands to the receptors FcγRIIa (antibodies 14A2 or VM58) or GPVI (collagen, CRP, convulxin) leads to (a) extracellular metalloproteinase-mediated ectodomain shedding of GPVI and (b) intracellular calpain-mediated cleavage of FcγRIIa. Both mechanisms result in deletion of the intracellular ITAM domain. Both pathways are also induced by the calmodulin inhibitor, W7, which dissociates calmodulin from the cytoplasmic domain of GPVI and FcγRIIa. Taken from: Gardiner EE *et al*., *Blood*, 2008[94].

1.5 Comparison of signal transduction pathways of GPVI and CLEC-2

As described above, the signaling pathway of the hemITAM-bearing receptor CLEC-2 shares some similarities with signaling mediated by the ITAM-bearing GPVI/FcRγ-chain complex (Fig 1.8)[36]. It was demonstrated that signaling of CLEC-2 is mediated via Src and Syk tyrosine kinases leading to a downstream tyrosine phosphorylation cascade and recruitment of several adapter proteins, such as Tec family tyrosine kinases and effector proteins including PI 3-kinase, Vav, Rac1 and PLCγ2[14,32] (see also Fig 1.5).

Comparable to GPVI signaling, several of these proteins are critical for activation including Syk and PLCγ2[14], whereas the role of others can be overcome at higher agonist concentrations, such as LAT and Gads which play very similar roles to those of GPVI signaling in the regulation of PLCγ2[39]. Furthermore, signaling by both receptors, CLEC-2 and GPVI, takes place in lipid rafts, with the respective receptor moving to the cholesterol-rich membrane domains upon activation[43]. The only notable difference in signaling by GPVI compared to CLEC-2 downstream of Syk is the absolute requirement for SLP-76 in signaling by GPVI, while high concentrations of rhodocytin mediate weak platelet activation by CLEC-2 also in the absence of the adapter protein[14,32]. Additionally, it was shown that phosphorylation of CLEC-2, but not of the FcRγ-chain of GPVI, is also dependent on actin polymerization, release of ADP and TxA$_2$ and the small G protein Rac, proving a critical role for feedback events in CLEC-2 signaling[43]. A study has proposed a model in which Syk rather than Src kinases mediates phosphorylation of the hemITAM sequence of CLEC-2, with Src kinases regulating activation of Syk[95].

However, a unique feature in the CLEC-2 signaling cascade is that Src kinase-dependent tyrosine phosphorylation of CLEC-2 on a single hemITAM appears to be sufficient to confer binding to Syk, thereby initiating downstream signaling events. This contrasts with the signaling cascade used by the GPVI/FcRγ-chain, which recruits Syk to a doubly phosphorylated ITAM on the FcRγ-chain. Thus, it seems that signaling through sequential activation of Src and Syk downstream of the hemITAM motif of CLEC-2 is a novel variation of the commonly known ITAM signaling pathways[36,96].
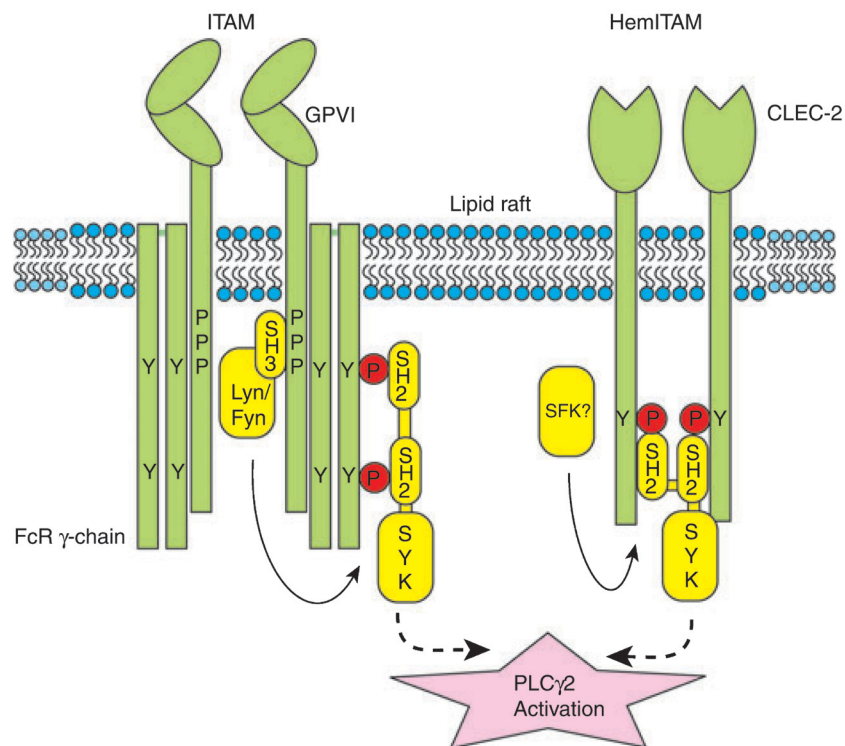
Fig 1.8 Comparison of signaling via the ITAM-bearing GPVI-FcRγ-chain complex and the hemITAM-bearing receptor CLEC-2. As GPVI interacts via a salt bridge with a covalent dimer of the FcRγ-chain, the complex forms a higher oligomer. Each FcRγ-chain contains an ITAM motif. Phosphorylation (P, red) of the tyrosine residues (Y) within the ITAM motif by the Src family kinases Lyn and Fyn within lipid rafts leads to the recruitment and activation of Syk. CLEC-2 also forms a dimer and phosphorylation of the tyrosine within the hemITAM motif leads to recruitment and activation of Syk. In both cases the recruitment and activation of Syk leads to the activation of PLCγ2. Taken from: Watson SP *et al.*, *J Thromb Haemost*, 2010[36].

1.6 Immunodepletion of platelet surface receptors as a novel strategy for anti-thrombotic therapy

Platelets are central mediators of pathological thrombus formation in ischemic diseases like myocardial infarction or stroke. Therefore, anti-platelet agents have evolved as the prime therapeutic tools in prevention and management of these diseases[97]. However, all available anti-platelet as well as anti-coagulant therapies exhibit unwanted side effects such as a high risk of bleeding, especially when used in combination[97-98]. Thus, the identification of novel platelet activation pathways as well as the validation of new methods of platelet inhibition is equally important, in order to develop novel, safe therapeutic agents.

Currently at least 23 antibody-based therapeutics are successfully being used in the clinic for the treatment of a wide range of diseases, such as autoimmune disorders, malignancies and infections[99]. Consistently, the platelet integrin αIIbβ3 inhibitor abciximab (trade name "ReoPro") represents a powerful tool for inhibition of unwanted platelet activation in clinical

settings. This chimeric (humanized) Fab-fragment binds non-specifically to the integrin and blocks its function, but does not lead to down-regulation of the glycoprotein on platelets[97,100]. In contrast, antibody-mediated temporary "immunodepletion" of prominent platelet surface receptors might represent a novel potential strategy of anti-thrombotic therapy. This approach has so far only been described for the platelet collagen receptor GPVI in the murine model[66]. Here, administration of the α-GPVI antibodies JAQ1, 2 and 3 leads to highly specific down-regulation of GPVI on the platelet surface, thereby inhibiting its signaling, while leaving platelets otherwise fully functional, a process that has been described in detail above (see chapter 1.4.2). Interestingly, while this potential strategy was elaborately analyzed in mice, antibody-induced loss of GPVI was also found in platelets of two patients who had developed anti-GPVI autoantibodies[80,101] as well as in human platelets circulating in nonobese diabetic/ severe combined immunodeficient (NOD/SCID) mice[102]. Importantly, one of the patients developing autoantibodies against GPVI suffered from mild thrombocytopenia and had platelets that were unresponsive towards collagen in consequence of "immunodepleted" GPVI. Bleeding times, however, were found to be only very moderately increased. Together, these findings indicate that antibody-based α-GPVI treatment may be a powerful novel strategy to specifically shut off this central activation pathway in platelets not only in mice but also in humans.

Importantly, the present study demonstrates that immunodepletion can also be achieved for another, newly identified platelet surface receptor, namely CLEC-2, and raises speculations whether this strategy might also be applicable for other receptors, not only in platelets, but also in other cell types.

1.7 Aim of the Study

The platelet surface receptors GPVI and CLEC-2 have been proposed as potential anti-thrombotic targets and share similarities in their intracellular signaling pathways. Whereas GPVI has been extensively studied, the physiological function of CLEC-2 was largely unknown.

The aim of the present study was i) to analyze the role of CLEC-2 in murine models of hemostasis and thrombosis and to clarify whether the receptor could indeed represent a potential anti-thrombotic target and ii) to investigate whether GPVI and CLEC-2 have redundant functions in physiological processes of hemostasis and thrombosis. For this purpose, an antibody-mediated "immunodepletion"-approach in mice was utilized and the resulting CLEC-2 single-deficient mice were analyzed. Secondly, analyses of antibody-induced double-deficiency of GPVI and CLEC-2 in platelets and of the resulting effect on hemostasis and thrombosis were performed.

2 Materials and methods

2.1 Materials

2.1.1 Kits and chemicals

Acetic acid	Roth (Karlsruhe, Germany)
ADP	Sigma (Deisenhofen, Germany)
Agarose	Roth (Karlsruhe, Germany)
Agarose, low melting	Euromedex (Souffelweyersheim, France)
Alexa Fluor 488	Invitrogen (Karlsruhe, Germany)
Ammonium peroxodisulphate (APS)	Roth (Karlsruhe, Germany)
Apyrase (grade III)	Sigma (Deisenhofen, Germany)
Atipamezole	Pfizer (Karlsruhe, Germany)
ATP release kit	Roche Diagnostics (Mannheim)
Avertin (2,2,2-tribromoethanol and 2-methyl-2-butanol)	Sigma (Deisenhofen, Germany)
Beta-mercaptoethanol	Roth (Karlsruhe, Germany)
Bovine serum albumin (BSA)	AppliChem (Darmstadt, Germany)
Calcium chloride	Roth (Karlsruhe, Germany)
Complete mini protease inhibitors (+EDTA)	Roche Diagnostics (Mannheim, Germany)
Convulxin	Alexis Biochemicals (San Diego, USA)
Disodiumhydrogenphosphate	Roth (Karlsruhe, Germany)
Dry milk, fat-free	AppliChem (Darmstadt, Germany)
Dylight-488	Pierce (Rockford, IL, USA)
EDTA	AppliChem (Darmstadt, Germany)
Enhanced chemoluminiscence (ECL)-detection substrate	PerkinElmer LAS (Boston, USA)
Eosin	Roth (Karlsruhe, Germany)
Ethanol	Roth (Karlsruhe, Germany)
Ethidium bromide	Roth (Karlsruhe, Germany)
EZ-Link sulfo-NHS-LC-biotin	Pierce (Rockford, IL, USA)
Fentanyl	Janssen-Cilag GmbH (Neuss, Germany)
Fibrillar type I collagen (Horm)	Nycomed (Munich, Germany)
Flumazenil	Delta Select GmbH (Dreieich, Germany)
Fluorescein-isothiocyanate (FITC)	Molecular Probes (Oregon, USA)
Freund's Adjuvant	Sigma (Deisenhofen, Germany)
GeneRuler 1kb DNA Ladder	Fermentas (St. Leon-Rot, Germany)
Glucose	Roth (Karlsruhe, Germany)

Glutaraldehyde	Roth (Karlsruhe, Germany)
Glycerol	Roth (Karlsruhe, Germany)
Hematoxylin	Sigma (Deisenhofen, Germany)
HEPES	Roth (Karlsruhe, Germany)
High molecular weight heparin	Sigma (Deisenhofen, Germany)
Human fibrinogen	Sigma (Deisenhofen, Germany)
Human vWF	CSL Behring (Hattersheim, Germany)
Igepal CA-630	Sigma (Deisenhofen, Germany)
Indomethacin	Sigma (Deisenhofen, Germany)
Isopropanol	Roth (Karlsruhe, Germany)
Loading Dye Solution, 6x	Fermentas (St. Leon-Rot, Germany)
Magnesium chloride	Roth (Karlsruhe, Germany)
Magnesium sulfate	Roth (Karlsruhe, Germany)
Medetomidine (Dormitor)	Pfizer (Karlsruhe, Germany)
Midazolam (Dormicum)	Roche Pharma AG (Grenzach-Wyhlen, Germany)
MOPS	AppliChem (Darmstadt, Germany)
Naloxon	Delta Select GmbH (Dreieich, Germany)
4-12% NuPage Bis-Tris gradient gels	Invitrogen (Karlsruhe, Germany)
PageRuler Prestained Protein Ladder	Fermentas (St. Leon-Rot, Germany)
Paraformaldehyde (PFA)	Roth (Karlsruhe, Germany)
Phalloidin-rhodamine	Invitrogen (Karlsruhe, Germany)
Phenol/chloroform/isoamylalcohol	AppliChem (Darmstadt, Germany)
Potassium acetate	Roth (Karlsruhe, Germany)
Potassium chloride	Roth (Karlsruhe, Germany)
Prostacyclin	Calbiochem (Bad Soden, Germany)
Protein G-Sepharose	GE Healthcare (Uppsala, Sweden)
QIAquick gel extraction kit	Qiagen (Hilden, Germany)
Rat Immunoglobulin Isotyping ELISA kit	BD Pharmingen (Heidelberg, Germany)
RNeasy Mini Kit	Qiagen (Hilden, Germany)
R-phycoerythrin (PE)	EUROPA (Cambridge, UK)
Rotiphorese Gel 30 (PAA)	Roth (Karlsruhe, Germany)
Sodium chloride	AppliChem (Darmstadt, Germany)
Sodium cacodylate	Roth (Karlsruhe, Germany)
Sodium citrate	AppliChem (Darmstadt, Germany)
Sodiumdihydrogenphosphate	Roth (Karlsruhe, Germany)
Sodium hydroxide	AppliChem (Darmstadt, Germany)

TEMED	Roth (Karlsruhe, Germany)
3,3,5,5-tetramethylbenzidine (TMB)	EUROPA (Cambridge, UK)
Thrombin	Roche Diagnostics (Mannheim, Germany)
Titan One Tube RT-PCR-Kit	Roche (Ingelheim, Germany)
TRIS ultra	Roth (Karlsruhe, Germany)
Triton X-100	AppliChem (Darmstadt, Germany)
U46619	Alexis Biochemicals (San Diego, USA)

Collagen-related peptide (CRP) was kindly provided by S.P. Watson (University of Birmingham, UK). Rhodocytin was a generous gift from J. Eble (University Hospital Frankfurt, Germany). All enzymes were purchased from Fermentas (St. Leon-Rot, Germany) or obtained from Invitrogen (Karlsruhe, Germany). All other chemicals were obtained from Sigma (Deisenhofen, Germany) or Roth (Karlsruhe, Germany).

2.1.2 Cell culture materials

BSA, low endotoxin	PAA Laboratories (Cölbe, Germany)
Cell strainer, 100 µm	BD Falcon (Bedford, USA)
Concentrator tube, exclusion size 10 kDa	VivaScience (Hannover, Germany)
DL-Dithiothreitol	Sigma (Deisenhofen, Germany)
DMEM + GlutaMAX-I	Gibco (Karlsruhe, Germany)
D-PBS	Gibco (Karlsruhe, Germany)
Dimethyl sulfoxide (DMSO)	AppliChem (Darmstadt, Germany)
Effectene Transfection Reagent	Invitrogen (Karlsruhe, Germany)
Foetal Bovine Serum (FCS)	Gibco (Karlsruhe, Germany)
Geneticin (G-418 sulphate)	Gibco (Karlsruhe, Germany)
HAT (hypoxanthine-aminopterin-thymidine, 50x)	Roche Diagnostics (Mannheim, Germany)
Iodacetamide	Merck (Darmstadt, Germany)
Panserin 410	PAN (Aidenbach, Germany)
Papain, immobilized	Pierce, Thermo Fisher Scientific (Bonn, Germany)
Penicillin-Streptomycin	Gibco (Karlsruhe, Germany)
Pepsin, immobilized	Merck (Darmstadt, Germany)
Polyethylene glycol 1500 (PEG 1500)	Roche Diagnostics (Mannheim, Germany)
Protein A-column, immobilized	Bio-Rad, (Munich, Germany)
Protein G-column, immobilized	GE Healthcare (Uppsala, Sweden)
RPMI	Gibco (Karlsruhe, Germany)
Steritop Bottle Top Filter 0.22 µm	Millipore (Massachusetts, USA)

Superdex 200 (SD) column	Amersham Biosciences (Freiburg, Germany)
Tissue culture dishes (100x20 mm)	Greiner (Frickenhausen, Germany)
Tissue culture flasks	Greiner (Frickenhausen, Germany)
Trypsin-EDTA	Gibco (Karlsruhe, Germany)
Well plates (6-well, 24-well or 96-well)	Greiner (Frickenhausen, Germany)

2.1.3 Antibodies

2.1.3.1 Purchased primary and secondary antibodies

Anti-phosphotyrosine 4G10	Upstate (CA, USA)
Rat anti-mouse IgG-HRP	DAKO (Hamburg, Germany)
Irrelevant anti-rat IgG-FITC	EMFRET Analytics (Eibelstadt, Germany)
Rabbit anti-rat Ig-FITC	DAKO (Hamburg, Germany)
Anti-human vWF Ig	DAKO (Hamburg, Germany)

2.1.3.2 Monoclonal antibodies (mAbs)

Monoclonal antibodies (mAbs) generated and modified in our laboratory:

antibody	isotype	antigen	described in
DOM2	IgG1	GPV	[103]
INU1	IgG1κ	CLEC-2	[104]
JAQ1	IgG2a	GPVI	[66]
JON/A	IgG2b	GPIIb/IIIa	[105]
JON1	IgG2a	GPIIb/IIIa	[103]
JON6 (14A3)	IgG2b	GPIIb/IIIa	unpublished
MWReg 30	IgG1	α2 integrin	unpublished
p0p4	IgG2b	GPIbα	[103]
p0p6	IgG2b	GPIX	[103]
ULF1	IgG2a	CD9	[103]
WUG1.9	IgG1	P-selectin	unpublished
12C6	IgG2b	α2 integrin	unpublished

2.1.4 Animals

Specific-pathogen-free male mice (NMRI, C57Bl/6J) and rats (WISTAR) 4 to 10 weeks of age were obtained from Harlan Laboratories (Eystrupp, Germany) or from Janvier (Le Genest-Saint-Isle, France). GPVI-deficient mice were generated by Markus Bender in our

own laboratories as described[106] and maintained on a mixed SV/129/C57Bl/6J background. For experiments with GPVI-deficient mice, animals of the same genetic background were used as controls. Animal studies were approved by the district government of Lower Franconia (Bezirksregierung Unterfranken).

2.1.5 Cell lines

The mouse myeloma cell line Sp2/0-Ag14 was kindly provided by D. Männel, University Hospital Regensburg, Germany. The Human Embryonic Kidney (HEK) 293 cell line was purchased at ATCC, Wesel, Germany.

2.1.6 Buffers and media

All buffers were prepared and diluted using *aqua ad injectabilia* Delta Select (Pfullingen, Germany) or double-distilled water (ddH$_2$O).

- *Acid-citrate-dextrose (ACD) buffer, pH 4.5*

Trisodium citrate dehydrate	85 mM
Citric acid anhydrous	65 mM
Glucose anhydrous	110 mM

- *Biotinylation buffer*

NaHCO$_3$	50 mM
NaCl	0.9%
add H$_2$O	

- *Blocking solution (immunoblotting)*

BSA or fat-free dry milk	5%
in PBS or washing buffer	

- *Blotting buffer A (immunoblotting)*

TRIS, pH 10.4	0.3 M
Methanol	20%

- *Blotting buffer B (immunoblotting)*

TRIS, pH 10.4	25 mM
Methanol	20%

- *Blotting buffer C (immunoblotting)*

ε-amino-n-caproic acid, pH 7.6	4 mM

Methanol	20%

- *Coating buffer (ELISA), pH 9.0*

NaHCO$_3$	50 mM

- *Coomassie staining solution*

Acetic acid	10%
Methanol	40%
Coomassie Brilliant blue	1 g

- *Coomassie destaining solution*

Acetic acid	10%
Methanol	40%

- *Coupling buffer 2x, pH 9.0*

NaHCO$_3$	14 g/l
Na$_2$CO$_3$	8.5 g/l

- *Digestion buffer, pH 7.0*

NaH$_2$PO$_4$ x H$_2$O	20 mM
NaCl	10 mM
Cystein-HCl	20 mM

- *DMEM growth medium*

DMEM	
FCS	10%
Penicillin-Streptomycin	1%

- *DMEM selection medium I*

DMEM	
FCS	10%
Penicillin-Streptomycin	1%
Geneticin (G-418)	700 µg/ml

- *DMEM selection medium II*

DMEM	
FCS	10%
Penicillin-Streptomycin	1%
Geneticin (G-418)	300-400 µg/ml

- *Elution buffer (affinity chromatography)*

Glycine (pH 2.8)	0.1 M
add H_2O	

- *FCS-free medium*

Panserin 401	
Penicillin-Streptomycin	1%
Geneticin (G-418)	300-400 µg/ml

- *IP buffer*

TRIS HCl, pH 8.0	15 mM
NaCl	155 mM
EDTA	1 mM
NaN_3	0.005%

- *Laemmli buffer (SDS-PAGE)*

TRIS	40 mM
Glycine	0.95 M
SDS	0.5%

- *Lysis buffer (DNA isolation)*

TRIS base	100 mM
EDTA	5 mM
NaCl	200 mM
SDS	0.2%
add Proteinase K (20 mg/ml)	100 µg/ml

- *Lysis buffer (tyrosine phosphorylation), pH 7.5*

NaCl	300 mM
Tris	20 mM
EGTA	2 mM
EDTA	2 mM
Na_3VO_4	2 mM
Igepal CA-630	2%
add 1 tablet of complete mini protease inhibitors	

- *Neutralization buffer (affinity chromatography)*

TRIS base (pH 9.0)	1.0 M

- *Phosphate buffered saline (PBS), pH 7.14*

NaCl	137 mM (0.9%)
KCl	2.7 mM
KH_2PO_4	1.5 mM
Na_2HPO_4	8 mM

- *SDS sample buffer, 2x*

β-mercaptoethanol (reduced conditions)	10%
TRIS buffer (1.25 M), pH 6.8	10%
Glycerin	20%
SDS	4%
Bromophenolblue	0.02%

- *Separating gel buffer*

TRIS/HCl, pH 8.8	1.5 M

- *Sodium citrate buffer*

Na citrate , HCl pH 4.0	0.1 mol/l

- *Stacking gel buffer*

TRIS/HCl, pH 6.8	0.5 M

- *Stripping buffer*

Tris/HCl, pH 6.8	62.5 mM
SDS	2%
β-mercaptoethanol	100 mM

- *Superdex 200 (SD) column buffer (pH 7.2)*

NaCl	0.15 M
Na_2HPO_4	0.05 Ml

- *50x TAE*

TRIS base	0.2 M
Acetic acid	5.7%
EDTA (0.5 M, pH 8)	10%

- *TE buffer, pH 8*

TRIS base	10 mM
EDTA	1 mM

- *Tris-buffered saline (TBS), pH 7.3*

NaCl	137 mM (0.9%)
Tris/HCl	20 mM

- *Tyrode-HEPES buffer, pH 7.3*

NaCl	137 mM (0.9%)
KCl	2.7 mM
$NaHCO_3$	12 mM
NaH_2PO_4	0.43 mM
$CaCl_2$	1 mM
$MgCl_2$	1 mM
HEPES	5 mM
BSA	0.35%
Glucose	0.1%

- *Washing buffer*

Tween 20	0.1%
in PBS	

2.2 Methods

2.2.1 Human embryonic kidney (HEK) 293 cell culture

2.2.1.1 Thawing and culture of HEK 293 cells

Frozen non-transfected human embryonic kidney (HEK) 293 cells were shortly thawed at 37°C and resuspended in DMEM growth medium. After centrifugation for 5 min at 900 rpm the cells were resuspended in fresh DMEM growth medium. Cells were grown in DMEM growth medium at 37°C and 5% CO_2 in monolayer in a T25 flask.

2.2.1.2 Splitting of HEK 293 cells

When cells had grown to 80-90% confluency, they were split into three separate tissue culture flasks of the same or the next larger size. For this purpose, cells were washed with 10 ml PBS. To detach the cells, 4 ml trypsin were added and incubated at 37°C for 5 min. After adding 5 ml DMEM growth medium the collected cells were again centrifuged, the pellet was resuspended in 5 ml DMEM growth medium and transferred to the tissue culture flasks. For further culturing of the cells, 20 ml DMEM growth medium were added and cells were incubated at 37°C and 5% CO_2.

2.2.1.3 Transfection of HEK 293 cells

The transfection of HEK 293 cells was performed using Effectene Transfection Reagent (Invitrogen, Karlsruhe, Germany) according to the manufacturer's protocol. This step was accomplished during my diploma thesis in the same laboratory[33].

For 6-well plates 0.4 µg DNA (murine CLEC-2 cDNA in Signal pIgplus-vector) per well were used for transfection. Transfection was performed when cells had reached confluency of 70-80%. The DNA was diluted in TE-buffer to a concentration of 0.2 µg/µl and 2 µg DNA were mixed with DNA-condensation buffer EC to a total volume of 100 µl. Next, 3.2 µl Enhancer were added, shortly mixed and incubated at RT for 5 min. Then, 10 µl Effectene Transfection Reagent were applied and incubated for 5-10 min at RT. 600 µl DMEM growth medium were added to the transfection complex and mixed carefully. This solution was then drop-wise added to the HEK 293 cells. Cells were cultured at 37°C and 5% CO_2 for 24-48 h. For positive selection, the medium was replaced by DMEM selection medium I containing 700 µg/ml geneticin (G418). After 3-4 days medium was changed. After further 7 days, the geneticin concentration was decreased to 300-400 µg/ml. Stably transfected HEK 293 cells were obtained and split into a fresh 12-well plate, and wells were monitored for monoclonal cell populations. Monoclonal cells were cultured further and tested for production of fusion protein by western blot analysis.

2.2.1.4 Freezing HEK 293 cells

CLEC-2 transfected monoclonal HEK 293 cells were grown until 85% confluency, trypsinized as described before, spun down and the pellet was resuspended in 5 ml ice-cold Freezing medium. Cell suspension aliquots of 1 ml in Cryo-tubes were immediately put on dry ice and stored in liquid N_2.

2.2.1.5 Purification of mCLEC-2 Fc-Fusion protein

For large scale production of the mCLEC-2 Fc-fusion protein (see chapter 2.2.2.3 and[33]), stably transfected HEK 293 cells were cultured in FCS-free medium (Panserin 410) and 6 l of medium containing the mCLEC-2 Fc-fusion protein were collected. The mCLEC-2 Fc-fusion protein was purified from the medium via affinity chromatography using a protein G-Sepharose column.

2.2.2 Production of monoclonal antibodies

2.2.2.1 Immunization

For generation of anti-CLEC-2 antibodies, three female WISTAR rats, 6 weeks of age, were immunized with either of the following antigens: washed mouse platelets, purified mCLEC-2 Fc-fusion protein or immuno-precipitate from wild-type platelet lysate using INU1. For this, 0.5×10^9 washed mouse platelets (resting state, washed in sterile PBS) were used per animal for each immunization. Alternatively, immuno-precipitate from wild-type platelet lysate with INU1 was utilized (lysate from 0.5×10^9 washed mouse platelets, pull-down with 5 µg/ml INU1 and 25 µl protein G-Sepharose per rat). In a third attempt, purified mCLEC-2 Fc-fusion protein (100 µg/ rat for the initial, 50 µg/ rat for all following immunizations) was used. Each antigen was resolved in Freund's adjuvant. For the initial immunization, antigens were solubilized in Freund's adjuvant complete and injected subcutaneously in three bolus injections of 50 µl per rat. All following immunizations were performed in Freund's adjuvant incomplete. Rats were repeatedly (minimum 7 times, intervals of 21 days) subcutaneously immunized with the immunogens.

2.2.2.2 Generation of hybridoma cells

The rat spleen was removed under sterile conditions and filtered through a 100 µm cell strainer to obtain a single cell suspension. For the fusion of mouse myeloma and rat splenic cells, spleen cells were washed twice in RPMI/pen-strep medium (160 x g, 5 min, RT), mixed with mouse myeloma cells (Ag14, 10^8 cells per fusion) and washed twice with RPMI/pen-strep by centrifugation at 900 rpm for 5 min. Supernatant was removed carefully and 1 ml of polyethylene glycol 1500 (37°C) was drop-wise added over a time period of 2 min. This was followed by slow addition of 10 ml RPMI/pen-strep medium (37°C) over a time period of 10 min. Cells were then seeded into 16 or 15 96-well plates and fed with selection medium

containing hypoxanthine-aminopterin-thymidine (HAT) that enabled only fused hybrid cells to survive until screening.

2.2.2.3 mCLEC-2 Fc-fusion protein

For cloning of the extracellular domain of mouse CLEC-2, RNA from mouse bone marrow was isolated using the RNeasy Mini Kit (Qiagen, Hilden, Germany) according to the manufacturer's protocol and reverse transcription was performed (Titan One Tube RT-PCR-Kit, Roche, Ingelheim, Germany). 100 ng RNA was used as a template and the oligonucleotide AA <u>CTC GAG</u> ACA CAG CAA AAG TAT CTA (*Xho*I restriction site underlined) and AA <u>GGA TCC</u> AGC AGT TTG TCC ACT CTT (*Bam*HI restriction site underlined) as the forward and reverse primer, respectively. The PCR-product was purified using a QIAquick gel extraction kit (Qiagen, Hilden, Germany) digested with *Xho*I and *Bam*HI enzymes, purified again and ligated to the Signal pIg plus vector containing the human immunoglobulin Fc-domain. The ligation mixture was transformed into *E. coli* DH5α cells. The obtained construct was verified by restriction enzyme digestion and DNA-sequencing. This work had been performed during my diploma thesis in the same laboratory[33]. HEK 293 cells were transfected with the construct as described above.

2.2.2.4 Screening of hybridoma clones by ELISA

To detect hybridoma clones producing mAbs directed against the respective antigen (mCLEC-2), hybridoma supernatant was tested by Enzyme-linked immunosorbent assay (ELISA). Therefore, ELISA plates were coated o/n at 4°C with the mCLEC-2 Fc-fusion protein (5 µg/ml in coating buffer). After blocking with 5% BSA in H_2O for 1 h at 37°C, the hybridoma supernatant was added and left to incubate for 1 h at 37°C. ELISA plates were washed 3 times with washing buffer and left to incubate with the secondary antibody α-rat HRP (1:3,000) in washing buffer. After extensive washing, the ELISA was developed using TMB substrate. False-positive clones producing mAbs directed against the Fc-part of the fusion protein were detected using a second ELISA in parallel with an unspecific Fc-fusion protein generated in our laboratory.

2.2.2.5 Screening of hybridoma clones by flow cytometry

To detect hybridoma clones producing mAbs against the respective antigen (mCLEC-2) by flow cytometry, a 1:1 mixture of resting and thrombin-activated platelets (10^6) was incubated with 100 µl of the hybridoma supernatant for 15 min at 37°C. To prepare this mixture, washed platelets were divided into two parts. One part was left untreated and the other was activated by thrombin (0.2 U/ml; 5 min, 37°C). Samples were then washed once with 500 µl PBS (2,800 rpm, 10 min) and stained with FITC-conjugated rabbit α-rat Ig for 15 min at 37°C. Samples were finally analyzed on a FACSCalibur (Becton Dickinson, Heidelberg, Germany).

Positive hybridoma clones were further cultured at 37°C and 5% CO_2 and allowed to adapt to HAT-free RPMI/pen-strep/ medium with 10% fetal calf serum.

2.2.2.6 Large-scale production of antibodies

Positive hybridoma clones were subcloned twice and allowed to adapt to FCS-free medium (Panserin 410) in tissue culture flasks (T175). Positive hybridoma clones that stably expressed the antibodies were cultured at 37°C and 5% CO_2 until 4 l of medium containing the secreted antibody were collected. The medium was sterile filtered and approximately 20 mg antibody was purified from the medium via affinity chromatography using an immobilized protein G-column. Bound antibodies were eluted from the column using elution buffer and collected into supplied neutralization buffer to prevent precipitation of the antibody. Eluted antibodies were dialyzed o/n at 4°C against PBS.

2.2.2.7 Determination of isotype subclass

To determine the Ig isotype subclass of the purified antibodies Rat Immunoglobulin Isotyping ELISA kit was used according to the manufacturer's instructions. Briefly, 96-well ELISA plates were coated with different isotype-specific monoclonal mouse α-rat Ig antibodies (1:50 in coating buffer) o/n at 4°C and after 30 min blocking, antibodies to be analyzed were added (1 h, 37°C). Plates were washed and subsequently incubated for 1 h with AP-conjugated antibodies (1:100, 37°C). After several washing steps, Sigma104 substrate was added to each well and absorbance at 405 nm was recorded on ELISA reader (Thermo Scientific Multiskan Ascent).

2.2.3 Modification of antibodies

2.2.3.1 Preparation of Fab-fragments using papain

Whole IgG (3 mg) was dialyzed o/n against digestion buffer at 4°C. The antibody was then concentrated using a concentrator tube (VivaSpin®, exclusion size 10 kDa) by centrifugation at 4,000 rpm until a volume of 0.5-1.0 ml was reached (~10 min). To generate fragment antigen-binding (Fab-fragments) of antibodies, dialyzed IgG was mixed with digestion buffer and immobilized papain (washed twice with digestion buffer) in the ratio of 1:1:1 and left to incubate at 37°C for 4-6 h under shaking conditions. To test the efficacy of the digestion, samples (20 µl) were taken at different time points (0, 1, 2, 4, and 6 h), mixed with 20 µl non-reducing sample buffer and separated by SDS-PAGE (15%). To visualize the protein bands, the gel was coomassie-stained and destained. If the digestion was not complete, incubation was prolonged for further 2-4 h. The antibody was then dialyzed o/n against PBS at 4°C and the preparations were then applied to an immobilized protein A-column followed by an immobilized protein G-column to remove Fc-fragments and undigested IgG. Samples (20 µl) were taken before and after the clearing process, mixed with 20 µl non-reducing sample

buffer and separated by SDS-PAGE (15%). Finally, low-endotoxin BSA (0.2% f.c.) was added to the Fab-fragments.

2.2.3.2 Preparation of Fab$_2$-fragments using pepsin

To generate Fab$_2$-fragments, dialyzed IgG was mixed with digestion buffer and immobilized pepsin (washed twice with digestion buffer) in the ratio of 1:1:1 and left to incubate at 37°C for 48 h under shaking conditions. Samples (20 µl) were taken at 0, 6, 24, and 48 h, mixed with 20 µl non-reducing sample buffer and separated by SDS-PAGE (15%). Fab$_2$-fragments were purified as described above using an immobilized protein A-column followed by an immobilized protein G-column.

2.2.3.3 Preparation of Fab$_2$- and Fab-fragments via size chromatography

To generate Fab$_2$-fragments, concentrated and dialyzed IgG (4.0 mg/ml) in 0.1 mol/l sodium citrate buffer was incubated with immobilized pepsin in the ratio of 5:1 and left to incubate at 37°C for 4 h under shaking conditions. For size chromatography, samples were dialyzed against Superdex 200 column buffer and pH was adjusted to pH 7.2. Then, the digested solution was added to a Superdex 200 column with a flow rate of 2.0 ml/min (~25 cm/h). Fractions were collected and tested on SDS-PAGE (15%) for sufficient digestion and purity. The Fab$_2$ fractions were concentrated by centrifugation using a concentrator tube (VivaSpin$^®$, exclusion size 10 kDa), sterile filtrated and stored at -20°C until use or further digestion to Fab-fragments.

For generation of Fab-fragments, Fab$_2$-fragments (1 mg/ml) were dialyzed against TRIS/HCl (50 mmol/l, pH 8.0) o/n at 4°C. For digestion 10mmol/l DL-dithiothreitol were added and samples were incubated for 30 min at 37°C followed by incubation with 20 mmol/l iodacetamide at 37°C for 30 min. The digested Fab-fragments were added to a Superdex 200 column with a flow rate of 2.0 ml/min (~25 cm/h) and fractions were collected and tested on SDS-PAGE (15%) for sufficient digestion and purity. The Fab fractions were concentrated by centrifugation, sterile filtrated and stored at -20°C until use.

2.2.3.4 Alexa Fluor 488 labeling

Affinity purified antibodies were Alexa Fluor 488-labeled to a fluorophore/protein-ratio of approximately 3:1. The purified antibody (4 mg) was dialyzed against coupling buffer o/n at 4°C. Alexa Fluor 488 NHS-ester was dissolved in anhydrous DMSO to a final concentration of 1 mg/ml. This solution was added to the antibody and left to incubate at RT for 2 h. The reaction was stopped by addition of 100 µl of 1 M NH$_4$Cl. Alexa Fluor 488-labeled antibody was separated from the uncoupled fluorophore by gel filtration on a PD-10 column.

2.2.3.5 FITC labeling

Affinity purified antibodies were FITC-labeled to a fluorescein/protein-ratio of approximately 3:1. The purified antibody (4 mg) was dialyzed against coupling buffer o/n at 4°C. FITC was dissolved in anhydrous DMSO to a final concentration of 1 mg/ml. This solution was added to the antibody and left to incubate at 4°C o/n. The reaction was then stopped by addition of 100 µl of 1 M NH_4Cl. FITC-labeled antibody was separated from the uncoupled FITC by gel filtration on a PD-10 column.

2.2.4 Mouse treatment with antibodies

To deplete mice from the CLEC-2 receptor, adult mice received 200 µg of the antibody INU1 (~8 µg/g body weight) intravenously 5-6 days prior to experiments, if not other stated. For intravital microscopy of thrombus formation in $FeCl_3$-injured mesenteric arterioles, mice received 100 µg of the antibody INU1 intraperitoneally 5-6 days prior to experiments. To deplete mice from the GPVI receptor, adult mice received 100 µg of the antibody JAQ1 intravenously 5-6 days prior to experiments, if not other stated. For intravital microscopy of thrombus formation in $FeCl_3$-injured mesenteric arterioles, mice received 75 µg of the antibody JAQ1 intraperitoneally 5-6 days prior to experiments.

2.2.5 Mouse genotyping using flow cytometry

Gp6$^{-/-}$ mice were generated by Markus Bender as described in[106] and Bender M, May F *et al.*, (manuscript in preparation). Genotyping of the mice was performed via flow cytometry. For this purpose, 50 µl of 1:20 diluted whole mouse blood were incubated with the α-GPVI antibody JAQ1 in saturating concentrations for 15 min at RT and analyzed on a FACSCalibur (Becton Dickinson, Heidelberg, Germany).

2.2.6 Immunoprecipitation and immunoblotting

2.2.6.1 Immunoprecipitation

For precipitation of surface receptors, washed platelets (10^8) were prepared and surface proteins were labeled with EZ-Link sulfo-NHS-LC-biotin as described below. After effective biotinylation, platelets were solubilized in 1 ml lysis buffer. Cell debris were removed by centrifugation (15,000x *g*, 10 min). Following pre-clearing (8 h), 10 µg mAb were added to 25 µl protein G-Sepharose and precipitation was carried out o/n at 4°C. Samples were separated on SDS-PAGE (12%) along with a molecular weight marker and transferred onto a polyvinylidene difluoride (PVDF) membrane. The membrane was incubated with streptavidin-horseradish peroxidase (1 µg/ml) for 1 h after blocking. After extensive washing (4x 15 min), biotinylated proteins were visualized by ECL.

2.2.6.2 Immunoblotting

For western blot analysis, prp was prepared as described and centrifuged at 1,500 rpm for 5 min. Platelets were washed twice in PBS containing 5 mM EDTA. The platelet pellet was resuspended in IP buffer containing protease inhibitors to a final concentration of 500,000 platelets/µl and Igepal was added to 1% f.c.. After incubation for 10 min at 4°C and centrifugation at 14,000 rpm for 5 min, the supernatant was mixed with an equal amount of 2x SDS sample buffer and incubated at 95°C for 5 min. Samples were separated by 12 or 15% SDS-PAGE and transferred onto a PVDF membrane. To prevent non-specific antibody binding, membranes were blocked in 5% fat-free milk or 5% BSA dissolved in washing buffer for 2 h at RT or o/n at 4°C. Membranes were incubated with the required primary antibody (5 µg/ml) o/n with gentle shaking at 4°C. Afterwards, membranes were washed three times with washing buffer for 15 min at RT. Next, membranes were incubated with appropriate HRP-labeled secondary antibodies for 1 h at RT. After three washing steps, proteins were visualized by ECL.

2.2.6.3 Tyrosin phosphorylation assay

For tyrosine phosphorylation studies, 0.7×10^6 platelets/µl were activated with 1 µg/ml convulxin, 0.24 µg/ml rhodocytin or 20 µg/ml INU1 antibody under constant stirring conditions (1,000 rpm) at 37°C. Stimulation was stopped by the addition of an equal volume ice-cold lysis buffer after the indicated time points. For whole-cell tyrosine-phosphorylation, 4x NuPage sample buffer (Invitrogen) was added. Samples were incubated at 70°C for 10 min and separated by SDS-PAGE on 4-12% NuPage Bis-Tris gradient gels under reducing conditions followed by transfer onto a PVDF membrane. Membranes were blocked for 1 h at RT in 5% BSA in PBS and then incubated with the primary α-phosphotyrosine antibody 4G10 o/n at 4°C. The membranes were then washed 4x 15 min in washing buffer before incubation with secondary α-mouse horseradish peroxidase-conjugated antibody in washing buffer (1:2,000). Following extensive washing, proteins were visualized by ECL.

2.2.7 *In vitro* analysis of platelet function

2.2.7.1 Platelet preparation and washing

Mice were bled under ether or isofluran anesthesia from the retroorbital plexus. 700 µl blood were collected in a reaction tube containing either 300 µl heparin in TBS (20 U/ml, pH 7.3) or 300 µl acid citrate dextrose (ACD). Blood was centrifuged at 1,800 rpm for 5 min at RT. Supernatant and buffy coat were transferred into a new tube and centrifuged at 800 rpm for 6 min at RT to obtain platelet rich plasma (prp). To prepare washed platelets, prp was centrifuged at 2,500 rpm for 5 min at RT and the pellet was resuspended in 1 ml Ca^{2+}-free Tyrode's buffer containing apyrase (0.02 U/ml) and PGI_2 (0.1 µg/ml). After 10 min incubation

at 37°C the sample was centrifuged at 2,500 rpm for 5 min. After a second washing step, the platelet pellet was resuspended in the appropriate volume of Tyrode's buffer containing apyrase (0.02 U/ml, 500,000 platelets/µl) and left to incubate for at least 30 min at 37°C before analysis.

2.2.7.2   Platelet counting

For determination of platelet count and size, 100 µl blood were drawn from the retroorbital plexus of anesthetized mice using heparinized microcapillaries and collected into a reaction tube containing 100 µl heparin in TBS (20 U/ml, pH 7.3). Platelet count and size were determined using a Sysmex KX-21N automated hematology analyzer (Sysmex Corp., Kobe, Japan).

2.2.7.3   Biotinylation of platelet surface receptors

To biotinylate platelet surface receptors, washed platelets (in PBS/EDTA, $2x10^9$ platelets/ml) were incubated in PBS containing 5 mM EDTA with EZ-link sulfo-NHS-LC-biotin (f.c. 100 µg/ml) rotating for 10 min at RT. Reaction was stopped by addition of Tris buffer (f.c. 10 µM). The sample was centrifuged at 2,200 rpm for 5 min and the platelet pellet was resuspended in Tyrode's buffer with 2 mM Ca^{2+} containing apyrase (0.02 U/ml) and PGI_2 (0.1 µg/ml). To test for the efficacy of the biotinylation, a platelet sample (1:20 diluted in PBS; 50 µl) was incubated with FITC-labeled streptavidin (1.5 µg/ml; 10 min, RT). The reaction was stopped by the addition of 500 µl PBS and samples were analyzed immediately by flow cytometry.

2.2.7.4   Aggregometry

To determine platelet aggregation, light transmission was measured using washed platelets in Tyrode's buffer without Ca^{2+} adjusted to a concentration of $0.3x10^8$ platelets/ml. Alternatively, heparinized prp was used and diluted 1:3 in Tyrode's buffer. For determination of aggregation, agonists or reagents (100-fold concentrated) were added and light transmission was recorded over 10 min on a Fibrintimer 4 channel aggregometer (Apact 4-channel optical aggregation system, APACT, Hamburg, Germany). For calibration, Tyrode's buffer (for washed platelets) or 1:3-diluted plasma (for prp) was set as 100% aggregation and washed platelet suspension or prp was set as 0% aggregation. For activation with thrombin, washed platelets were diluted in Tyrode's buffer containing 2 mM Ca^{2+}, for all other agonists platelets were diluted in the same buffer in presence of 70 µg/ml human fibrinogen.

2.2.7.5   Flow cytometry

For determination of basal glycoprotein expression levels, platelets ($1x10^6$) were stained for 10 min at RT with saturating amounts of fluorophore-conjugated antibodies. The reaction was stopped by addition of 500 µl PBS, and samples were analyzed directly on a

FACSCalibur instrument (Becton Dickinson, Heidelberg, Germany). For activation studies, platelets were activated with the indicated agonists or reagents for 15 min at RT in the presence of saturating amounts of phycoerythrin (PE)-coupled JON/A and fluorescein isothiocyanate (FITC)-coupled α-P-selectin antibody. The reaction was stopped by addition of 500 µl PBS and samples were analyzed. For a two-color staining, the following settings were used:

Detectors/Amps:

Parameter	Detector	Voltage
P1	FSC	E01
P2	SSC	380
P3	Fl1	650
P4	Fl2	580
P5	Fl3	150

Threshold:

Value	Parameter
253	FSC-H
52	SSC-H
52	Fl1-H
52	Fl2-H
52	Fl3-H

Compensation:

Fl1	2.4% of Fl2
Fl2	7.0% of Fl1
Fl2	0% of Fl3
Fl3	0% of Fl2

2.2.7.6 Immunofluorescent microscopy of platelets

Washed platelets were fixed in PHEM buffer containing 1% PFA for 20 min at 4°C, blocked with 5% BSA for 2 h at 37°C, and stained with 1:25 INU1-Alexa Fluor 488 and 1:200 phalloidin-rhodamine for 2 h at 37°C. Samples were washed with PBS and mounted using ProLong Antifade reagent (Invitrogen, Karlsruhe, Germany). For permeablization the same procedure was followed using PHEM buffer containing 1% PFA and 1% NP40. Samples were visualized using a Leica SP5 confocal microscope with 100x oil objective (Leica Microsystems, Mannheim, Germany).

2.2.7.7 Measurement of ATP release

Washed platelets were adjusted to a concentration of $0.4 \times 10^6/\mu l$ in Tyrode's buffer. For activation, platelets were incubated with the indicated agonists for 2 min at 37°C under stirring conditions (1,000 rpm). Following activation, EDTA (3 mM f.c.) and formaldehyde (0.1% f.c.) were added and platelets were fixed for 2 h. Platelets were then centrifuged for 1 min at 13,000 rpm and 100 µl supernatant were added to 100 µl absolute ethanol. Samples were stored at -20°C until use. Levels of ATP in 12.5 µl sample were quantified using a bioluminescence assay kit according to the manufacturer's instructions and a Fluostar Optima Luminometer (BMG Lab Technologies, Germany).

2.2.7.8 Adhesion under flow conditions

Rectangular coverslips (24 x 60 mm) were coated with 0.2 mg/ml fibrillar type I collagen (Horm, Nycomed) o/n at 37°C and blocked for 1 h with 1% BSA in H_2O. Blood (700 µl) was collected into 300 µl heparin (20 U/ml in TBS, pH 7.3) or ACD-buffer (for studies under non-anticoagulated conditions). Platelets were labeled with a Dylight-488 conjugated α-GPIX Ig derivative (0.2 µg/ml) for 5 min at 37°C. Whole blood was diluted 2:1 in Tyrode's buffer containing Ca^{2+} and filled into a 1 ml syringe. Transparent flow chambers with a slit depth of 50 µm, equipped with the coated coverslips, were connected to the syringe filled with diluted whole blood. Perfusion was performed using a pulse-free pump under high shear stress equivalent to a wall shear rate of 1,000 sec^{-1} or 1,700 sec^{-1} (for 4 min). Thereafter, coverslips were washed for 1 min by perfusion with Tyrode's buffer at the same shear stress and phase-contrast and fluorescent images were recorded from at least five different microscopic fields (40x objective). Image analysis was performed off-line using MetaVue® software. Thrombus formation was expressed as the mean percentage of total area covered by thrombi and as the mean integrated fluorescence intensity per mm^2.

For studies determining the binding of platelets to vWF under flow conditions, flow adhesion was performed as described. Cover slips were coated with human α-vWF antibody at 37°C o/n, washed with PBS, incubated with 100 µl murine serum obtained from control mice and blocked for 1 h with 1% BSA in H_2O. Adhesion of platelets to bound vWF was determined 90 sec after perfusion of the slide.

2.2.8 *In vivo* analysis of platelet function

2.2.8.1 Tail bleeding time assay

Mice were anesthetized by intraperitoneally injection of the substances dormitor, dormicum and fentanyl, and a 1 mm segment of the tail tip was ablated with a scalpel. Tail bleeding was monitored by gently absorbing the drop of blood with a filter paper in 20 sec intervals without interfering with the wound site. When no blood was observed on the paper, bleeding was

determined to have ceased. The experiment was manually stopped after 20 min by cauterization.

Alternatively, tail bleeding times were determined in 37°C warm saline (0.9% NaCl). Upon amputation, the tail tip was placed in a plastic tube containing 4 ml saline, bleeding was observed and determined to have ceased when stopped for >1 min. Lost blood volume was determined via weight against a saline filled reference tube and increased weight of the tube was multiplied by the density of blood.

2.2.8.2 Intravital microscopy of thrombus formation in FeCl₃-injured mesenteric arterioles

Mice (4-5 weeks of age, weight 15-18 g) were anesthetized with 2.5% avertin and the mesentery was exteriorized through a midline abdominal incision. Arterioles (35-60 µm in diameter) were visualized with a Zeiss Axiovert 200 inverted microscope (10x objective) equipped with a 100-W HBO fluorescent lamp source, and a CoolSNAP-EZ camera (Visitron, Munich, Germany). Digital images were recorded and analyzed off-line using MetaVue® software. Injury was induced by topical application of a 3 mm² filter paper saturated with $FeCl_3$ (20%). Adhesion and aggregation of fluorescently labeled platelets (Dylight-488 conjugated α-GPIX Ig derivative) in arterioles was monitored for 40 min or until complete occlusion occurred (blood flow stopped for >1 min). This work was performed by Ina Hagedorn in the group of Prof. Bernhard Nieswandt.

2.2.8.3 Intravital microscopy of thrombus formation in the abdominal aorta

To open the abdominal cavity of anesthetized mice (~6 weeks of age), a longitudinal midline incision was performed and the abdominal aorta exposed. A Doppler ultrasonic flow probe (Transonic Systems, New York, USA) was placed around the aorta and thrombosis was induced by mechanical injury with a single firm compression (5 sec) of forceps upstream of the flow probe. Blood flow was monitored until complete occlusion occurred or 30 min had elapsed. This work was performed by Ina Hagedorn in the group of Prof. Bernhard Nieswandt.

2.2.8.4 Transient middle cerebral artery occlusion model (tMCAO)

Experiments were conducted on 6-8 weeks old male C57Bl/6J mice according to published recommendations for research in mechanism-driven basic stroke studies[107]. Transient middle cerebral artery occlusion (tMCAO) was induced under inhalation anesthesia using the intraluminal filament (6021PK10; Doccol Company) technique[83]. After 60 min, the filament was withdrawn to allow reperfusion. For measurements of ischemic brain (infarct) volume, animals were sacrificed 24 h after induction of tMCAO and brain sections were stained with 2% 2,3,5-triphenyltetrazolium chloride (TTC; Sigma-Aldrich, Germany). Brain infarct volumes were calculated and corrected for edema as described[83]. Neurological function and motor

function were assessed by two independent and blinded investigators 24 h after tMCAO. This work was performed by and in collaboration with Stefan Bräuninger in the group of Prof. Guido Stoll, Department of Neurology, University Hospital Würzburg.

2.2.9 Histology

2.2.9.1 Preparation of paraffin sections

Tissue from adult mice were washed in PBS and fixed o/n in PBS containing 4% PFA. Afterwards, organs were washed 3 times with PBS and were directly dehydrated and embedded in paraffin. Organs were cut using a Microm Cool Cut microtome (Thermo Scientific, Braunschweig, Germany) to prepare 5 µm thin sections.

2.2.9.2 Hematoxylin/eosin staining of paraffin sections

Sections were deparaffinated by two incubations in xylol (3 min each). Rehydration was carried out using decreasing ethanol concentrations (100, 96, 90, 80 and 70%) with two incubation steps in each solution and final 2 min incubation in deionized water. Next, sections were stained for 2 min with hematoxylin, followed by a 10 min washing step using running tab water and 2 min staining with 0.05% Eosin G. The sections were washed shortly and dehydration was carried out using the same ethanol concentrations and incubation times as described above in reversed order. Finally, sections were incubated twice in xylol for each 3 min, dried and mounted using Eukitt mounting medium. Samples were analyzed using a Leica DHI 4000B inverse microscope equipped with a Leica digital camera.

2.2.10 Data analysis

The results presented in this thesis are mean ± SD from at least three independent experiments per group, if not other stated. Differences between the groups were statistically analysed using the Mann-Whitney-U-test. p-values <0.05 were considered as statistically significant (*), $p < 0.01 = $ ** and $p < 0.001$ was taken as the level of highest significance (***).

3   Results

3.1   Characterization of the anti-mouse CLEC-2 antibody INU1

3.1.1   Generation of the monoclonal anti-mouse CLEC-2 antibody, INU1

Since at the beginning of this project no antibody directed against mouse CLEC-2 was commercially available, it was decided to generate such an antibody in our laboratory.

For this purpose in a previous work performed during my diploma thesis a recombinant murine CLEC-2 (mCLEC-2) Fc-fusion protein composed of the extracellular domain of mCLEC-2 and Fc-fragment of the human IgG was generated[33]. Therefore, the extracellular domain (CTLD) of the murine CLEC-2 protein was stably expressed in HEK 293 cells using a recombinant mammalian expression vector system termed Signal pIgplus-vector (Fig 3.1A). This vector system contained a constitutively active human cytomegalovirus (CMV) immediate early promoter upstream of the multiple cloning site (MCS). The promoter was followed by a DNA sequence, encoding the signal peptide of CD33, which facilitates the secretion of the produced mCLEC-2 Fc-fusion protein into the cell culture medium. Downstream of CD33, a sequence coding for the Fc-fragment of human IgG1 was inserted, which allows the purification of the protein from the cell culture medium. The Fc-fragment was followed by a neomycin resistance gene enabling negative selection of the transfected HEK 293 cell clones. The DNA sequence coding for the extracellular domain of murine CLEC-2 was ligated into the MCS in frame with the DNA sequences encoding the CD33 protein and the Fc-part of human IgG1 (Fig 3.1A). As CLEC-2 is expressed as a type II transmembrane receptor on the surface of human and mouse platelets[18], the extracellular domain of the native protein contains the carboxyl-terminus. However, in the finally expressed mCLEC-2 Fc-fusion protein the carboxyl-terminus of the extracellular domain is fused to the Fc-fragment of human IgG1 and thus the amino-terminus of the extracellular domain is freely exposed.

It was shown previously that HEK 293 cells were successfully transfected with the vector system encoding for the mCLEC-2 Fc-fusion protein, since bands of the expected size of the recombinant protein were detected by western blot analysis[33]. The transfected HEK 293 cell clone no.6 was used for large scale production in FCS-free medium and approximately 6 liters of medium containing the secreted mCLEC-2 Fc-fusion protein were collected. The secreted protein was then purified from the medium by affinity chromatography via an immobilized protein G-column (Fig 3.1B+C). In this process the Fc-part of the human IgG binds to protein G-Sepharose and thus the fusion protein is extracted from the medium. From the collected medium approximately 13 mg of protein were purified.

Due to the fact that the CLEC-2 protein is a type II receptor[18], it was difficult, if not impossible, to obtain correctly folded protein by the Fc-fusion protein system (Fig 3.1A+B).

Thus, to generate specific α-murine CLEC-2 antibodies mouse washed platelets were used for repeated immunizations of three rats.

Then, the antibody titer in the serum of immunized rats was tested by western blot analysis. For this purpose, blood was drawn from the tail vain; the serum was purified and tested on mouse platelet lysate. Serum from rat no. 2 produced a detectable band at the expected size of murine CLEC-2 (32-33 kDa) and showed the highest α-CLEC-2 antibody titer from all three tested rats (Fig 3.1D, middle). Therefore, the spleen of this rat was taken for the generation of antibody-producing hybridoma cells.
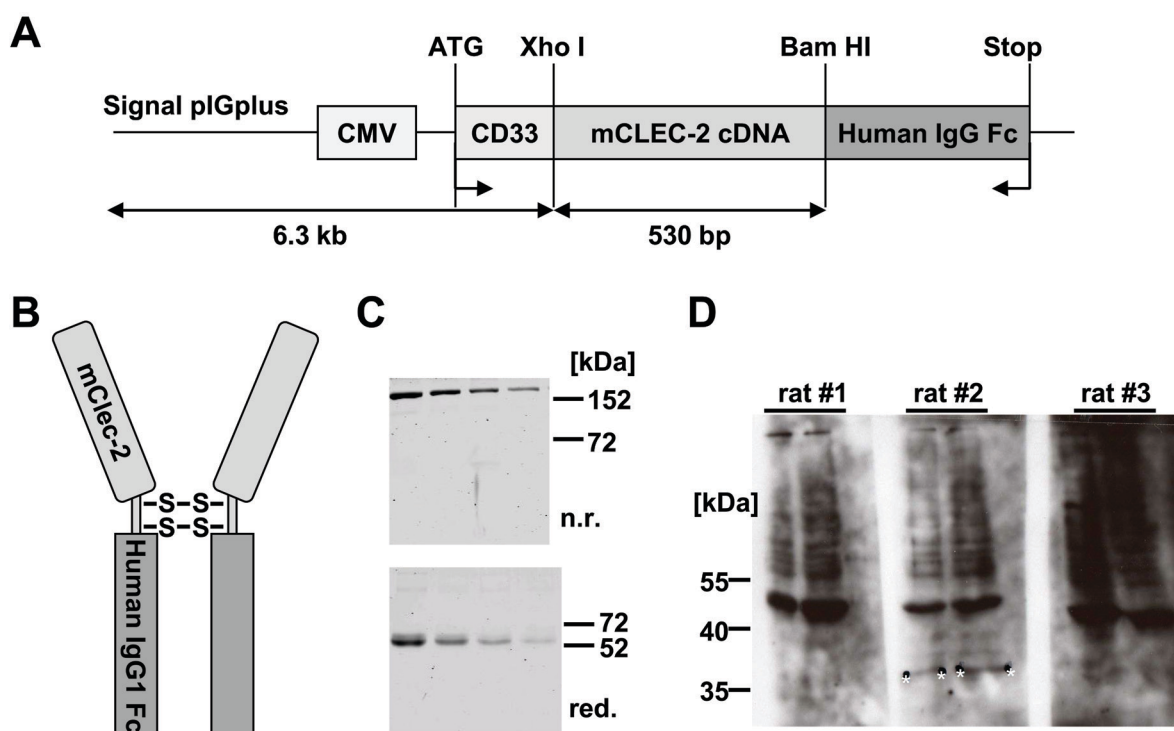

Fig 3.1 Generation of the mCLEC-2 Fc-fusion protein and antibody titer in rats. A. The Signal pIGplus vector map containing the extracellular domain of mCLEC-2 is depicted. B. Scheme of the expressed mCLEC-2 Fc-fusion protein. Upon translation in HEK 293 cells the CD33 signaling peptide is cleaved off and the protein is secreted as a dimer linked by disulfide bonds. C. The purified mCLEC-2 Fc-fusion protein has an apparent molecular weight of approximately 120-150 kDa under non-reducing (n.r., upper panel) and of 55-60 kDa under reducing conditions (red., lower panel). D. Antibody titer was tested on mouse platelet lysate (12% SDS-PAGE, red. conditions, rat serum 1:200 in PBS) and detected by α-rat IgG-HRP (1:300). A band of the expected molecular size of 32-33 kDa was observed upon incubation with serum from rat no. 2 (marked with stars, middle).

For generation of hybridoma cells producing α-CLEC-2 antibodies, the rat spleen cells were isolated to obtain a single cell suspension, mixed with mouse myeloma cells (Ag14) and fusion of the cells was induced by addition of PEG. Cells were then seeded into sixteen 96-well plates. In almost every well hybridoma clones were observed resulting in approximately 1,500 clones to be tested. To detect hybridoma clones producing antibodies directed against CLEC-2, medium of the cells was screened in an Enzyme-linked immunosorbent assay (ELISA) system using the generated mCLEC-2 Fc-fusion protein. By this method 180 positive clones were registered (data not shown). To identify false-positive clones that

non-specifically bound to the Fc-part of the fusion protein a second ELISA was performed in parallel where plates were coated with a different non-specific Fc-fusion protein generated in our laboratory. Out of the 180 positively tested clones only six clones were found to produce antibodies specifically directed against the extracellular part of the mCLEC-2 Fc-fusion protein (data not shown). Antibodies produced by these six clones were further tested by flow cytometry using mouse platelets. Therefore, a mixture of resting and thrombin-activated platelets (10^6) was incubated with the hybridoma supernatant containing the produced antibodies and after washing stained with a secondary FITC-conjugated rabbit α-rat IgG. Samples were analyzed on a FACSCalibur. Antibodies from all 6 clones specifically bound to platelets with a relatively high mean fluorescence intensity (MFI) of approximately 300 (data not shown). To obtain monoclonal antibodies, the positive hybridoma clones were subcloned twice. During this process only one clone (clone 11E9) stably expressed the antibody, whereas the other 5 clones lost the expression of the antibody. For large scale production of the antibody the hybridoma cell clone 11E9 was cultured in FCS-free medium and the antibody was purified from the medium by affinity chromatography via a protein G-column. Thus, a new and at that time point the only known rat monoclonal antibody (mAb) against mouse CLEC-2 was generated and termed INU1.

3.1.2 INU1 recognizes mouse CLEC-2 on platelets

The antibody INU1 was tested by western blot analysis using mouse platelet lysate. Unexpectedly, INU1 did not recognize CLEC-2 under these conditions indicating that the antibody binds to a three-dimensional epitope on the receptor that is lost under the denaturing conditions during SDS-PAGE (data not shown). However, FITC-conjugated INU1 specifically bound to mouse platelets as demonstrated in flow cytometry (Fig 3.2A). To test whether the antibody detected murine CLEC-2, immunoprecipitation was performed from surface-biotinylated mouse platelets. INU1 precipitated a protein of an apparent molecular weight of approximately 32-38 kDa under reducing and non-reducing conditions (Fig 3.2B), strongly indicating that the antibody was directed against murine CLEC-2 and demonstrating that the apparent molecular weight of mouse CLEC-2 is similar to its human homologue[18]. The specificity of INU1 for CLEC-2 was further confirmed by ELISA where it bound specifically to the extracellular domain of mCLEC-2 Fc-fusion protein, but not to a murine (m)GPVI-Fc fusion protein[82]. In contrast, in a control experiment the α-mouse GPVI antibody, JAQ1[66-67], bound to the mGPVI-Fc, but not to the mCLEC-2 Fc-fusion protein (Fig 3.2C). Furthermore, the subclass of the antibody INU1 was tested using Rat Immunoglobulin Isotyping ELISA kit and defined INU1 as a rat IgG1 of the subclass κ (data not shown).

Upon incubation of mouse platelets with INU1-FITC, a shape change visible as a characteristic shift in the FFC/SSC pattern was observed by flow cytometry indicating

activation of platelets (data not shown). To further analyze this phenomenon, INU1-IgG was incubated with mouse platelets at 37°C under stirring conditions in a standard aggregometer. Here, INU1 induced profound aggregation of mouse platelets. This response occurred in a dose-dependent manner that was evident as a decrease in the delay before the onset of aggregation (termed lag phase) rather than an increase in the maximal aggregation response (Fig 3.2D). A similar effect is known to occur upon activation with the CLEC-2-specific agonist rhodocytin (RC) on human and mouse platelets[14,45]. Furthermore, these results are in line with previous observations made on human platelets which were activated using polyclonal α-human CLEC-2 antibody[14]. Additionally, INU1-induced activation of platelets was associated with changes in tyrosine phosphorylation patterns of downstream signaling proteins that were comparable with those induced by rhodocytin demonstrating that the binding of INU1 to mouse platelets elicits profound signaling of the receptor (Fig 3.2E).
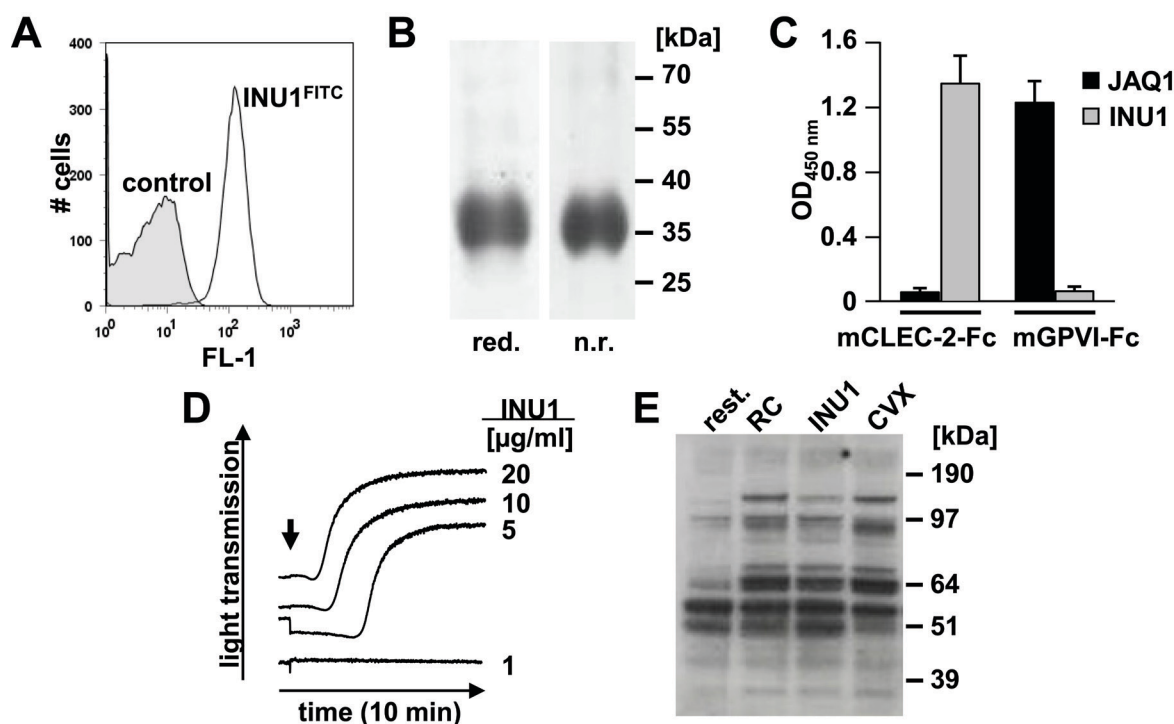

Fig 3.2 INU1 recognizes murine CLEC-2. A. Flow cytometric detection of CLEC-2. Mouse platelets were incubated with INU1-FITC (solid line) or an irrelevant rat IgG-FITC (shaded area). B. Immunoprecipitation of CLEC-2 from surface-biotinylated platelets with INU1 (10 µg/ml). Proteins were separated under reducing (red.) or non-reducing (n.r.) conditions and detected by streptavidin-HRP. C. Binding of INU1 to mCLEC-2 Fc-fusion protein was tested by ELISA. Binding of α-GPVI antibody JAQ1 to mGPVI-Fc fusion protein served as control. D. Washed platelets were incubated with the indicated concentrations of INU1 and light transmission was recorded on an aggregometer. E. Washed platelets (rest.= resting state) were stimulated with 0.24 µg/ml rhodocytin (RC), 20 µg/ml INU1 or 1 µg/ml convulxin (CVX) and lysed after 90 sec. Tyrosine phosphorylated proteins were visualized by probing with the phosphotyrosine-specific antibody 4G10, α-mouse-HRP and ECL. The results are representative of 3-4 individual experiments. (May F et al., *Blood*, 2009[104].)

3.1.3 INU1-alexa488 is suitable for immuno-fluorescent stainings on platelets

To further study the expression of CLEC-2, washed platelets were stained with INU1 coupled to the fluorophore Alexa Fluor 488 (INU1-Alexa Fluor 488) and analyzed by confocal microscopy (Leica SP5 confocal microscope, Leica Microsystems, Mannheim, Germany). As the platelets were not treated with detergents (non-permeabilized), CLEC-2 expression was observed only on the platelet membrane whereas no intracellular protein was detected (Fig 3.3A). In contrast, no fluorescent signal was detected upon staining of washed platelets from CLEC-2-depleted animals with the antibody suggesting the complete depletion of the receptor from the plasma membrane (data not shown). Additionally, platelets from control and INU1-treated mice were stained with INU1-Alexa Fluor 488 under permeabilizing conditions thus allowing the antibody to enter the cells. In control platelets, an intracellular fluorescence signal was observed as a dotted structure indicating the presence of the CLEC-2 protein in vesicles (Fig 3.3B). Interestingly, under this condition, in platelets from CLEC-2-depleted mice a residual fluorescence signal was observed intracellularly that was, however, of lower intensity when compared to controls (data not shown). This signal could be derived from the internalized receptor upon down-regulation or from splice variants of CLEC-2 that have been described to be expressed intracellularly[27].
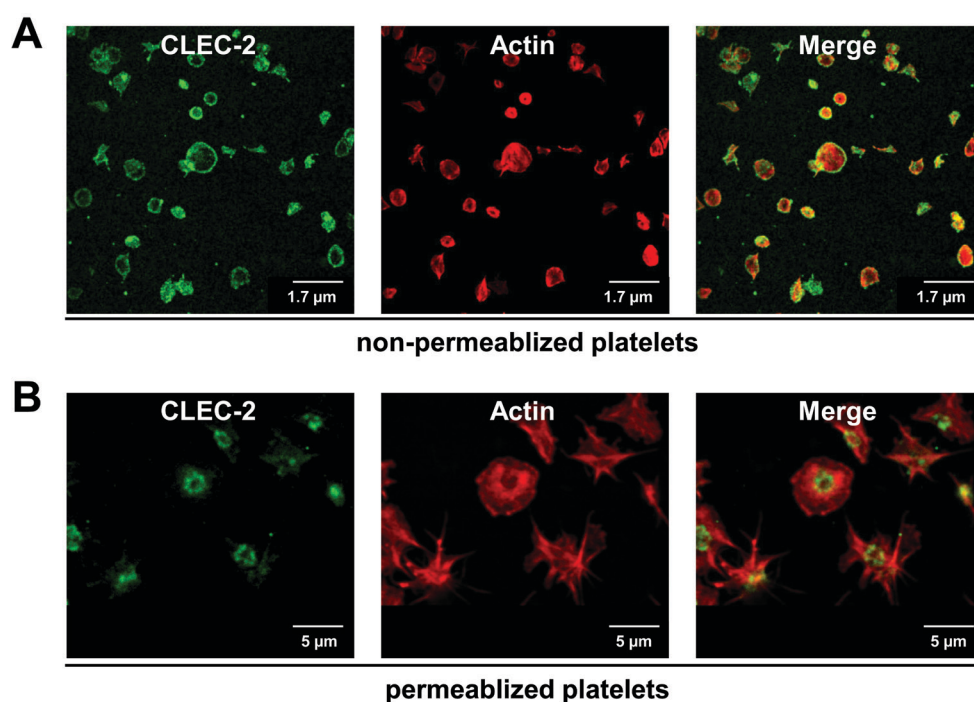

Fig 3.3 Confocal images of platelets stained with INU1-Alexa Fluor 488. Washed platelets of control mice were fixed and stained with INU1-Alexa Fluor 488 (CLEC-2, left) and phalloidin-rhodamine (actin, middle). Merged images are given (right). A. Staining of non-permeabilized platelets. Note the ring-like structure of CLEC-2 expression on the platelet surface. B. Staining of permeabilized platelets. INU1 detected CLEC-2 protein in intracellular vesicles in platelets whereas less protein expression was detected on the platelet surface due to the conditions used in sample preparation.

3.1.4 Analysis of CLEC-2 expression on immune cells

To test whether INU1 could detect CLEC-2 on murine immune cells, cells were isolated from murine spleen, lymph nodes and thymus. Furthermore, macrophages were obtained from peritoneal lavage. Single cell suspensions were prepared, stained with INU1-FITC or the corresponding isotype control and analyzed by flow cytometry. The different cell populations were identified by light scatter characteristics in combination with specific staining of surface markers. These experiments were performed together with Timo Vögtle.

As described earlier, in our experimental settings CLEC-2 expression was detected on murine platelets (see also Fig 3.2A). However, INU1 did not stain both CD4$^+$ and CD8$^+$ cells as well as B cells (B220$^+$ cells) isolated from lymph nodes and spleen. Furthermore, CLEC-2 was not found on CD4$^+$/CD8$^+$ double-positive cells, the major cell population of the thymus, and also not on CD4$^-$/CD8$^-$ double-negative cells, which provide a small fraction of thymocytes by staining with INU1. Additionally, CLEC-2 expression was also not detected on peritoneal macrophages that were gated using the macrophage-specific marker F4/80 (Fig 3.4A). Interestingly, CLEC-2 has been reported to be expressed on mouse peripheral CD11b$^+$/Gr1$^+$ double-positive blood neutrophils by Kerrigan *et al.*[26]. To test whether the antibody INU1 could detect CLEC-2 under the same conditions on these cells, granulocytes were prepared from mouse blood and stained with the neutrophil-specific marker combination CD11b and Gr1. CD11b$^+$/Gr1$^+$ double-positive neutrophils represented a clearly defined population in the FSC/SSC dotplots, and therefore could be identified by FSC/SSC characteristics and CD11b expression in the following experiments (data not shown). Under these experimental settings, CLEC-2 expression was clearly detectable by INU1-FITC on neutrophils (Fig 3.4B, left) being in line with data shown by Kerrigan *et al.*[26].

In a next step, the CLEC-2 positive population was co-stained with the platelet-specific marker JON6-PE (14A3, α-integrin αIIbβ3) and very surprisingly the same population yielded positive MFI signals (Fig 3.4B, right) suggesting that the CLEC-2 signal was not derived from neutrophils but rather from platelets that were possibly captured by the immune cells. A compensation error was excluded since i) compensation was performed prior to each measurement and ii) the JON6-PE signal (14A3, FL-2) was also observed in the sample with the INU1-FITC (FL-1) negative isotype control. Also, the FACS dot plot data showed a direct correlation between the platelet-marker positive and the INU1-FITC positive cells. There were no platelet-marker positive but INU1-FITC negative cells observed and *vice versa*. In line with this observation, in further experiments a positive CLEC-2 signal was not consistently observed on neutrophils depending on the preparation of the sample but rather found to be decreased with reducing concentrations of platelets in the tested samples (data not shown). This further strengthened the hypothesis that the gated neutrophil population was contaminated with platelets.
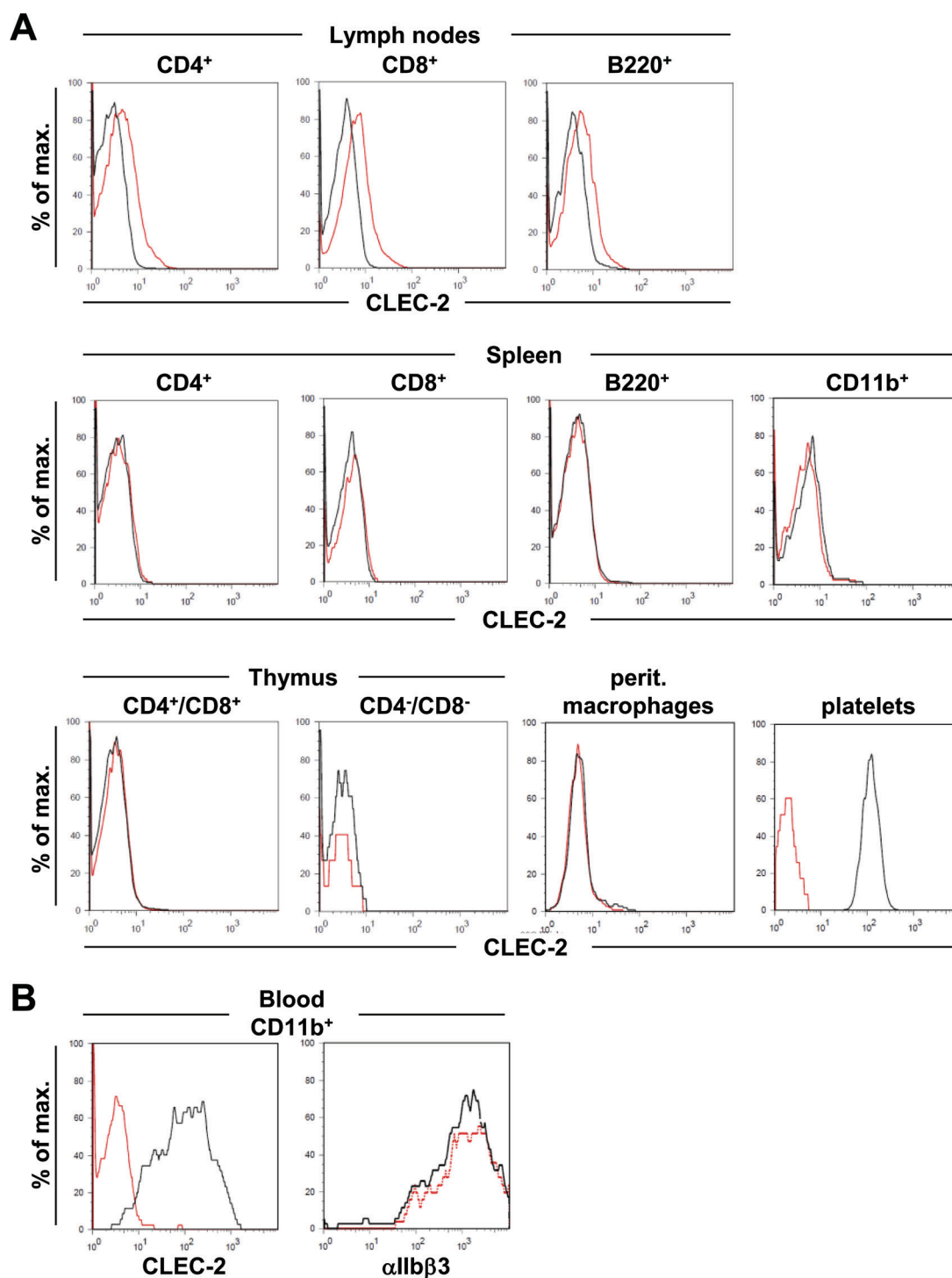
Fig 3.4 CLEC-2 expression on murine T cells, B cells, macrophages and granulocytes. CLEC-2 expression was qualitatively assessed by flow cytometry, using INU1-FITC (black line). FITC-labeled rat IgG without detectable specificity for mouse tissue served as isotype control (red line). A. INU1-FITC specifically detected CLEC-2 on murine platelets, but not on the tested murine immune cells. Peritoneal macrophages were gated by the specific F4/80 marker and B cells by B220. B. In two samples of peripheral blood cells neutrophils were gated using the marker CD11b. Left: INU1-FITC (black solid line) detected CLEC-2 on CD11b^{+} cells. FITC-labeled rat IgG without detectable specificity for mouse tissue served as isotype control (red line). Right: the platelet-specific marker JON6-PE (black line, $\alpha IIb\beta 3$) clearly detected platelets in the CLEC-2 positive neutrophil population. A compensation error was excluded as the JON6-PE signal was also observed in the sample labeled with the negative isotype control (dotted red line).

To analyze the discrepancies between results published by Kerrigan *et al.*[26] and our findings, splenic CD11b^{+} cells that were initially CLEC-2 negative (Fig 3.4A) were co-incubated with increasing concentrations of isolated resting platelets, stained with the appropriate markers, the isotype controls and INU1-FITC and directly analyzed via flow cytometry. Under these conditions, expression of CLEC-2 was only detectable when platelets were present in the sample and the MFI signals of INU1-FITC were found to be increasing with raising concentrations of co-incubated platelets (Timo Vögtle, personal communication). These results indicate that CLEC-2 is not expressed on peripheral immune cells in mice but that rather the CLEC-2 signal was attributed to platelets.

3.1.5 Fab-fragments of INU1 partially inhibit CLEC-2 function *in vitro*

To further characterize INU1, monovalent *fragment antigen-binding* (Fab)-fragments of the antibody (INU1-Fab) were prepared by enzymatic digestion of the full IgG using papain.

In contrast to INU1-IgG, INU1-Fab did not induce aggregation of mouse platelets at concentrations up to 20 µg/ml (Fig 3.5A), suggesting that dimerization or clustering of the CLEC-2 receptor is a critical prerequisite for INU1-IgG-mediated platelet activation. This was confirmed by cross-linking of the bound INU1-Fab using a secondary antibody (rabbit α-rat IgG) which induced robust platelet aggregation (Fig 3.5A). INU1-Fab (20 µg/ml) had no effect on the aggregation response to the stable TxA_2 analog U46619, to the GPVI agonist convulxin (CVX) or to thrombin. However, ADP-induced aggregation was consistently increased in the presence of INU1-Fab (83.53 ± 4.57% versus 58.76 ± 5.12% in control) (Fig 3.5B). In contrast, INU1-Fab had a significant inhibitory effect on rhodocytin-induced platelet aggregation at low and intermediate agonist concentrations (visible as a delay in the onset of aggregation) which was, however, overcome at high rhodocytin concentrations (Fig 3.5C). These results suggest that INU1 binds to an epitope on the CLEC-2 receptor that is at least partially overlapping with the rhodocytin binding site.
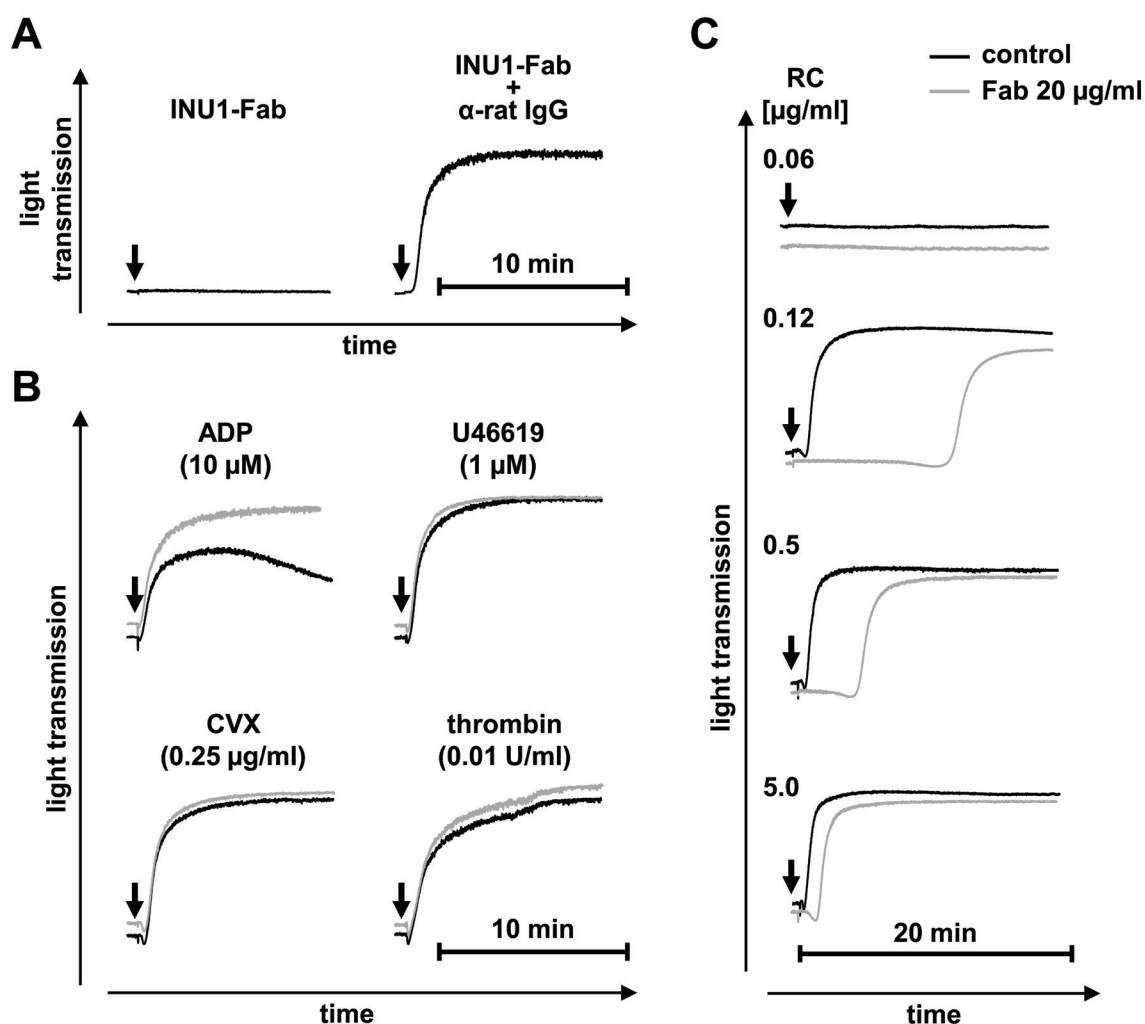
Fig 3.5 INU1-Fab partially inhibits CLEC-2 function *in vitro*. A. INU1-Fab (20 µg/ml) alone does not induce aggregation of washed control platelets, but elicits profound aggregation when cross-linked by addition of 20 µg/ml α-rat IgG. B+C. Washed control platelets were incubated with PBS (black line) or INU1-Fab (20 µg/ml, gray line) for 5 min at 37°C and then stimulated with the indicated agonists under stirring conditions. Light transmission was recorded on an aggregometer. The results are representative of 4 individual measurements. Abbreviations: RC= rhodocytin, ADP= adenosine diphosphate, CVX= convulxin. (May F *et al.*, *Blood*, 2009[104].)

3.1.6 INU1-IgG induces the loss of CLEC-2 in circulating platelets *in vivo*

To study the effect of INU1 on platelets *in vivo*, mice received 2 µg/g body weight (~50 µg/ mouse) of the antibody intravenously (i.v.) and circulating platelets were studied *ex vivo* at different time points after injection. Surprisingly, treatment of mice with INU1-IgG induced a transient thrombocytopenia in the animals with a maximal drop of platelet counts of more than 85% on day 1. Platelet counts returned back to normal 3-4 days (d) post injection (p.i.) and were observed to be slightly increased on d5 and 6 indicating an overshooting platelet production. Then, they remained on normal levels compared to controls for at least 6 more days (Fig 3.6A). Parallel analyses on an automated cell analyzer (Sysmex) yielded similar results (data not shown). In a preliminary set of experiments, thrombocytopenia was also observed upon injection of Fab-fragments of INU1 (2 µg/g body weight) (Fig 3.6A). Thus, it

was concluded that the observed thrombocytopenia was not Fc-dependent or caused by antibody-induced receptor dimerization. INU1-treated mice did not develop spontaneous bleeding for at least 3 weeks (data not shown).

To further analyze the mechanism of receptor down-regulation, plasma of INU1-IgG-treated mice was tested for free antibody by ELISA. Here, free INU1-IgG was detectable for approximately 2-3 days after treatment in plasma of the animals (data not shown). To further investigate the consequences of INU1-treatment *in vivo*, platelets from treated mice were isolated and analyzed. On days 1 and 3 p.i. of INU1-IgG (2 µg/g body weight), platelets from INU1-IgG- or INU1-Fab-treated mice were refractory towards rhodocytin (1 µg/ml) as revealed by flow cytometry (Fig 3.6B). However, the response was partially restored on d5 in a subpopulation of platelets and back to normal on d7 compared to controls (data not shown). To test whether this inhibitory effect was due to a blockade of the CLEC-2 receptor by the antibody, platelets were stained with a secondary FITC-conjugated α-rat IgG antibody. Remarkably, the secondary antibody failed to detect INU1-IgG (or INU1-Fab) on the surface of the cells on d1 and 3 p.i., whereas control platelets incubated *in vitro* with INU1-IgG or INU1-Fab yielded strong MFI signals (Fig 3.6C). Additionally, INU1-FITC did not bind to platelets from INU1-IgG- or INU1-Fab-treated mice on d1 and 3, whereas a subpopulation of the cells was stained on d5 and more than 90% were stained on d6 of mice that were treated with lower doses of the antibody (2 µg/g body weight) (Fig 3.6D). These results indicated that treatment with INU1 induced the loss of CLEC-2 in circulating platelets within 24 h. Furthermore, it was shown that the resulting thrombocytopenia was overcome by the production of new platelets completely lacking the receptor thus allowing to study mice with a CLEC-2 "knock-out like" phenotype for a defined period of time.

To study the functional consequences of CLEC-2 deficiency in more detail and to test whether a prolonged loss of the receptor could be achieved, mice received 8 µg/g body weight INU1-IgG i.v. (~200 µg per mouse). Interestingly, in these animals free INU1-IgG was detectable in plasma samples by ELISA up to 8 days after treatment (data not shown). Animals that had been subjected to the higher dose treatment also showed a transient thrombocytopenia and the kinetics of CLEC-2 loss were comparable with the effects caused by the lower dose treatment with 2 µg/g body weight (Fig 3.6A). However, importantly, CLEC-2 was not detectable on the surface of the cells for at least 6 days (Fig 3.6C-D).
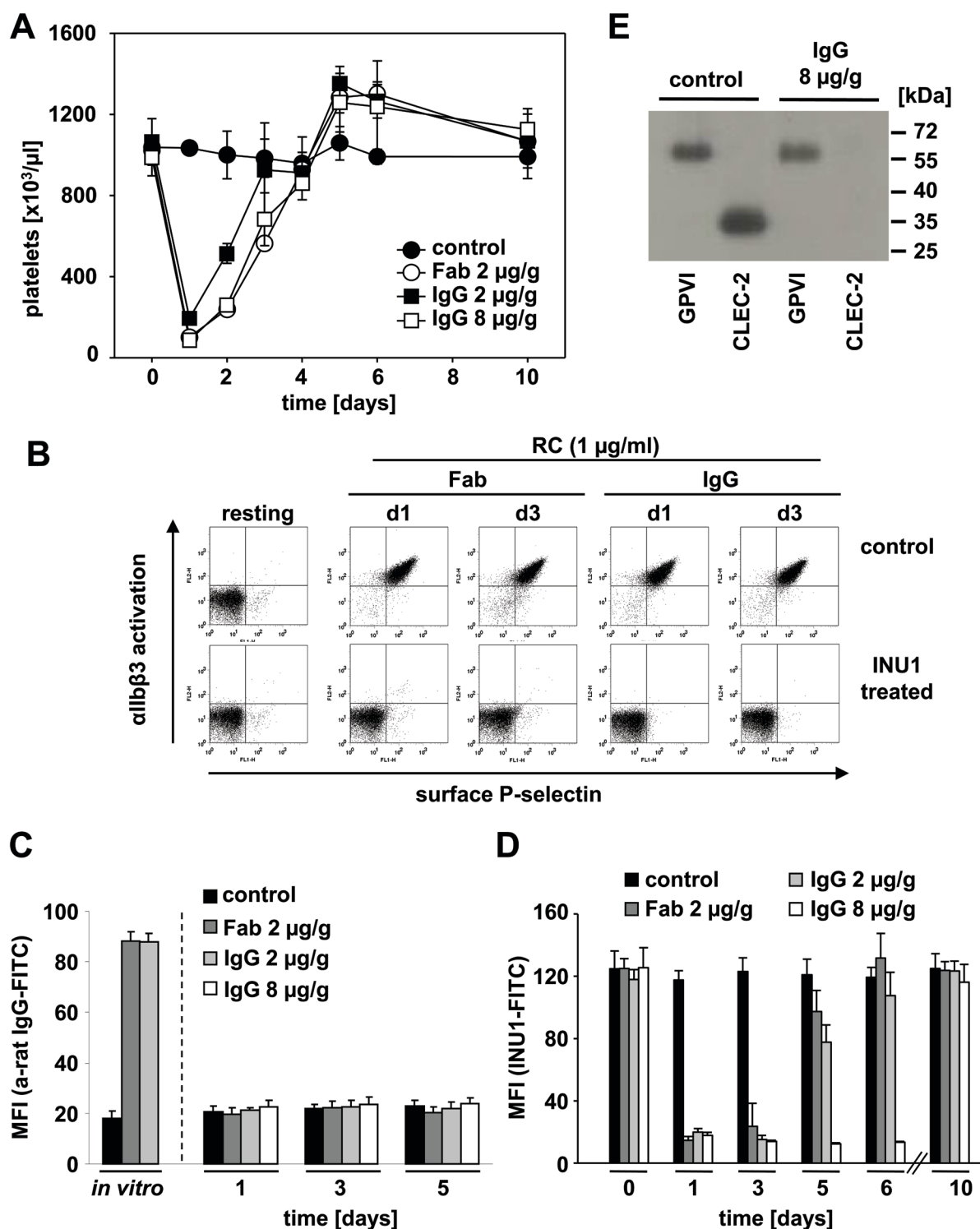
Fig 3.6 INU1 induces the loss of CLEC-2 in circulating platelets *in vivo*. Mice received the indicated amounts of INU1-IgG or INU1-Fab i.v.. A. Platelet counts were determined by flow cytometry at the indicated time points. Results are expressed as the mean platelet count ± SD for groups of each n=4 and are representative of 3 individual experiments. B. Two color flow cytometric analysis of integrin αIIbβ3 activation (JON/A-PE) and P-selectin exposure (FITC) in platelets from mice on d1 or d3 p.i.. Diluted whole blood was stimulated with 1 µg/ml rhodocytin (RC). The results are representative of 8 mice per group. C. Surface-bound IgG or Fab was detected by flow cytometry using α-rat IgG-FITC. Maximal binding was determined by incubating platelets from untreated mice with INU1-IgG or INU1-Fab (10 µg/ml) *in vitro* following staining with α-rat IgG-FITC. D. Binding of INU1-FITC to platelets from the indicated mice. E. Immunoprecipitation of CLEC-2 and GPVI from surface-biotinylated platelets from control and INU1 (8 µg/g b.w.)-treated mice on d5 under reducing conditions. (May F *et al.*, *Blood*, 2009[104].)

To further investigate whether other surface receptors of platelets were affected by the antibody treatment, flow cytometric analysis of basal surface expression levels of glycoproteins (GP) was performed on day 5 p.i.. Here, expression levels of all tested proteins such as GPVI, GPIb-V-IX, CD9, and integrins $\alpha IIb\beta 3$ and $\alpha 2\beta 1$ were unaltered compared to controls (Tab 3.1). This was also demonstrated by immunoprecipitation experiments performed on d5 after antibody injection which confirmed complete loss of CLEC-2, whereas other receptors such as GPVI were not affected (Fig 3.6E).

	control	INU1
HCT [%]	53.3 ± 1.76	48.7 ± 4.41
WBC [x10^6]	11.1 ± 1.19	11.05 ± 1.74
CLEC-2	119 ± 10	14 ± 1
GPIb	398 ± 5	391 ± 19
GPV	354± 5	364 ± 14
GPIX	550 ± 13	563 ± 20
CD9	1496 ± 27	1338 ± 66
GPVI	61 ± 3	56 ± 3
α2	76 ± 5	69 ± 1
β1	173 ± 11	165 ± 12
αIIβ3	888 ± 40	854 ± 51
plt. size	403 ±14	456 ± 33

Tab 3.1 Hematology and platelet glycoprotein expression in control and INU1-treated mice. Hematocrit (HCT) in per cent and white blood cell counts (WBC) per ml for control and INU1-treated mice (d5) were measured by an automated blood cell analyzer. Expression of glycoproteins on the platelet surface and platelet (plt.) size was determined by flow cytometry. Diluted whole blood from the indicated mice was incubated with FITC-labeled antibodies at saturating concentrations and platelets were analyzed directly on a FACSCalibur. Mean platelet size is given as mean FSC and was determined by FSC characteristics. Results are expressed as mean fluorescence intensity ± SD for n=6 mice per group. (May F *et al.*, *Blood* 2009.[104])

Furthermore, the hematocrit and white blood cell counts were not significantly different between control and INU1-treated mice (Tab 3.1). As newly produced platelets were depleted of CLEC-2, it was assumed that the antibody INU1 not only targeted platelets but also megakaryocytes in the bone marrow. Indeed, CLEC-2 is expressed on megakaryocytes[18-19] and INU1 detected the receptor on isolated megakaryocytes from bone marrow of control animals but not from INU1-treated mice 60 min after treatment (data not shown).

3.1.7 CLEC-2-deficient platelets show an abolished response to rhodocytin but normal responses to classic agonists.

To test the effect of INU1-treatment on different signaling pathways in platelets, standard aggregometry assays were performed with CLEC-2-depleted and control platelets. The analyses showed that platelets from mice on d5 after INU1-treatment (8 µg/g body weight) were completely resistant to activation with rhodocytin at any concentration tested (up to

10 µg/ml), whereas responses to classic platelet agonists such as ADP, U46619, convulxin, collagen and thrombin were normal (Fig 3.7).
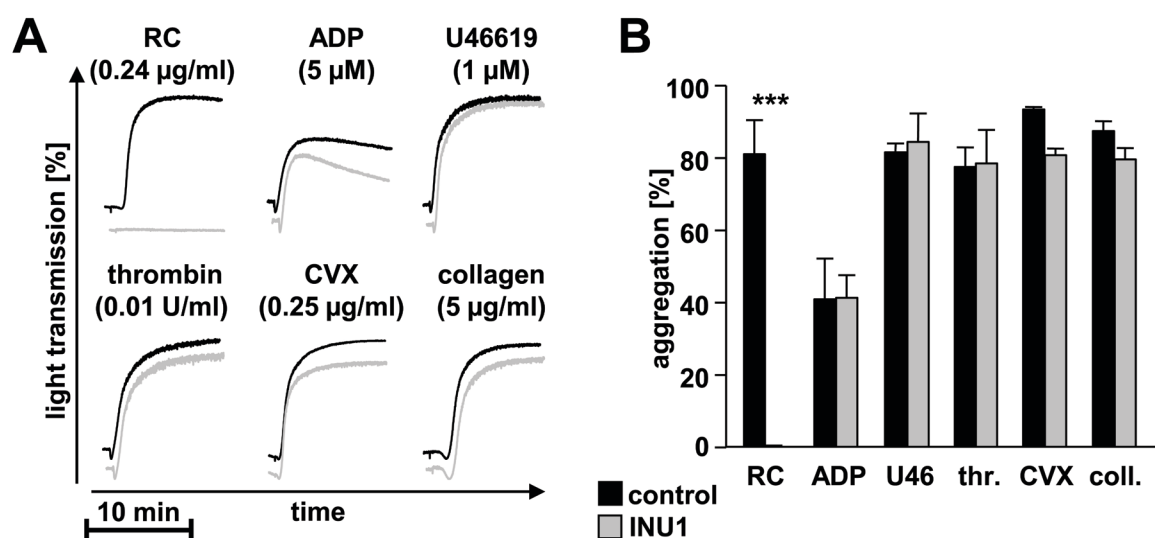

Fig 3.7 Activation of CLEC-2-deficient platelets in aggregometry. Mice were treated with vehicle (PBS) or 8 µg/g body weight INU1-IgG and platelets were analyzed on d5 p.i.. Washed platelets from control (black) or INU1-treated (gray) mice were stimulated with the indicated agonists and light transmission was recorded. The results are representative of 6 individual experiments. A. Representative light transmission curves. B. Bar graphs of results obtained by aggregometry. Agonist concentrations correspond to aggregometry curves in A. Abbreviations: RC= rhodocytin, ADP= adenosine diphosphate, U46= U46619, thr.= thrombin, CVX= convulxin. ***$p<0.001$. (May F *et al.*, *Blood*, 2009[104].)

Furthermore, flow cytometric analyses of integrin $\alpha IIb\beta 3$ activation and degranulation-dependent P-selectin exposure as a measure of the activation of platelets also confirmed that the INU1-induced CLEC-2 deficiency had no significant effect on other activation pathways induced by ADP, U46619, CVX or thrombin, whereas responses to rhodocytin were completely blunted as expected (Fig 3.8A+B). On d10 after INU1 injection of both high and low dose treatment, CLEC-2 expression (Fig 3.6D) and rhodocytin-induced responses (data not shown) were fully restored in all tested animals.

Together, these results demonstrate that INU1-induced CLEC-2 deficiency very specifically abolished one activation pathway in platelets while the other tested pathways were left intact. To further analyze whether INU1-treatment had an impact on dense granule release of platelets, thrombin- and CRP-induced ATP release from dense granules was determined. It was demonstrated that the ATP release was not significantly altered in platelets from INU1-treated mice compared to controls. This further confirmed that the antibody-induced loss of CLEC-2 had no general effect on the degranulation machinery of platelets (Fig 3.8C).
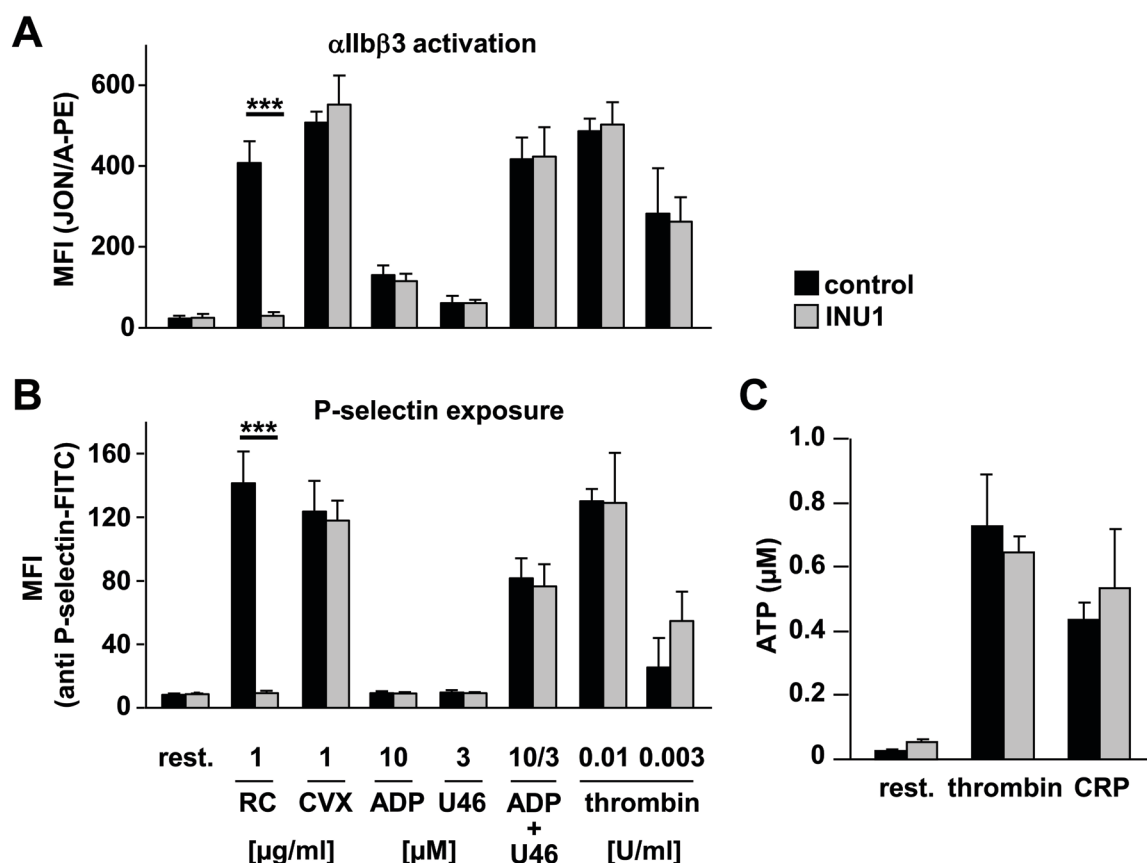
A

B

C

Fig 3.8 Activation of CLEC-2-deficient platelets in flow cytometry and measurement of released ATP. Mice were treated with vehicle (PBS, black) or 8 μg/g body weight INU1-IgG (gray) and washed platelets were analyzed on d5 p.i.. A. Flow cytometric analyses of αIIbβ3 integrin activation (JON/A-PE, upper panel) and B. degranulation-dependent P-selectin exposure (lower panel) in response to stimulation with the indicated agonists. Results are given as mean fluorescence intensities (MFI) ± SD of n=6 mice per group. C. Washed platelets were incubated for 2 min at 37°C with PBS (rest.), 0.1 U/ml thrombin or 10 μg/ml CRP and fixed. ATP present in the supernatant was measured using a luminometric assay according to the manufacturer's protocol. Results are given as mean ATP concentration (μM) ± SD (n=6 per group) and are representative of 2 individual experiments. Abbreviations: rest.= resting state, ATP= adenosine-5'-triphosphate, U46= U46619, CRP= collagen related peptide. ***$p<0.001$. (May F *et al.*, *Blood*, 2009[104].)

3.1.8 CLEC-2 is required for stable thrombus formation under flow

At sites of vascular injury, the signals generated by multiple platelet receptor-ligand interactions are integrated to ensure efficient platelet attachment and thrombus formation under flow conditions[7]. As a possible function of CLEC-2 in this process had not been assessed, we analyzed the ability of CLEC-2-deficient platelets to form thrombi under flow conditions. To do so, whole blood was perfused over a collagen-coated surface using a pulse-free pump. Under high shear conditions (1,700 sec^{-1}), control platelets adhered to collagen fibers and formed aggregates within 2 min that consistently grew into large thrombi by the end of the perfusion period of 4 min. In INU1-treated blood, platelets adhered to collagen, but, in marked contrast to the control, the subsequent formation of three-dimensional aggregates was severely impaired (Fig 3.9C). During the entire perfusion time,

adherent platelets recruited numerous new platelets from the blood flow, but these were consistently unable to firmly attach and were released after a few seconds. As a consequence, the surface area covered by platelets and the total thrombus volume at the end of the experiment were reduced by 36% and 82% in CLEC-2-deficient blood, respectively (Fig 3.9C).

This phenotype was, however, not due to altered initial adhesion on collagen under flow as, comparable to control platelets, CLEC-2-deficient platelets exhibited unaltered adhesion to collagen fibers after 30 sec of perfusion (Fig 3.9A). Furthermore, formation of GPIb-V-IX complex seemed not to be altered as the adhesion to a vWF-coated surface under flow was also unaltered in CLEC-2-deficient platelets (Fig 3.9B).

Similar results were obtained in the same model at intermediate shear rates (1,000 sec^{-1}, Fig 3.10A). Here, the disturbed platelet adhesion in INU1-treated blood was also visible. As newly recruited platelets were not able to firmly attach to the already adherent first layer of platelets, they were constantly released from the thrombus surface. Those already activated but released platelets seemed to bind a second time to free collagen fibers on the cover slip and therefore lead to a rather high surface coverage compared to controls. However, it was evident that the overall thrombus growth was markedly reduced demonstrated by the strongly decreased thrombus volume measured via fluorescence of the platelets (Fig 3.10A). Furthermore, the same phenotype of CLEC-2-deficient blood was also obtained under flow conditions of very high shear (3,400 sec^{-1}, Fig 3.10B). These findings suggest that CLEC-2-dependent processes are essential for stable aggregate formation under flow, whereas the receptor is not required for the adhesion process on collagen (Fig 3.10A).
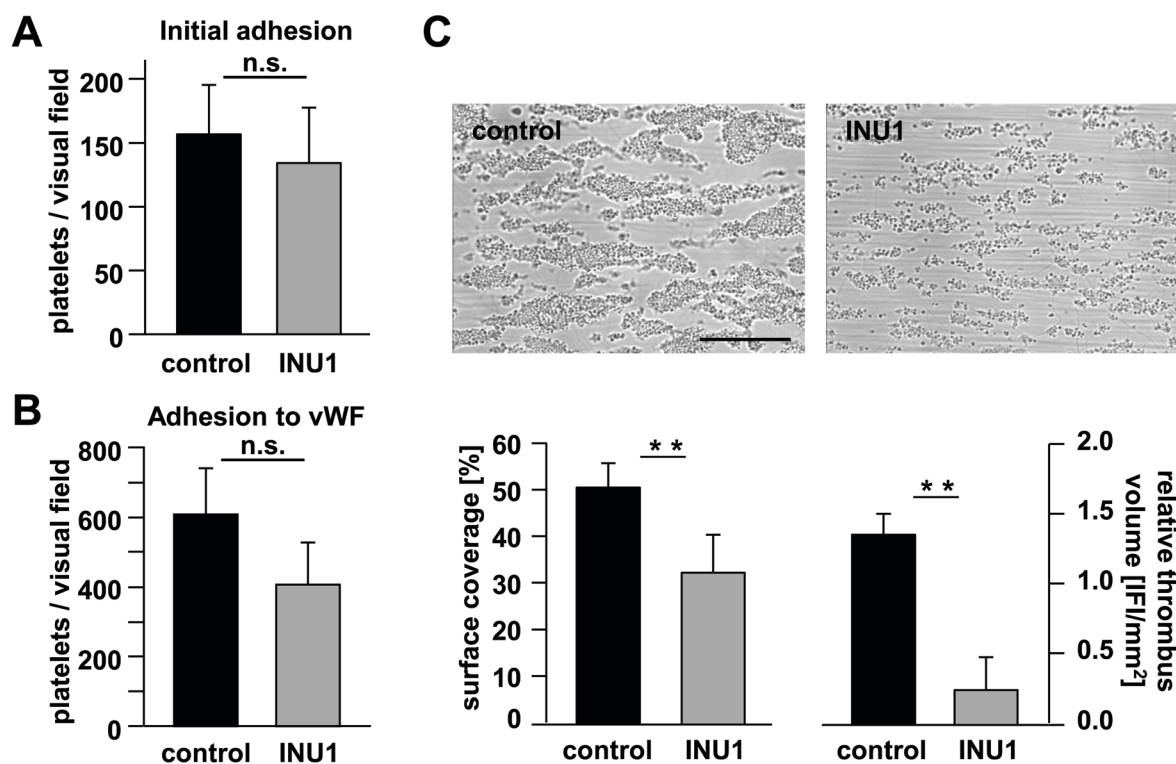
Fig 3.9 CLEC-2-deficient platelets fail to form stable aggregates under flow. Whole blood from control or INU1-treated mice (8 µg/g body weight, d5) was perfused over a collagen- (A+C) or vWF-coated surface (B) under anticoagulated conditions (whole blood in 20 U/ml heparin) at a shear rate of 1,700 sec^{-1} (A+C) or 3,400 sec^{-1} (B). A. Initial platelet adhesion on collagen after 30 sec perfusion of the slide indicated as number of platelets per visual field. B. Platelet adhesion to vWF-coated surface after 150 sec of perfusion. C. Aggregate formation on collagen after 4 min of perfusion. Top: representative phase contrast images. Bar, 100 µm. Bottom: Mean surface coverage (left) and relative thrombus volume expressed as integrated fluorescence intensity (IFI) per mm^2 (right) ± SD of n=6 mice per group, **$p<0.01$. (May F *et al.*, *Blood*, 2009[104].)

To test whether the thrombus instability was based on impaired platelet activation *per se*, we performed further flow adhesion studies with whole blood in Acid Citrate Dextrose (ACD) buffer causing non-anticoagulated conditions. In contrast to heparinized anticoagulated whole-blood where thrombin formation is inhibited, under non-anticoagulated conditions thrombin generation is allowed. Under these conditions, both control and CLEC-2-deficient platelets formed large stable thrombi (Fig 3.10C), indicating that in the presence of high amounts of thrombin, platelet activation via CLEC-2 signaling is not essential for thrombus stabilization in this flow-system. Similarly, co-infusion of a mixture of ADP (10 µM) and the stable thromboxane analog U46619 (1 µM) into anticoagulated blood shortly before entering the flow chamber likewise resulted in the formation of large and stable aggregates in both control and CLEC-2-deficient blood (data not shown).

Taken together, these data indicate that CLEC-2 functions as an activatory receptor in platelets that is required for thrombus stabilization under conditions where other agonists are not present in concentrations sufficient to fully activate the cells.
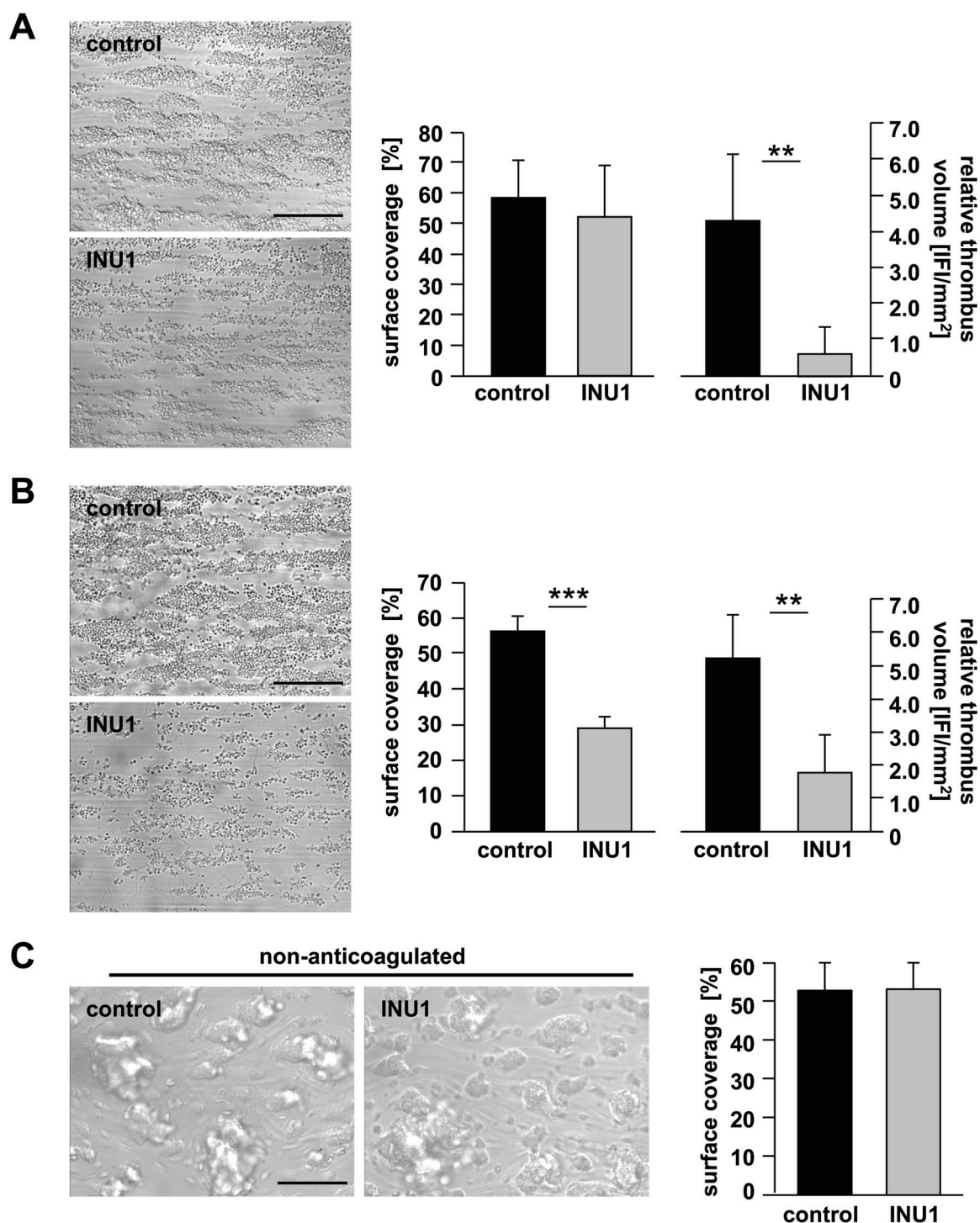
Fig 3.10 Aggregate formation of CLEC-2-deficient platelets. Whole blood from control or INU1-treated mice (8 µg/g body weight, d5) was perfused over a collagen-coated surface (0.2 mg/ml). Left: representative phase contrast images. Right: Mean surface coverage and relative thrombus volume expressed as integrated fluorescence intensity (IFI) per mm^2 ± SD. Bar, 100 µm. **$p<0.01$. A. Aggregate formation on collagen after 4 min perfusion time under anticoagulated conditions (whole blood in 20 U/ml heparin) at a shear rate of 1,000 sec^{-1}. n=5 mice per group. B. Aggregate formation on collagen after 4 min perfusion time under anticoagulated conditions (whole blood in 20 U/ml heparin) at a shear rate of 3,400 sec^{-1}. n=4 mice per group. C. Aggregate formation on collagen after 4 min perfusion time under non-anticoagulated conditions in ACD-buffer. n=6 mice per group. (May F et al., *Blood*, 2009[104].)

3.1.9   Increased tail bleeding times in CLEC-2-deficient mice

To test whether the INU1-induced CLEC-2 deficiency had an impact on hemostasis, a tail bleeding time assay was performed. To this end, mice were anesthetized and upon a 1 mm dissection of the tail tip the blood was absorbed with a filter paper avoiding contact with the wound site. In this series of experiments it was found that whereas bleeding stopped in all (22/22) control mice during the 20-min observation period (mean bleeding time: 6.1 ± 3.9 min), bleeding times were variable and overall increased in INU1-treated mice, with 8 (33.3%) of 24 mice bleeding for more than 20 min and a mean bleeding time of 10.8 ± 6.0 min for the other animals ($p<0.05$; Fig 3.11). However, even those animals that were not able to arrest bleeding within the observation period displayed a rather mild blood loss (data not shown). These results show that CLEC-2 plays a significant role in normal hemostasis under the conditions of this experiment.
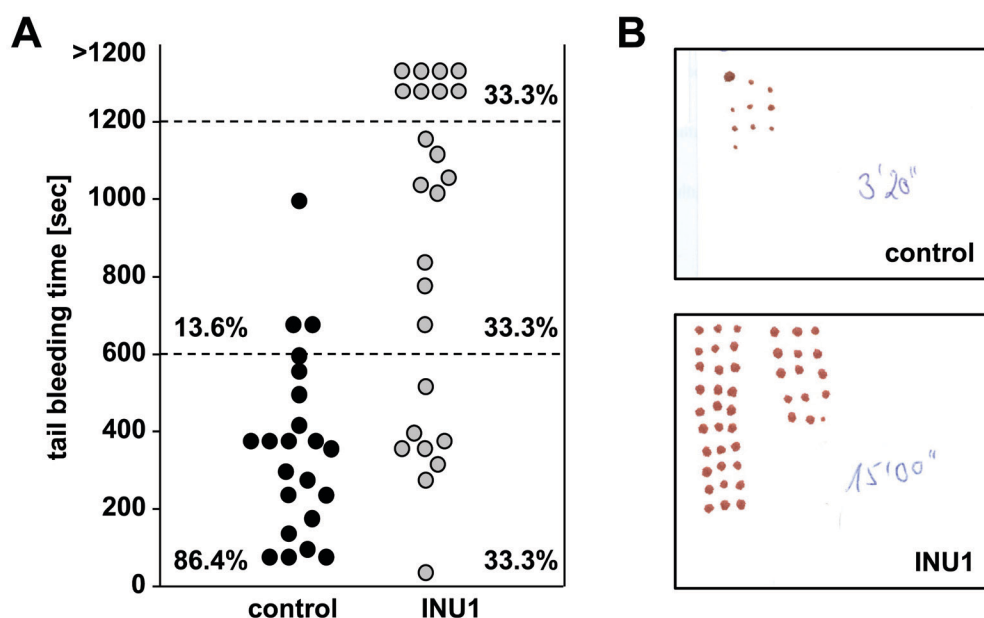

Fig 3.11 Tail bleeding times in control and CLEC-2-deficient mice. Mice received vehicle (PBS) or INU1 (8 µg/g body weight) and were analyzed on d5 p.i.. A. Each symbol represents one individual. Tail bleeding times were performed by amputation of a 1 mm segment of the tail tip of anesthetized mice and subsequent absorbance of the blood drop with a filter paper. B. Representative pictures of a filter paper from control (upper panel) and INU1-treated mice (lower panel). Note the size of the blood drop as a measure of the severity of blood loss. (May F *et al.*, *Blood*, 2009[104].)

3.1.10 CLEC-2-deficient mice in models of arterial thrombosis and ischemic stroke

3.1.10.1 CLEC-2-deficient mice are protected from FeCl₃-induced arterial thrombus formation

As platelet aggregation is a major pathomechanism in acute ischemic cardiovascular events, we studied the effects of CLEC-2 deficiency on pathologic occlusive thrombus formation by *in vivo* fluorescence microscopy after ferric chloride ($FeCl_3$)-induced mesenteric arteriole

injury. To do so, the mesentery of the animals was exposed and injury was induced by topical application of a filter paper saturated with $FeCl_3$ (20%). These experiments were performed in collaboration with Ina Hagedorn in our laboratories. In all control mice, the formation of small platelet aggregates was observed approximately 5-7 min after injury, with progression to complete vessel occlusion within 20 min (mean occlusion time: 16.4 ± 2.2 min; Fig 3.12). Interestingly, initial adhesion and formation of small aggregates occurred with similar kinetics in CLEC-2-deficient mice (6.9 ± 1.5 min *versus* 6.5 ± 1.5 min in control, *p*>0.05), showing that the receptor CLEC-2 is not essential for the first step of platelet adhesion/activation. Remarkably, in contrast to controls, progression to stable large thrombi was almost completely abrogated in CLEC-2-deficient animals. This defect was to a great extent caused by the release of individual platelets from the thrombus surface, but also embolization of small thrombus fragments was observed. Consequently, the blood flow was maintained throughout the 40-min observation period in all CLEC-2-deficient mice and thus the treated animals were protected from arterial thrombosis. These results indicate that in this model of vessel wall injury CLEC-2 plays a crucial role in the process of occlusive thrombus formation.
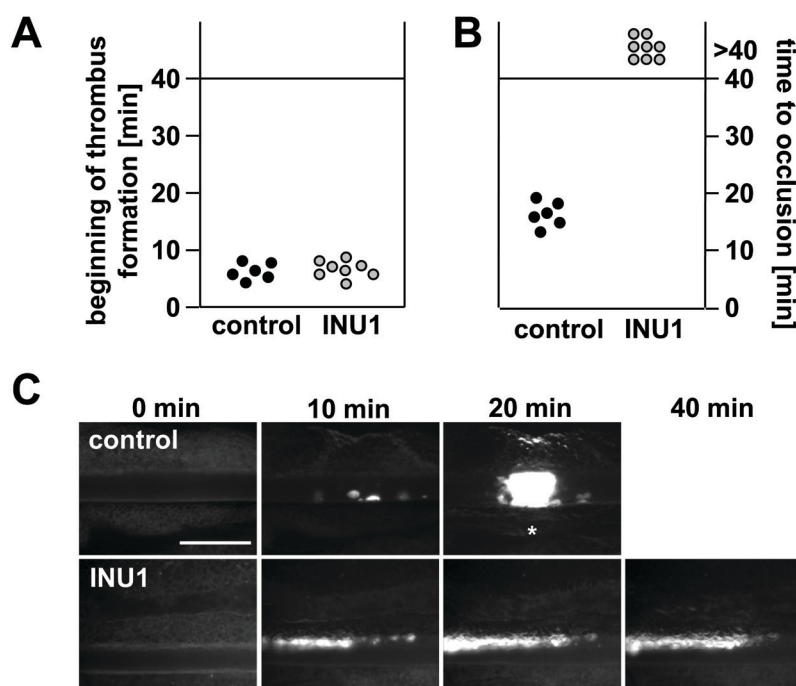
Fig 3.12 Defective thrombus formation in CLEC-2-deficient mice. Mice received vehicle (PBS) or INU1 (8 µg/g body weight) and were analyzed on d5 p.i.. (A-C) Mesenteric arterioles were injured with $FeCl_3$ and adhesion and thrombus formation of fluorescently-labeled platelets were monitored *in vivo* by fluorescence microscopy. A. Time to appearance of first thrombus >10 µm, and B time to vessel occlusion are shown. Each symbol represents one arteriole. C. Representative images are depicted. Bar, 50 µm. The asterisk indicates occlusion of the vessel. Data are representative of two individual experiments. (May F *et al.*, *Blood*, 2009[104].)

3.1.10.2 CLEC-2 deficiency does not protect from mechanically induced occlusive thrombus formation in the aorta

To further analyze the role of CLEC-2 in pathological thrombus formation, INU1-treated CLEC-2-deficient mice were subjected to a thrombosis model where injury is mechanically induced in the aorta by a single, firm compression with a forceps, and blood flow is monitored with an ultrasonic perivascular Doppler flow-meter (Fig 3.13). These experiments were performed in collaboration with Ina Hagedorn in our laboratories.

After a transient increase directly after injury, blood flow progressively decreased for several minutes in all animals. In all tested control mice (7/7), this decrease resulted in complete and irreversible occlusion of the vessel within maximally 7 min thereafter. Surprisingly, CLEC-2 deficiency did not protect from occlusive thrombus formation in this model (7/7), although a trend to a later occlusion was found in INU1-treated animals (mean occlusion time 4.6 ± 1.2 min *versus* 7.1 ± 3.0 min, Fig 3.13). To analyze whether the observed effect is statistically significant, more mice will be subjected to this model in the near future.
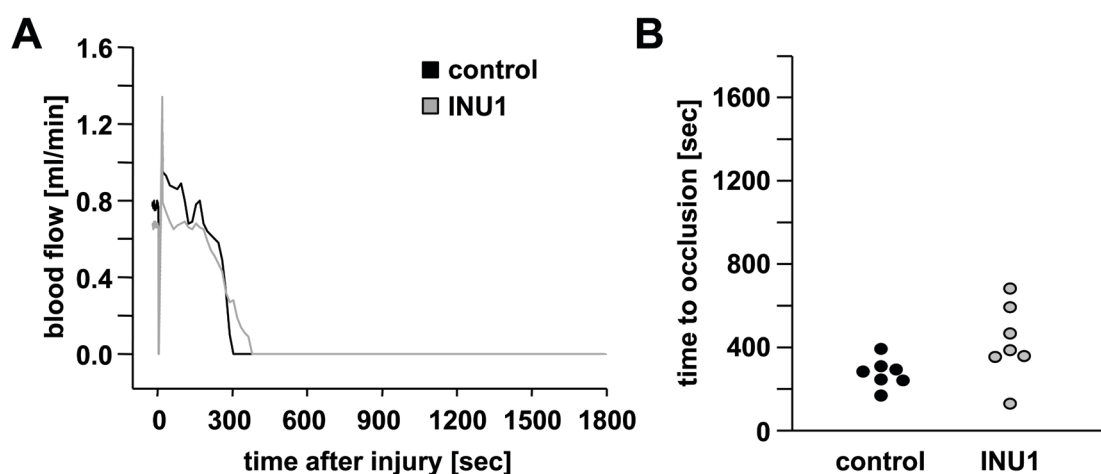
Fig 3.13 CLEC-2-deficient mice form stable thrombi in the aorta model. A. Representative graph of blood flow of a control (black) and INU1-treated CLEC-2-deficient mouse (gray) after mechanical injury of the aorta (at t=0). B. Occlusion time upon injury of the aorta. The aorta of all control and INU1-treated mice occluded during the 30-min observation period. Each symbol represents one individual, n= 7.

3.1.10.3 CLEC-2 deficiency has no significant impact on the outcome in a model of ischemic brain infarction

Ischemic stroke is the third leading cause of death and disability in industrialized countries[108]. Although it is well established that microvascular integrity is disturbed during cerebral ischemia[109], the signaling cascades involved in intravascular thrombus formation in the brain are still poorly understood. To determine the importance of CLEC-2 deficiency in this process, the development of neuronal damage in CLEC-2-deficient mice following transient cerebral ischemia was studied in a model that depends on thrombus formation in the

microvasculature downstream of an induced occlusion of the middle cerebral artery (MCA)[110]. These experiments were conducted by Stephan Bräuninger and performed in collaboration with the Neurology Department of the University of Würzburg. To initiate transient cerebral ischemia, a thread was advanced through the carotid artery into the MCA and allowed to remain for one hour (transient MCA occlusion, tMCAO), reducing regional cerebral flow by >90%[83]. After one hour the filament was removed to allow reperfusion and the animals were followed for another 24 h. Then, the brains were harvested and 2,3,5-triphenyltetrazolium chloride (TTC) staining was performed to analyze the extent of the infarct size of the contralateral hemisphere. In CLEC-2-deficient animals, infarct volumes 24 h after reperfusion were not significantly reduced compared to controls. The infarct size of controls was calculated to 50.9 ± 16.4% *versus* 42.7 ± 11.5% in INU1-treated animals. Although the values were not significantly decreased in CLEC-2-deficient animals, a trend to a better outcome was observed (Fig 3.15A). In consequence, the Bederson score assessing the global neurological function in surviving mice 24 h post operation was also not significantly altered compared to controls (3.1 ± 0.4 *versus* 3.0 ± 0.6, values 0-5, 0= best value, Fig 3.14B). Furthermore, the grip test, which specifically measures motor function and coordination of the challenged animals, was not significantly different in CLEC-2-deficient mice compared to controls (2.5 ± 1.1 *versus* 2.7 ± 1.4, values 0-5, 5= best value, Fig 3.14C). However, as a trend to less neurological deficits was observed and in order to further analyze whether treatment with INU1 could possibly lead to a better outcome in stroke, more mice will be subjected to this model in the near future.

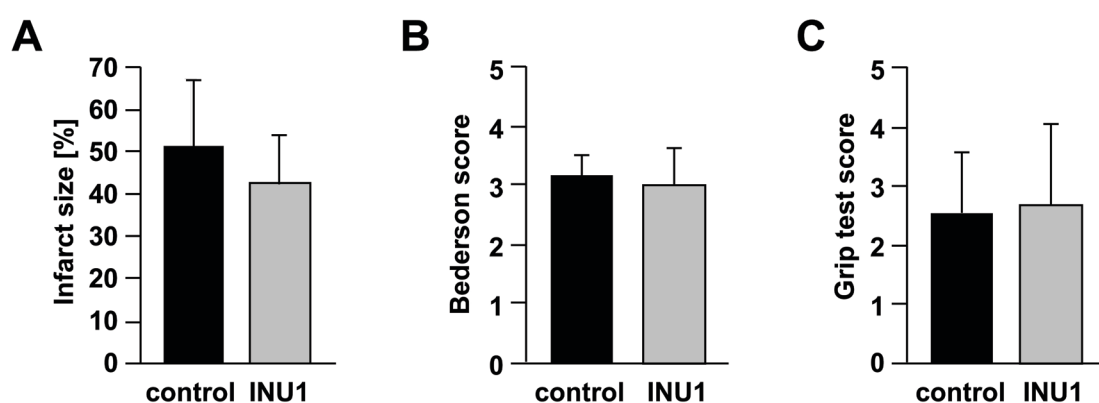**Fig 3.14 CLEC-2-deficient mice are not protected in a model of tMCAO.** A. The sizes of induced brain infarcts following tMCAO in control (n=8) and INU1-treated (n=6) mice in percent of contralateral hemisphere are not significantly reduced in INU1-treated mice although a trend is observed. B+C. Neurological Bederson score (middle) and grip test (right) assessed at day 1 following tMCAO of control (n=8) and INU1-treated (n=6) mice.

3.1.11 INU1-Fab-fragment-induced lethality in mice

In the above described experiments (Fig 3.5, Fig 3.6), a single batch of INU1-Fab-fragments was used, previously generated by enzymatic digestion of the full IgG using papain. Here, similar to the full INU1-IgG, treatment with INU1-Fab led to a profound thrombocytopenia in mice. However, similar to treatment with the full IgG all of the INU1-Fab-treated mice survived the treatment (data not shown).

To further analyze the effect of treatment with INU1-Fab, a second batch of INU1-Fab was generated using the same method. This batch was tested in aggregometry where it -as expected- failed to induce platelet aggregation. However, upon addition of α-rat IgG, full aggregation of platelets was observed (data not shown). Furthermore, flow cytometry studies confirmed that INU1-Fab-fragments (20 µg/ml) fully blocked the binding site of the antibody on washed mouse platelets *in vitro* (data not shown). Additionally, in line with previous results of the first batch presented before (see chapter 3.1.5) the CLEC-2-specific agonist rhodocytin (0.24 µg/ml f.c.) failed to induce activation of INU1-Fab-treated platelets but not of control platelets in aggregometry, as well as in flow cytometry (data not shown). These results indicated that the generated INU1-Fab-fragments were fully functional.

However, very unexpectedly, and in sharp contrast to the described initial experiments, *in vivo* administration of the second batch of INU1-Fab resulted in immediate lethality in mice. Animals treated with 100 µg INU1-Fab under short-term ether anesthesia displayed muscle spasms, paralysis, and symptoms of suffocation leading to death of all treated animals (10/10, Fig 3.15A) within 30 min after i.v. injection, whereas all controls (10/10, PBS treated) survived this challenge. However, inner bleeding or damage of internal organs was not visible (data not shown). Some of the observations made, could point to an anaphylactic shock reaction such as peripheral cyanosis observed on the tail veins of the treated animals. Other observations rather suggested an acute thrombotic event such as paralysis that is often observed upon stroke.

As these symptoms were totally unexpected and to exclude that contamination during preparation of the second batch caused this effect, a third batch of INU1-Fab was generated. The full IgG was enzymatically digested with papain utilizing the same method. As before, upon injection of 200 µg of INU1-Fab (third batch), the same symptoms were immediately observed (10-30 min after injection) causing mortality in the treated animal (1/1, data not shown). Even a lower dose of INU1-Fab (100 µg) induced lethality in a further treated mouse, whereas all control mice treated with PBS survived (3/3) (data not shown).

To further analyze this phenomenon, a fourth batch of INU1-Fab-fragments was generated using a modified method where the full IgG was digested with pepsin to Fab_2-fragments (10 mg were kept for further use) and subsequently to Fab-fragments with DL-dithiothreitol. The obtained fragments of the antibody were purified by gel filtration twice via a Superdex

200 column (SD) after each of the digestions, firstly with pepsin and secondly with DL-dithiothreitol, excluding residual Fc-portions of the digested IgG in the preparation. By use of this method, 40 mg of INU1-Fab (termed INU1-Fab^{SD}) were generated.

INU1-Fab^{SD} was again tested in aggregometry where it failed to induce aggregation of platelets *in vitro* but did so upon cross-linking with α-rat IgG as shown before (data not shown, compare Fig 3.5). Additionally, separation of the purified INU1-Fab^{SD} on SDS-PAGE further confirmed purity of the newly generated batch (data not shown), thereby excluding a possible contamination during preparation.

In all following experiments, mice were treated with INU1-Fab^{SD} or PBS only under long-term deep anesthesia using the narcotics fentanyl, dormitor and dormicum. To further determine whether treatment with INU1-Fab^{SD} also induced lethality, deeply anesthetized mice were treated with 100 µg of the antibody fragment. Under these conditions, all INU1-Fab^{SD} treated mice died within 30 min (3/3, Fig 3.15B). This process took significantly longer when compared to mice treated with INU1-Fab (third batch) under short-term anesthesia, probably due to a lower blood pressure under these conditions. In contrast, mice treated with either the full IgG or Fab$_2$-fragments of the antibody (INU1-Fab$_2$) survived the treatment and showed no symptoms of circulation problems similar to controls. To detect whether the lethal effect of INU1-Fab was platelet-mediated, mice were depleted of platelets by treatment with 100 µg of the α-GPIbα antibody p0p4 1 h prior to experiments[103]. Interestingly, all platelet-depleted mice (3/3, Fig 3.15C) survived the following treatment with INU1-Fab^{SD}, thus pointing to a role of platelets in this process. Furthermore, mice depleted of CLEC-2 on d5 after INU1-treatment also survived treatment with INU1-Fab^{SD} (3/3, Fig 3.15C). This indicated that the observed lethality was indeed platelet- and CLEC-2-mediated and further strengthens the hypothesis that lethality was not due to non-specific toxicity of the INU1-Fab^{SD} solution itself. Interestingly, even very low doses of INU1-Fab^{SD} (5 µg/ mouse) were lethal within 30 min in all treated animals (3/3, Fig 3.15C).

To further analyze the role of platelets in INU1-Fab^{SD}-mediated lethality, mice were treated with Fab-fragments of the antibodies p0p/B and JON/A (1 h prior to experiments) to induce blockage of platelet GPIbα and GPIIb/IIIa, respectively. GPIIb/IIIa (also known as integrin αIIbβ3) is a prominent target for anti-thrombotic therapy as blockage of the integrin profoundly inhibits platelet aggregation[111]. Therefore, it was unexpected that even under GPIIb/IIIa blockage 66.7% of the INU1-Fab^{SD} treated animals died (2/3, Fig 3.15D). Furthermore, blockage of GPIbα did not decrease mortality in INU1-Fab^{SD} treated animals as all INU1-Fab^{SD} treated mice died (3/3, Fig 3.15D). These results indicate that INU1-Fab^{SD}-induced lethality in mice is platelet- and CLEC-2-dependent since platelet- as well as CLEC-2-depleted mice were protected from lethality. However, blockage of the platelet glycoproteins GPIbα as well as GPIIb/IIIa did not protect from INU1-Fab^{SD}-induced lethality.
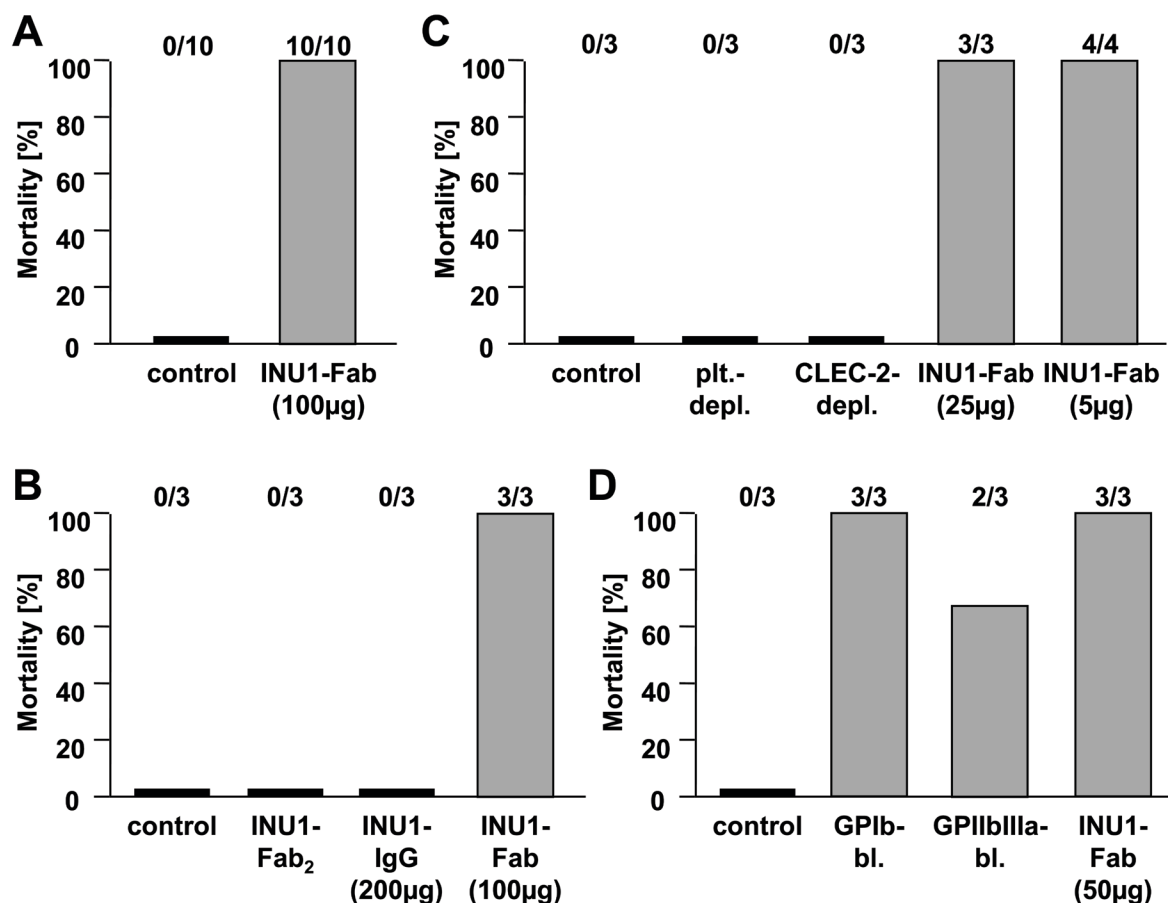
Fig 3.15 INU1-Fab-induced lethality in mice. Lethality in mice upon treatment with INU1-Fab-fragments (INU1-Fab) expressed as mortality in per cent of all treated animals. Controls were treated with sterile PBS. A. Treatment with INU1-Fab (100 µg) under ether anesthesia. B. Full IgG or Fab$_2$-fragments of INU1 (INU1-Fab$_2$, 100 µg) are not lethal, whereas INU1-Fab^{SD} (100 µg) leads to 100% mortality. C. To induce depletion of platelets, mice were treated with the antibody p0p4 (100 µg) 1 h prior to experiments. For CLEC-2 depletion, animals were treated with INU1-IgG (200 µg, 5 days prior to experiments). These groups received 50 µg INU1-Fab^{SD}. Treatment with 25 µg and 5 µg of INU1-Fab was lethal in all tested animals. These results are representative of two individual experiments. D. For blockage of GPIbα or GPIIb/IIIa, mice were treated with Fab-fragments of the antibodies p0p/B and JON/A, respectively (100 µg) 1 h prior to experiments and then treated with INU1-Fab^{SD} (50 µg).

Upon injection of INU1-Fab^{SD}, in long-term anesthetized mice symptoms of hypoxia were observed (data not shown). This led to the hypothesis that upon treatment with INU1-Fab^{SD}, micro-thrombi of clustered platelets could possibly block small arterioles and capillaries in the lung leading to pulmonary embolism or might potentially also cause cerebral ischemia. To test this hypothesis, long-term deep anesthetized mice were treated with PBS (control) or INU1-Fab^{SD} (100 µg) and organs were perfusion fixated by injection of 4% paraformaldehyde (PFA) into the beating heart 10 min after treatment. Organs were harvested, fixed in 4% PFA, cut into 5 µm thin sections and stained with hematoxylin-eosin. Interestingly, no major differences were observed between samples of INU1-Fab^{SD} treated mice and controls (data not shown). However, as the perfusion fixation was performed with rather high pressure, it could not be excluded that micro-thrombi or emboli were flushed away. To further test this hypothesis, organs of mice treated under the same conditions as described above were harvested and fixed using liquid N_2. These samples will be analyzed in the near future.

3.2   Generation of the second anti-murine CLEC-2 antibody INU2

To further characterize the mechanism of INU1-mediated down-regulation of CLEC-2 in platelets, additional anti-CLEC-2 antibodies were required e.g. to detect possibly cleaved fragments of the receptor in mouse plasma by a specific ELISA- or western blot-system as well as for further FACS analyses. For this purpose, two additional fusions of spleen cells from rats immunized with washed platelets were performed. Both fusions did not result in generation of any specific α-CLEC-2 antibody (data not shown). Therefore, repeated immunizations of three rats with native CLEC-2 protein were performed, previously immuno-precipitated from wild-type platelet lysate using INU1. However, these three fusions also failed and no specific α-CLEC-2 antibodies were generated (data not shown).

As the washed platelet and native CLEC-2 approach were not successful in antibody generation, a third method was considered by using the previously generated mCLEC-2 Fc-fusion protein. For this purpose, three rats were repeatedly immunized with the mCLEC-2 Fc-fusion protein. The antibody titer in the serum of the immunized rats was tested on mouse platelet lysate by western blot analysis. From all tested animals, only serum from rat no. 1 produced a detectable band at the expected size of murine CLEC-2 (32-33 kDa) and showed the highest antibody titer (data not shown). Therefore, the spleen from rat no. 1 was used for the generation of antibody-producing hybridoma cells as described above (see chapter 3.1.1). Approximately 1,400 hybridoma populations were obtained and screened for antibody production in the ELISA system using the mCLEC-2 Fc-fusion protein. To identify false-positive clones that non-specifically bound to the Fc-part of the fusion protein, a second ELISA was performed in parallel with the mGPVI Fc-fusion protein. By this method, 12 polyclonal hybridoma populations were detected that produced antibodies specifically directed against the mCLEC-2 Fc-fusion protein (data not shown).

These antibodies were seeded into 24-well plates and further tested by flow cytometry on mouse platelets. Unfortunately, none of the tested hybridoma clones produced antibodies that specifically bound to platelets (data not shown). However, the clones were again tested in the established ELISA system and one clone (clone 8C7) still yielded strong signals specifically directed against the mCLEC-2 Fc-fusion protein but not against the control mGPVI Fc-fusion protein (Fig 3.16A). Therefore, 8C7 was subcloned twice, and as it stably expressed the antibody, the clone was cultured in RPMI medium containing 5% FCS. Approximately 70 mg of the antibody were purified.

Thereafter, the antibody 8C7 was further tested on mouse platelet lysate by western blot analysis. Under reducing and non-reducing conditions a specific band of the approximate size of CLEC-2 at ~32-35 kDa was observed in platelet lysate. Furthermore, the antibody also detected the mCLEC-2 Fc-fusion protein (Fig 3.16B) as well as CLEC-2 protein that was pulled down from platelet lysate using INU1 (Fig 3.16C).

The antibody 8C7 was again tested on resting or activated platelets in flow cytometry where it failed to detect native CLEC-2 or any other protein on the surface of platelets (data not shown). However, as it clearly detected mCLEC-2 Fc-fusion protein in ELISA and in western blot, as well as a protein of the size of CLEC-2 from platelet lysate and immunoprecipitations in western blot under reducing conditions, it seems likely that 8C7 binds an epitope of CLEC-2 that is not recognized by the antibody under native conditions on the platelet surface but exclusively under denaturing conditions. Thus, this second rat monoclonal antibody against mouse CLEC-2 was termed INU2.
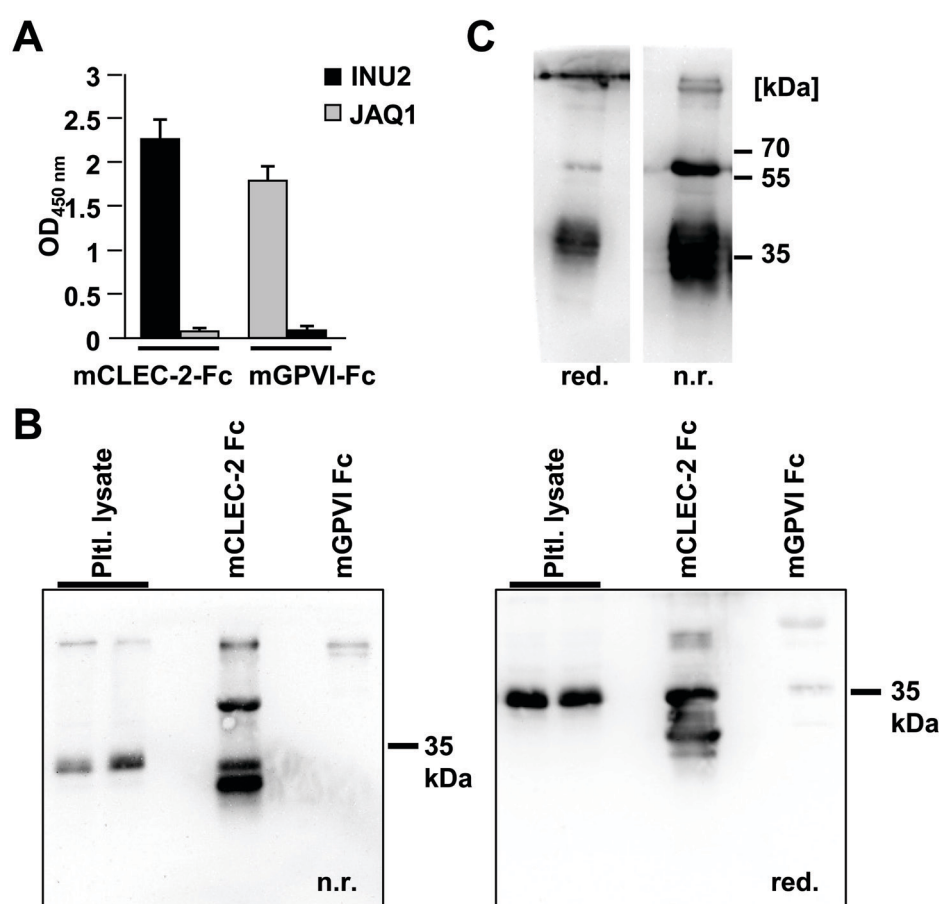
Fig 3.16 The novel antibody INU2 recognizes murine CLEC-2. A. Binding of INU2 to mCLEC-2 Fc-fusion protein (mCLEC-2-Fc) was tested by ELISA. As control, binding of the α-GPVI antibody JAQ1 to mGPVI Fc-fusion protein (mGPVI-Fc) was used. B. Western blots from murine platelet (pltl.) lysate and fusion proteins. INU2 detected a protein of ~32-35 kDa under non-reducing (n.r., left panel) and reducing (red.) conditions from platelet lysate and the mCLEC-2 Fc-fusion protein. C. Immunoprecipitation of CLEC-2 from platelet lysate using INU1. Platelets were lysed and incubated with 10 µg/ml INU1 followed by immunoprecipitation with protein G-Sepharose. Proteins were separated on a 12% SDS-PAGE under reducing or non-reducing conditions and detected by INU2 and α-rat HRP. Results are representative of 2-3 individual experiments.

3.3 Abolished arterial thrombus formation and severely defective hemostasis in GPVI/CLEC-2 double-deficient mice

3.3.1 Independent antibody-mediated down-regulation of GPVI and CLEC-2 in platelets *in vivo*

On human platelets it was demonstrated that individual activation of both ITAM-coupled receptors, GPVI and FcγRIIa, led to a proteolytic inactivation of both receptors simultaneously; a process that was termed trans-inhibition. However, the FcγRIIa receptor is not present on mouse platelets and it is not known whether a similar mechanism of trans-inhibition exists for GPVI and CLEC-2 on human or mouse platelets[94]. To address this question, the basal surface expression of both GPVI and CLEC-2 following INU1- or JAQ1-induced receptor deficiency on mouse platelets was analyzed by flow cytometry. As expected, JAQ1-treatment induced the complete loss of GPVI on the surface of platelets[66], however, it had no effect on basal surface expression levels of CLEC-2. Likewise, INU1-treatment induced the complete loss of CLEC-2 from the platelet surface but had no effect on GPVI expression (Fig 3.17A). Moreover, CRP-induced GPVI signaling in CLEC-2-depleted platelets was not affected and *vice versa* in GPVI-depleted platelets stimulation of CLEC-2 signaling by rhodocytin (RC) was unaltered (Fig 3.17B). These results indicate that trans-inhibition of (hem)ITAM-bearing receptors in murine platelets does not occur *in vivo* and that the independent down-regulation of either of the two proteins is possible without affecting signaling of the respective other receptor.
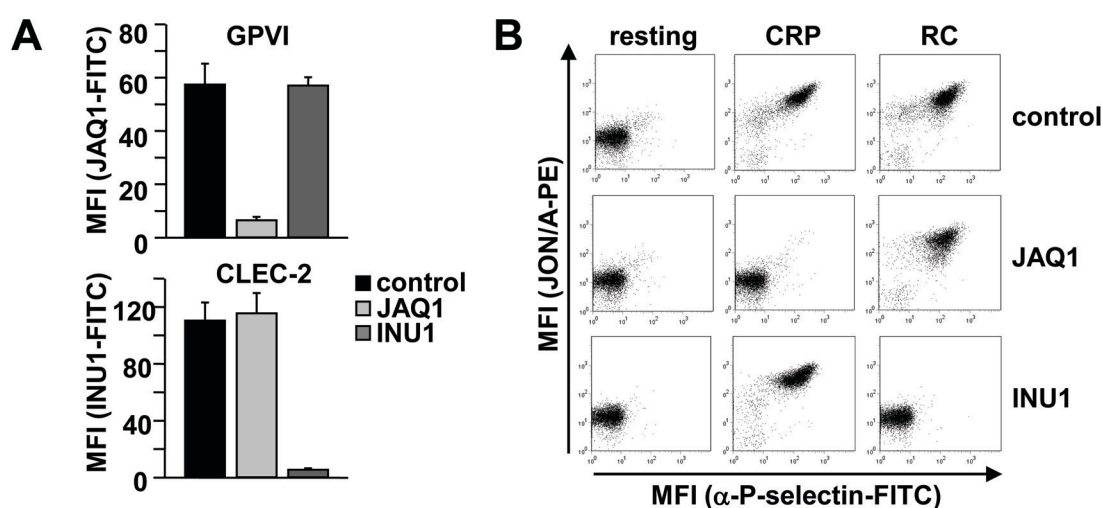
Fig 3.17 Surface expression and signaling of GPVI and CLEC-2 upon INU1- and JAQ1-treatment. Mice received 100 µg JAQ1 or 200 µg INU1 i.v. and were analyzed 5-6 days p.i.. Results are expressed as mean fluorescence intensity (MFI) ± SD. A. Expression levels of GPVI (upper) or CLEC-2 (lower panel) on the platelet surface were determined by flow cytometry. B. Representative dot plots of αIIbβ3 integrin activation (binding of JON/A-PE) and degranulation-dependent P-selectin exposure in response to the indicated agonists CRP (10 µg/ml) and rhodocytin (RC, 1 µg/ml) from control, JAQ1- or INU1-treated mice. (Bender M[§], May F[§] *et al.*, in revision).

3.3.2 *In vitro* analysis of platelet function upon antibody-induced GPVI and CLEC-2 double-deficiency

It has been speculated previously[14] that the (hem)ITAM receptors in platelets, GPVI and CLEC-2, may compensate for each other in preventing blood loss because, patients[80,101,112] as well as mice[67,113-114] lacking GPVI displayed only mild bleeding tendencies. To investigate whether GPVI and CLEC-2 have redundant functions in hemostasis as well as in thrombosis animals deficient in both receptors were analyzed.

Therefore, mice were injected i.v. with the α-GPVI antibody JAQ1 (100 µg), the α-CLEC-2 antibody INU1 (200 µg), or both antibodies in combination (JAQ1+INU1). In all antibody treated animals, a rapid thrombocytopenia was induced immediately (~30 min) upon injection of the respective antibody (Fig 3.18). However, in line with a previous study from our group, the JAQ1-induced thrombocytopenia was quickly reversible and platelet counts of the treated animals came back to ~80% of controls one day p.i. and fully recovered on d5 p.i. (Fig 3.18)[66]. In contrast, a more sustained thrombocytopenia was observed in mice treated with INU1 with recovery to normal platelet count levels on d4 post injection, as described earlier (see also Fig 3.6A). Similarly, upon combined treatment with JAQ1+INU1 platelet counts were found to recover fully on d5 p.i. (Fig 3.18). Remarkably, whereas in INU1- and JAQ1+INU1-treated mice an overshooting platelet production was observed on d5-6 p.i., this effect was not found in JAQ1-treated animals. As in the latter animals thrombocytopenia was quickly reversible this could suggest different mechanisms of receptor down-regulation and the subsequent thrombocytopenia upon treatment with JAQ1 or INU1. This hypothesis was underlined by a study from our group showing that upon JAQ1-treatment the same platelets were released to the blood stream after cleavage of the GPVI receptor which is assumed to take place in the spleen[66].
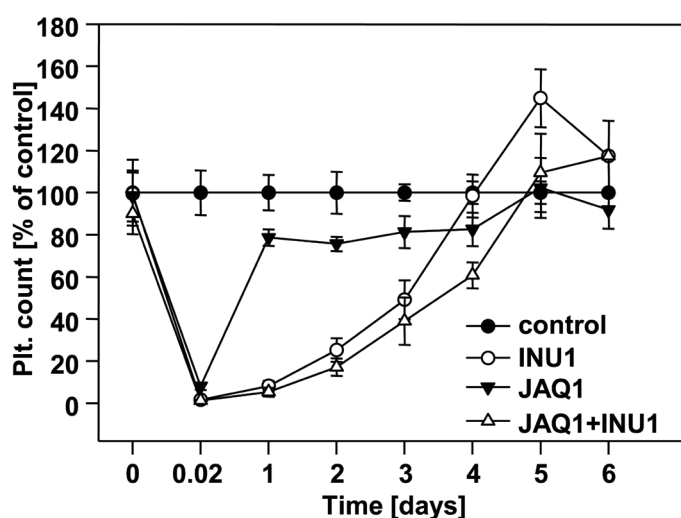
Fig 3.18 Antibody-induced thrombocytopenia and recovery of platelet counts. Mice received 100 µg JAQ1, 200 µg INU1 or a mixture of both antibodies (JAQ1 + INU1) i.v. and platelet counts were determined by flow cytometry at the indicated time points p.i. (0.02 days=~30 min). Results are expressed as the mean platelet count in percent of control $\pm$ SD for groups of each n=4 mice and are representative of 3 individual experiments. (Bender M[§], May F[§] *et al.*, in revision).

In contrast, upon INU1- and JAQ1+INU1-treatment, CLEC-2-depleted platelets found in the blood stream were increased in size (Tab 3.2) compared to platelets from the same animals before treatment or controls and the animals showed a more profound thrombocytopenia until platelet counts returned back to normal, indicating that the production of new platelets from megakaryocytes in the bone marrow was necessary. To investigate the effect of the double-depletion, using JAQ1+INU1, on platelet function, basal surface expression levels of glycoproteins were analyzed via flow cytometry.

It was found that platelets from JAQ1+INU1-treated mice -as expected- specifically lacked GPVI and CLEC-2 whereas expression of other surface proteins was largely unaltered (Tab 3.2). Expression of the glycoprotein (GP) IX was found to be only mildly increased, whereas expression of the integrin $\alpha2\beta1$ was slightly decreased. These effects were, however, assumed to be of minor importance to the physiological function of the cells as the changes in expression rate were very low. Notably, the platelet size of double-deficient animals was significantly increased compared to controls most probably due to the rapid and massive production of new platelets following the induced thrombocytopenia in the double-deficient animals.

	control	JAQ1+INU1	
GPVI	53 ± 3	7 ± 1	***
CLEC-2	130 ± 23	6 ± 1	***
GPIb	388 ± 29	395 ± 23	n.s.
GPIX	476 ± 36	524 ± 16	*
GPV	332 ± 24	337 ± 15	n.s.
CD9	1364 ± 116	1238 ± 40	n.s.
αIIbβ3	679 ± 39	684 ± 35	n.s.
α2	49 ± 2	44 ± 3	*
β1	153 ± 9	130 ± 3	**
plt. size	357 ± 19.7	421 ± 40.2	***

Tab 3.2 Platelet size and glycoprotein expression in control and JAQ1+INU1-treated mice. Expression of glycoproteins (GP) on the platelet surface was determined by flow cytometry on d5 p.i. of PBS (control) or JAQ1+INU1 (100 µg + 200 µg) treated mice. Diluted whole blood from the indicated mice was stained with fluorophore-labeled antibodies at saturating concentrations and platelets were analyzed on a FACSCalibur. Platelets were gated by FSC/SSC characteristics. Results are expressed as mean fluorescence intensity ± SD for n=6 mice per group. Mean platelet (plt.) size is given as mean FSC and was determined by FSC characteristics. Abbreviation: n.s.= not significant. *$p<0.05$, **$p<0.01$, ***$p<0.001$. (Bender M[§], May F[§] *et al.*, in revision).

To further investigate whether the lack of both receptors had an impact on other signaling pathways of the platelets, flow cytometric analyses were performed after activation of the cells with different agonists. On d5 p.i. double-deficient platelets were refractory to the GPVI-specific agonist convulxin and to the CLEC-2-specific agonist rhodocytin, respectively, as neither activated integrin αIIbβ3 (Fig 3.19A) nor degranulation-dependent P-selectin exposure was observed on the surface of the cells (Fig 3.19B). The same results were obtained on d6 p.i. (data not shown). Interestingly, no significant differences in integrin αIIbβ3

activation upon stimulation with the agonists ADP, U46619, combination of ADP+U46619 and thrombin were observed compared to controls (Fig 3.19A). However, degranulation-dependent P-selectin exposure was slightly but significantly decreased upon stimulation with thrombin in double-deficient animals, whereas responses to ADP and combination of ADP+U46619 were not significantly altered (Fig 3.19B, d5 p.i.). This observation is in line with a thrombin defect that has been reported in JAQ1-treated animals on d3 p.i. of the antibody by our group[115], which is -however- described to be lost at later time points. To test whether in double-deficient mice the thrombin defect was also lost at later time points, the same activation studies in double-deficient platelets were again performed on d6 p.i. where the thrombin-defect was -as expected- found to be further minimized (Fig 3.19C+D).
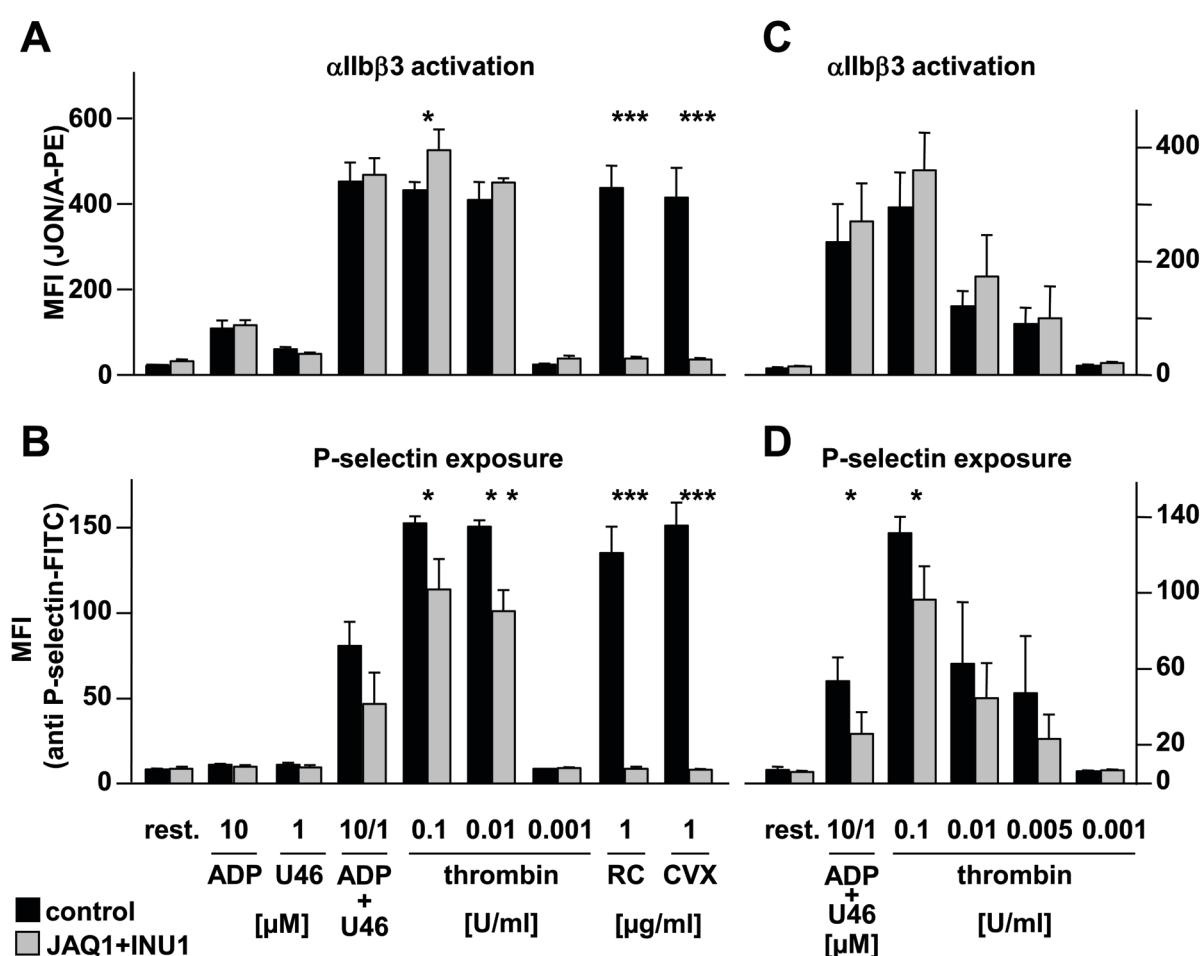
Fig 3.19 Flow cytometric analyses of GPVI-CLEC-2 double-deficient platelets. Integrin $\alpha IIb\beta 3$ activation (JON/A-PE, A+C) and degranulation-dependent P-selectin exposure (B+D) in platelets. Animals were tested on d5 (A+B) or d6 (C+D) post injection of PBS (control, black) or antibody mixture JAQ1+INU1 (100 µg and 200 µg, respectively, gray). Washed blood was incubated with the indicated agonists and analyzed on a FACSCalibur. Data shown are mean fluorescence intensities (MFI) ± SD (n=5 mice per group, representative of three individual experiments). Abbreviations: ADP= adenosine diphosphate; U46= U46619; RC= rhodocytin; CVX= convulxin. ***p<0.001. (Bender M[§], May F[§] *et al.*, in revision).

Under conditions used in flow cytometry studies, platelets and the activating agonists are significantly diluted. In contrast, under conditions of standard aggregometry, platelet aggregation is amplified by the released "second wave" mediators ADP and TxA_2. To analyze whether this might augment the observed thrombin defect in GPVI-CLEC-2 double-deficient platelets, the cells' response to different agonists was tested in aggregometry studies (Fig 3.20). Similar to the results obtained by FACS, no aggregation was observed in double-deficient platelets upon activation with the GPVI-specific agonists collagen, CRP or convulxin and the CLEC-2-specific agonist rhodocytin at all concentrations tested (Fig 3.20A). The thrombin-defect that was observed in flow cytometry studies (Fig 3.19) was also slightly visible under conditions of aggregometry. However, only intermediate concentrations of 0.0075 U/ml thrombin led to a significantly reduced aggregation in GPVI/CLEC-2 double-deficient platelets compared to controls, whereas upon all other tested concentrations of thrombin the platelets aggregated normally (Fig 3.20B+C). Similar to the stimulation with intermediate thrombin concentrations, upon activation with intermediate concentrations (0.1 µM) of the TxA_2 analog U46619, slightly reduced aggregation was observed in double-deficient platelets. Again, compared to controls no significant differences were observed using high and low concentrations of the agonist (Fig 3.20B+C). Interestingly, upon activation with the agonist ADP, no detectable differences were found in CLEC-2/GPVI double-deficient platelets. As only small differences in the aggregation response were observed in double-deficient platelets upon activation with intermediate concentrations of the agonists thrombin and U46619, it was proposed that this minor defect would have probably no major impact on platelet activation *in vivo*.

Together, these results demonstrate that ITAM and hemITAM signaling pathways in GPVI/CLEC-2 double-deficient platelets are completely absent. However, overall normal responses to G protein-coupled agonists were preserved.
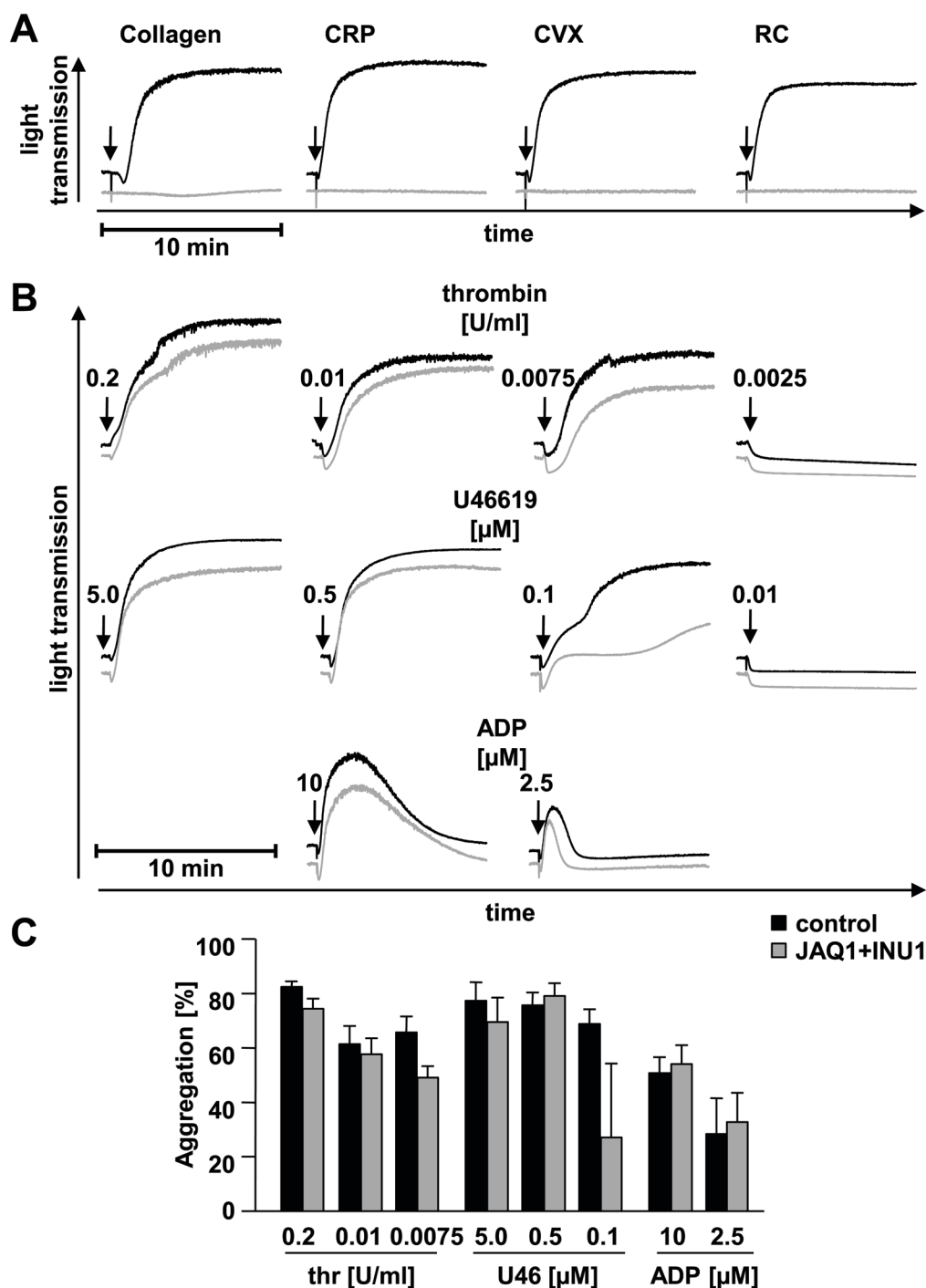
Fig 3.20 Aggregometry studies using GPVI-CLEC-2 double-deficient platelets. Washed platelets from control (black) or JAQ1+INU1-treated (gray) mice were stimulated with the indicated agonists and experiments were performed in the presence of 70 µg/ml human fibrinogen. Thrombin stimulation was performed in the absence of human fibrinogen. Light transmission was recorded on an aggregometer. ADP measurements were performed using platelet-rich plasma. The results shown are representative of 6 individual experiments. A+B representative aggregation curves. Abbreviations and concentrations used: Coll= collagen 10 µg/ml, CRP= collagen related peptide 20 µg/ml, CVX= convulxin 0.48 µg/ml, RC= rhodocytin 0.24 µg/ml. C. Bar graphs of results obtained by aggregometry. Abbreviations: thr= thrombin, U46= U46619, ADP= adenosine diphosphate. *p<0.05, **p<0.01, ***p<0.001. (Bender M[§], May F[§] *et al.*, in revision).

3.3.3 *In vivo* analysis of antibody-induced GPVI and CLEC-2 double-deficiency in mice

To analyze whether the receptors GPVI and CLEC-2 have redundant functions in hemostasis, tail bleeding times were determined in double-deficient mice. It was published previously that JAQ1-treated mice displayed only mildly prolonged bleeding times compared to controls[66]. Furthermore, in this thesis it was demonstrated that INU1-treated mice showed moderately increased and generally variable tail bleeding times (see Fig 3.11). Both results were accomplished in our laboratories using the filter paper method where upon amputation of the tail tip the resulting blood drops are absorbed by a filter paper without making contact with the wound site.

Utilizing the same assay, notably, the depletion of both (hem)ITAM-bearing receptors virtually lead to a complete loss of hemostatic function evident by infinite tail bleeding times (Fig 3.22A) and the lack of reduction in blood drop size on the filter paper during the entire observation period of 20 min (Fig 3.22B). Thus, GPVI/CLEC-2 double-deficient mice had to be cauterized to prevent an excessive blood loss.

In a second model of tail bleeding time comparable results were observed. Here, bleeding from the tail wound into saline (0.9% NaCl, 37°C) was monitored. Whereas in most control mice (14/15) bleeding stopped within 5 min after injury, 12 out of 18 double-depleted mice showed infinite bleeding times (Fig 3.22C) and none of the residual 6 animals could stop bleeding in less than 6 min. Additionally, the volume of blood loss as a measure of the severity of bleeding was analyzed in this model (Fig 3.22D). The lost blood volume was constantly very low in control (30.5 ± 107.5 µl), JAQ1- (90.9 ± 128.5 µl) and INU1-treated animals (7.8 ± 14.9 µl), whereas double-deficient mice suffered from an enormous blood loss (307.5 ± 223.8 µl). These results clearly demonstrate that the receptors GPVI and CLEC-2 have redundant functions in hemostasis.
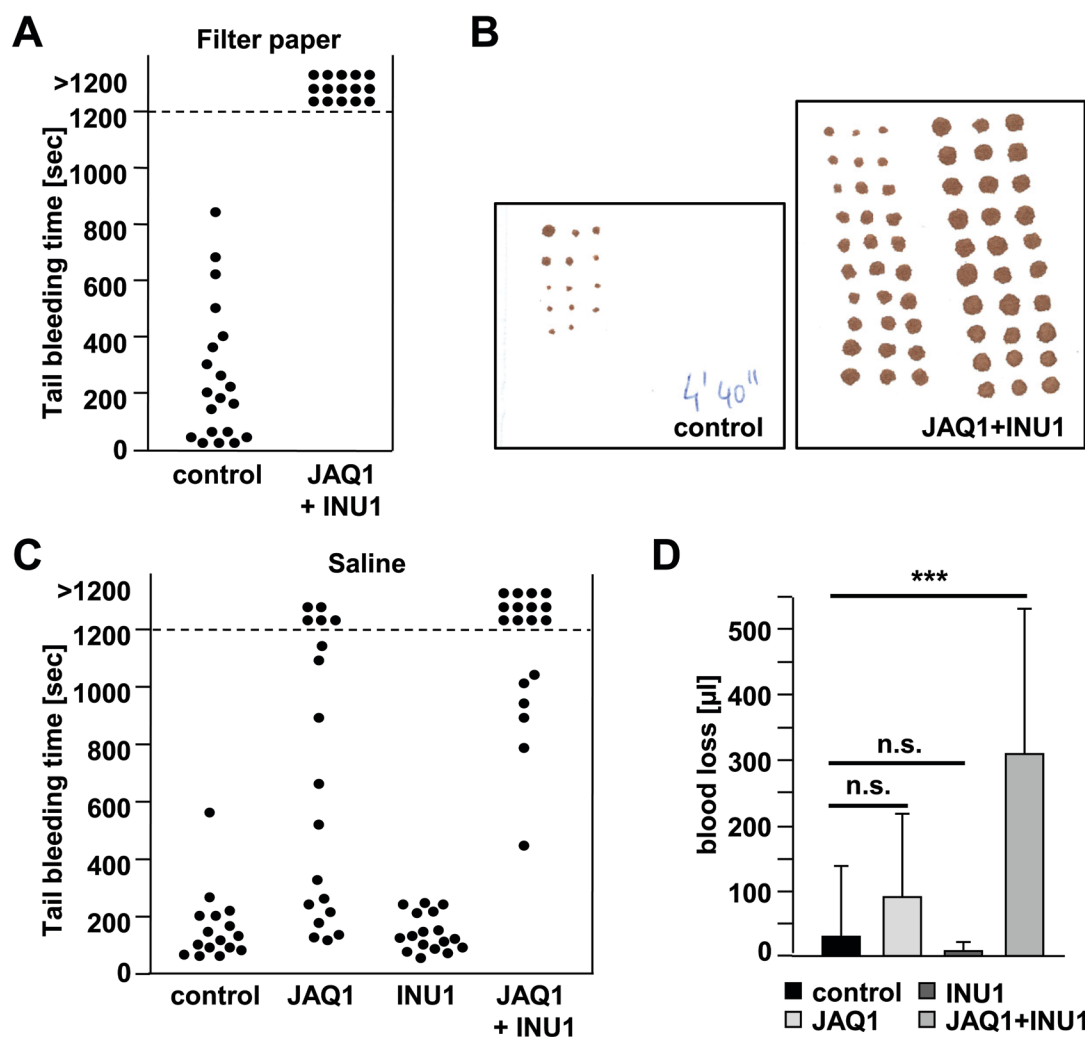
Fig 3.21 Infinite tail bleeding times in control and JAQ1+INU1-treated mice. Mice received vehicle (PBS) JAQ1 (100 µg), INU1 (200 µg) or JAQ1+INU1 (100 µg and 200 µg) and were analyzed on d5-6 p.i.. A+C. Each symbol represents one individual. Tail bleeding times were performed by amputation of a 1 mm segment of the tail tip of anesthetized mice. A. Subsequently, the blood drop was absorbed with a filter paper every 20 sec and bleeding was determined to have ceased when no blood was observed on the filter paper. B. Representative pictures of a filter paper from control (left panel) and double-deficient mice (JAQ1+INU1, right panel). Note the size of the blood drop as a measure of the severity of blood loss. C. Upon amputation of the tail tip, the tails were positioned in 37°C saline (0.9% NaCl). Bleeding was determined to have ceased when it stopped for >1min. D. Blood loss was determined by weight against a NaCl filled reference. ***p<0.001. (Bender M[§], May F[§] *et al.*, in revision).

Additionally, the effect of double receptor depletion on pathological thrombus formation was studied in the $FeCl_3$-induced injury model in mesenteric arterioles. In control mice, small aggregate formation was observed at 7.8 ± 1.2 min after injury (Fig 3.22A, left) with complete vessel occlusion at 16.4 ± 2.2 min. Formation of small aggregates followed similar kinetics in GPVI and CLEC-2 single-depleted mice, whereas in most cases the vessels did not occlude (GPVI-depleted: 8/12; CLEC-2-depleted: 7/10). Remarkably, the onset of small aggregate formation was significantly delayed in GPVI/CLEC-2-depleted mice compared to controls and single-deficient animals (Fig 3.22A, left) and the maximal vessel stenosis reached within the 40-min observation period was strongly decreased compared to all other groups (Fig 3.22A,

right). As a consequence, blood flow was maintained in all vessels (12/12) of GPVI/CLEC-2-depleted mice. These data demonstrate that the lack of both receptors, GPVI and CLEC-2, results in abolished occlusive thrombus formation further suggesting redundant functions of the two receptors *in vivo*.
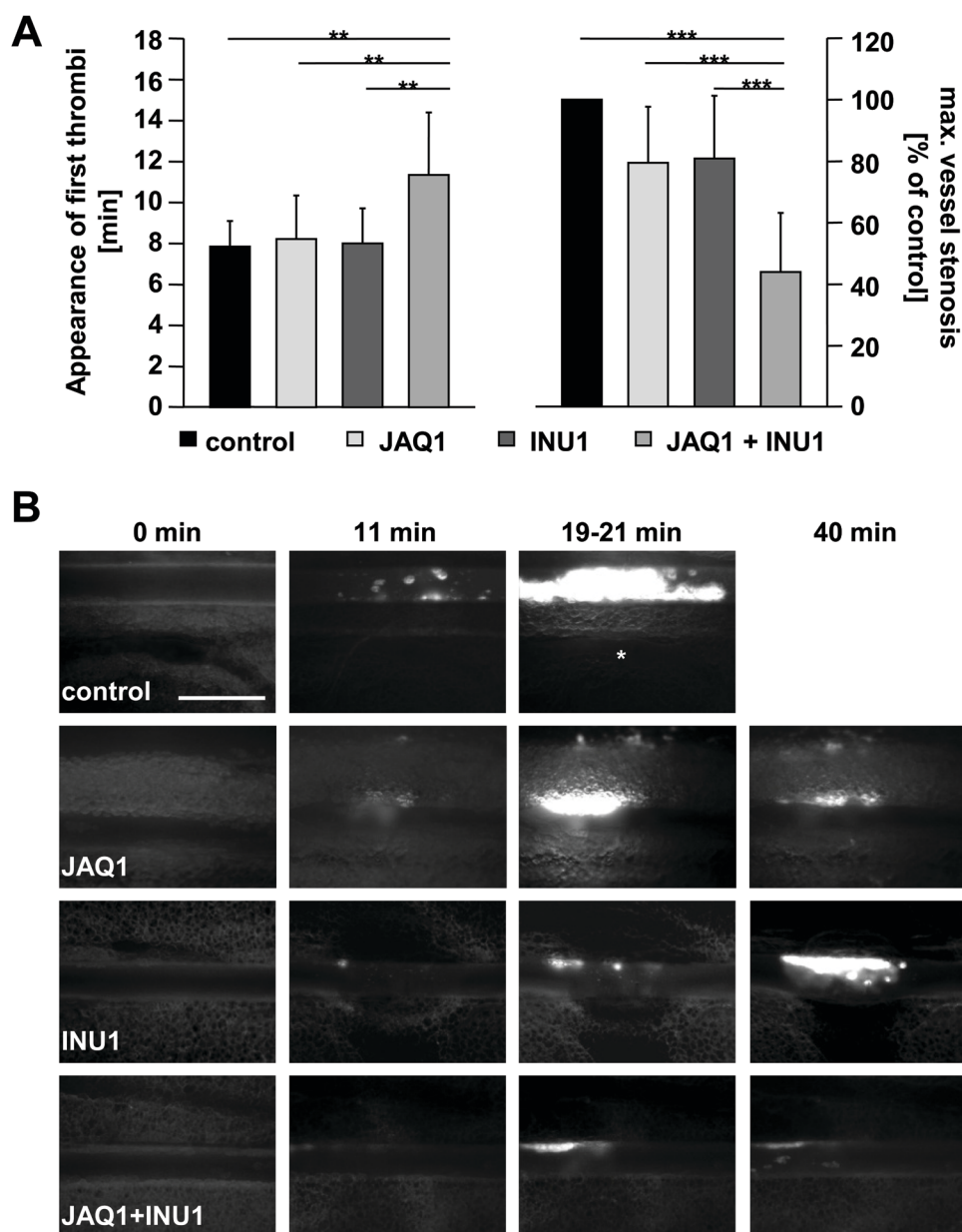
Fig 3.22 Abolished thrombus formation in JAQ1+INU1-treated mice. Mice received vehicle (PBS, control), JAQ1 (50 µg), INU1 (100 µg) or JAQ1+INU1 (50 µg and 100 µg) and were analyzed on d5-6 p.i.. Mesenteric arterioles were injured with $FeCl_3$ and adhesion and thrombus formation of fluorescently-labeled platelets was monitored *in vivo* by fluorescence microscopy. A. Time to appearance of first thrombus >10 µm (left panel) and vessel occlusion measured as maximal vessel stenosis (in percent of control, right panel) are shown. B. Representative images are depicted. Bar, 100 µm. The asterisk indicates occlusion of the vessel. n= minimum 5 mice per group. Data are representative of two individual experiments. **$p<0.01$, ***$p<0.001$. (Bender M[§], May F[§] *et al.*, in revision).

3.3.4 Analysis of *Gp6*^{-/-}/CLEC-2-deficient mice

As it could not be excluded that the JAQ1+INU1 antibody-induced deficiency of GPVI and CLEC-2 had unwanted side effects, the consequences of CLEC-2 deficiency were studied in newly generated GPVI knock-out mice (*Gp6*^{-/-}, Bender M, May F *et al.*, manuscript in preparation) on d5-6 after treatment with the α-CLEC-2 antibody INU1 (*Gp6*^{-/-}/INU1). The *Gp6*^{-/-} mice were generated by Markus Bender and the experiments were performed in collaboration in our laboratories.

Comparable to the results obtained in control mice that were treated with INU1, *Gp6*^{-/-} mice displayed a profound thrombocytopenia upon treatment with 200 µg INU1 (compare Fig 3.6A, data not shown). Similarly, on days 5 and 6 post treatment the resulting *Gp6*^{-/-}/CLEC-2-deficient (*Gp6*^{-/-}/INU1) mice showed normal platelet counts. Furthermore, these platelets fully lacked CLEC-2 expression (Fig 3.23A). It was thus decided to perform all further experiments on d5-6 p.i. of 200 µg INU1. To analyze whether platelets from these mice were physiologically functional and/or different to those obtained from JAQ1+INU1-treated mice, basal surface expression levels of glycoproteins were measured by flow cytometry. It was found that *Gp6*^{-/-}/INU1 platelets -as expected- specifically lacked GPVI and CLEC-2, whereas expression of other surface proteins was largely unaltered compared to controls (wildtype, wt; Fig 3.23A). Similar to JAQ1+INU1-treated mice, increased expression levels of GPIb were noted in *Gp6*^{-/-}/INU1 mice compared to controls, which could possibly be explained by the platelet size that was slightly but not significantly increased. Notably, expression levels of all other glycoproteins were not significantly altered. Likewise, increased platelet counts were observed in *Gp6*^{-/-}/INU1-treated animals that were probably due to the rapid production of new platelets upon thrombocytopenia that was induced by the antibody treatment. These results showed that treatment of *Gp6*^{-/-} mice with the α-CLEC-2 antibody INU1 had no overall impact on the expression levels of other platelet glycoproteins.

To test whether the downstream signaling pathways of the cells were affected, flow cytometric studies upon activation were performed. Here, as expected and similar to GPVI/CLEC-2 double-depleted mice, *Gp6*^{-/-}/INU1 platelets were refractory to the GPVI-specific agonists CRP and convulxin and to the CLEC-2-specific agonist rhodocytin, respectively, whereas all other tested activation pathways were unaffected (Fig 3.23B+C). Notably, in *Gp6*^{-/-}/INU1 platelets no defect in response to thrombin was observed even at intermediate concentrations of the agonist (data not shown). This strengthened the hypothesis that the observed thrombin defect in JAQ1+INU1-treated mice was mediated by JAQ1-treatment (see Fig 3.19 and Fig 3.20). Furthermore, these findings indicate that the specific down-regulation of CLEC-2 by treatment with INU1 is not only possible in wildtype but also in *Gp6*^{-/-} mice.
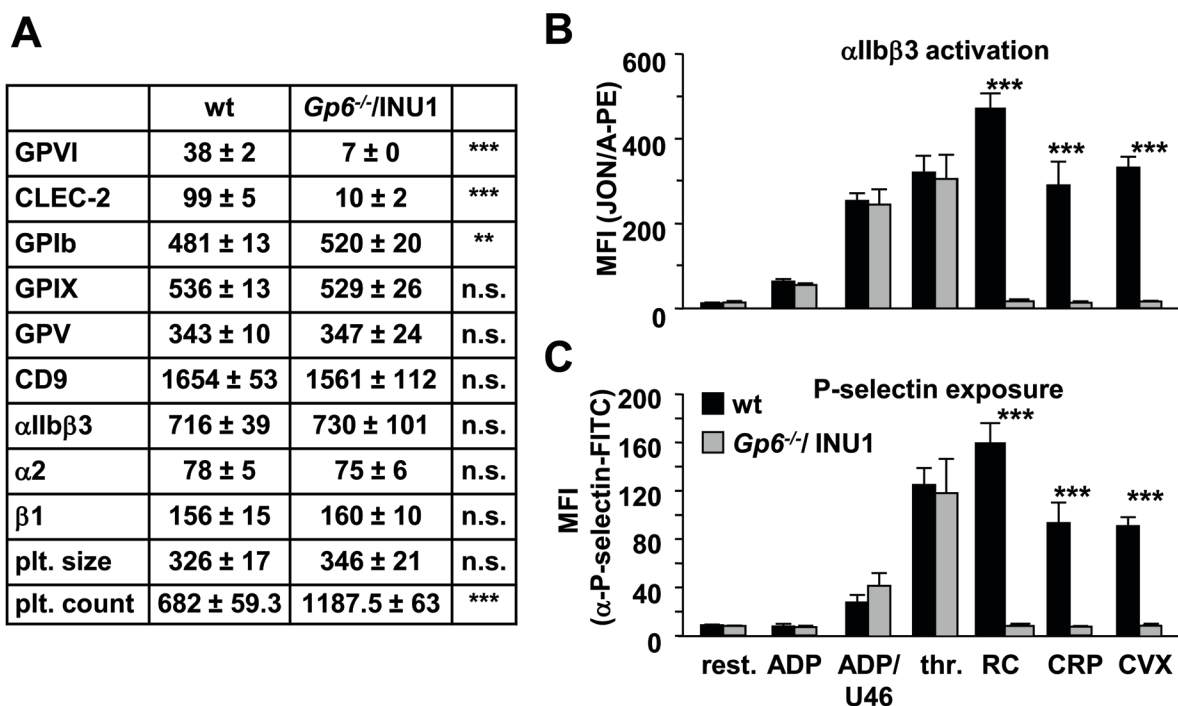
A

	wt	*Gp6*-/-/INU1	
GPVI	38 ± 2	7 ± 0	***
CLEC-2	99 ± 5	10 ± 2	***
GPIb	481 ± 13	520 ± 20	**
GPIX	536 ± 13	529 ± 26	n.s.
GPV	343 ± 10	347 ± 24	n.s.
CD9	1654 ± 53	1561 ± 112	n.s.
αIIbβ3	716 ± 39	730 ± 101	n.s.
α2	78 ± 5	75 ± 6	n.s.
β1	156 ± 15	160 ± 10	n.s.
plt. size	326 ± 17	346 ± 21	n.s.
plt. count	682 ± 59.3	1187.5 ± 63	***

Fig 3.23 CLEC-2-depleted *Gp6*-/- platelets lack GPVI and CLEC-2 signaling but show no major alterations in other signaling pathways. Analyses of platelet glycoprotein expression (A), integrin αIIbβ3 activation (JON/A-PE, B) and degranulation-dependent P-selectin exposure (C) was determined by flow cytometry on d5 p.i. of PBS (wt) or INU1 (200 µg, *Gp6*-/-/INU1) on a FACSCalibur. Results are expressed as mean fluorescence intensity (MFI) ± SD for n=6 mice per group. A. Mean platelet (plt.) size is given as mean FSC and was determined by FSC characteristics. Mean platelet count was determined using Sysmex and is given in platelets /µl *10^{-3}. B+C. Washed blood was incubated with the indicated agonists. Abbreviations and agonist concentrations: n.s.= not significant, ADP= adenosine diphosphate: 10 µM; U46(619): 3 µM; thr.= thrombin: 0.01 U/ml; RC= rhodocytin: 1 µg/ml; CRP= collagen related peptide: 10 µg/ml; CVX= convulxin: 1 µg/ml. **$p<0.01$, ***$p<0.001$. (Bender M[§], May F[§] *et al.*, in revision).

To further determine whether i) the two receptors GPVI and CLEC-2 play redundant roles in hemostasis and thrombosis and whether ii) the effect seen in JAQ1+INU1-treated mice was due to an antibody-induced side effect, tail bleeding times and pathological thrombus formation were analyzed in *Gp6*-/-/INU1 mice.

In the tail bleeding time assay performed by the filter paper method, no significant increase of bleeding times in *Gp6*-/- mice was observed compared to controls. This finding was in line with results from other groups, who had analyzed the constitutive knock-out of GPVI and also found no alteration of bleeding times[113-114]. Furthermore, it was previously shown by our group that JAQ1 treatment alone only mildly affects hemostasis[66,86,115] (see also Fig 3.21). Similar to double-depleted mice (JAQ1+INU1, Fig 3.21), *Gp6*-/-/INU1 mice showed a severe hemostatic defect with infinite bleeding times compared to controls (11/12, Fig 3.24A+B) mirroring the effect observed in JAQ1/INU1 antibody-induced double-deficient mice. Again, animals had to be cauterized to prevent an excessive blood loss. These results further underline the hypothesized redundant function of the two receptors GPVI and CLEC-2 in hemostasis.

Additionally, the effect of CLEC-2 receptor depletion in $Gp6^{-/-}$ mice on pathological thrombus formation was studied in the $FeCl_3$-injury model in mesenteric arterioles. Here, in all control mice formation of small platelet aggregates was observed at 6.4 ± 0.9 min after injury with $FeCl_3$ (Fig 3.24C, left) leading to complete vessel occlusion at 16.2 ± 2.0 min (Fig 3.24C, right). Remarkably, compared to controls the onset of small aggregate formation was significantly delayed in $Gp6^{-/-}$/INU1-treated mice (Fig 3.24C, left). Furthermore, the ratio of thrombi size to vessel diameter was significantly decreased (data not shown). As a consequence, blood flow was maintained in the majority of all vessels (8/12, Fig 3.24C, right). Furthermore, even in the occluded vessels of $Gp6^{-/-}$/INU1-treated animals a significant delay (4/12, 27.5 ± 4.6 min) was observed compared to controls (p= 0.013). The phenotype observed in $Gp6^{-/-}$/INU1-treated mice was found to mirror the effect seen in JAQ1/INU1 antibody-induced GPVI/CLEC-2 double-deficient mice.
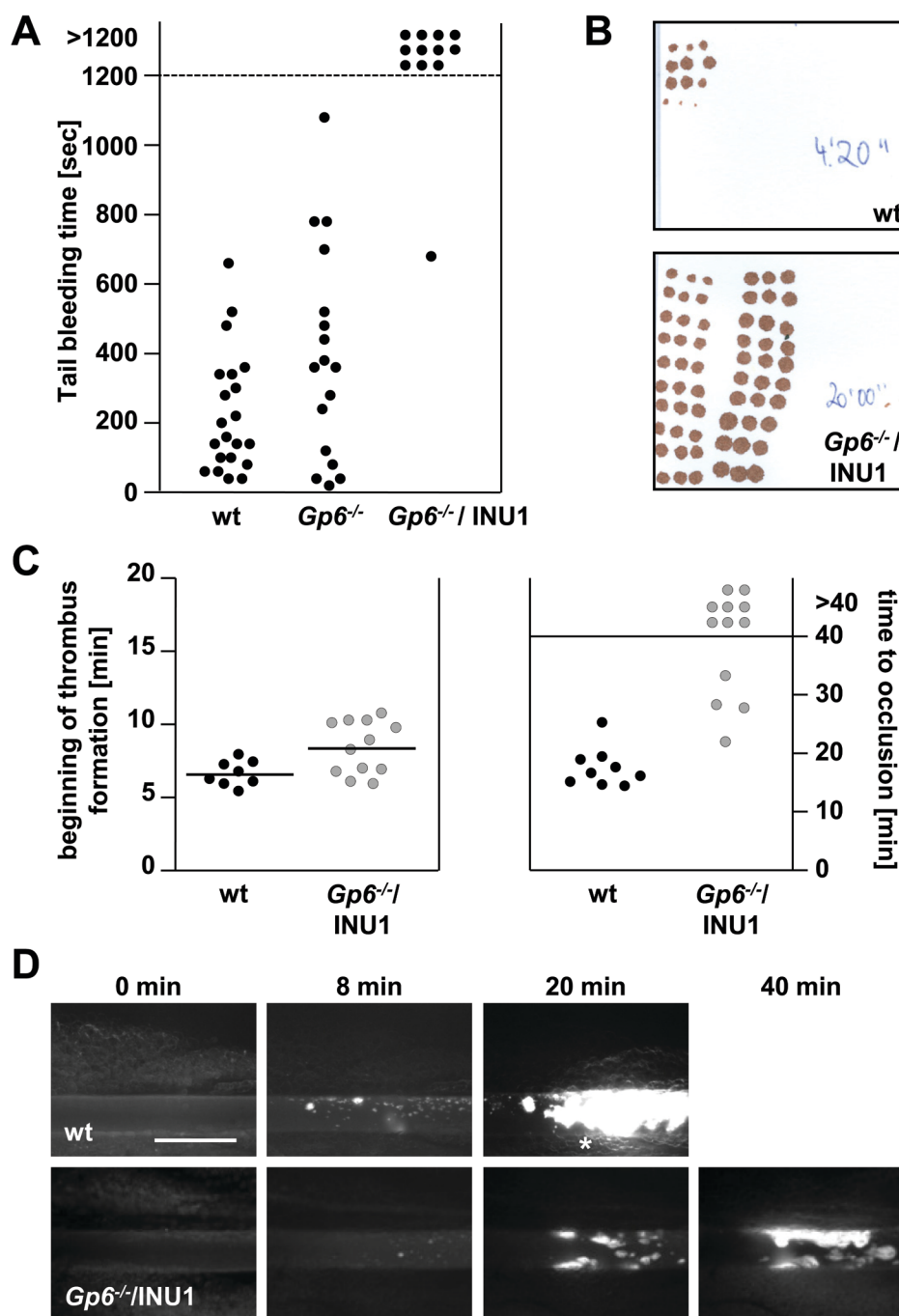
Fig 3.24 Tail bleeding times and pathological thrombus formation in control and CLEC-2-depleted *Gp6*^{-/-} mice. Mice received vehicle (PBS, wt) or INU1 and were analyzed on d5-6 p.i.. A+B. Tail bleeding times were performed by amputation of a 1 mm segment of the tail tip and blood was absorbed with a filter paper every 20 sec. Bleeding was determined to have ceased when no blood was observed. A. Each symbol represents one individual. B. Representative pictures of a filter paper from control (upper panel) and CLEC-2-depleted *Gp6*^{-/-} mice (*Gp6*^{-/-}/ INU1, lower panel). Note the size of blood drop as a measure of the severity of blood loss. C+D. Mesenteric arterioles were injured with FeCl$_3$ and adhesion and thrombus formation of fluorescently-labeled platelets was monitored *in vivo* by fluorescence microscopy. Data shown are representative of two individual experiments. A. Appearance of first thrombus (left) and time to vessel occlusion (right) are shown. Each symbol represents one arteriole. B. Representative images are depicted. Bar, 100 µm. The asterisk indicates occlusion of the vessel. (Bender M[§], May F[§] *et al.*, in revision).

4 Discussion

Platelets are a crucial component of the blood system as their activation and aggregation is essential to prevent blood loss and to seal vascular injuries. However, under pathological conditions, uncontrolled platelet aggregation may also cause arterial occlusion or embolism resulting in severe diseases such as myocardial infarction or stroke. Unfortunately, any currently available anti-thrombotic therapy of these diseases comes with unwanted side effects such as a high risk of bleeding. Therefore, not only the discovery of novel pathways of platelet activation but also the identification of new methods of platelet inhibition is essential for the development of future save anti-thrombotic therapies in human patients.

The C-type lectin-like receptor 2 (CLEC-2) has been proposed as such a new anti-thrombotic target in several studies[12,14]. At the beginning of the presented thesis, the role of CLEC-2 in hemostasis and thrombosis was not known. In addition, neither an α-murine CLEC-2 antibody nor a CLEC-2 knock-out mouse was available to analyze the role of CLEC-2 in experimental models of arterial thrombosis. Therefore, in the current study, the first α-murine CLEC-2 antibody, termed INU1, was generated. Importantly, it could be demonstrated for the first time that injection of INU1 in mice leads to the specific down-regulation of CLEC-2 from the platelet surface *in vivo*. This phenomenon of a "knock-out like" phenotype allowed the first studies to assess the role of CLEC-2 in hemostasis and thrombosis. In addition to treatment of mice with the full IgG of the antibody, also administration of INU1-Fab-fragments (INU1-Fab) was characterized in mice. Surprisingly however, treatment with INU1-Fab resulted in lethality and this very unexpected effect was further analyzed. Furthermore, during the course of this study a second α-murine CLEC-2 antibody, termed INU2, was successfully generated.

Antibody-mediated down-regulation as a novel method of anti-thrombotic therapy had already been presented in a former work from our group, namely the transient "immunodepletion" of GPVI, the major platelet collagen receptor[66]. To investigate a potential reciprocal regulation of GPVI and CLEC-2 expression and signaling[94], in the second part of the present thesis, antibody-induced double-deficiency of GPVI and CLEC-2 in mice was analyzed and revealed unexpected redundant functions of the receptors in hemostasis and thrombosis.

4.1 Challenges during the generation of anti-mouse CLEC-2 antibodies

In the current study, the first rat anti-murine CLEC-2 antibody, termed INU1, was generated (Fig 3.2). In the first attempt, only one clone from more than 1,500 resulting hybridoma clones stably expressed an α-CLEC-2 antibody. Two other fusions of spleen cells from further immunized rats were performed; each yielding similarly high numbers of tested

hybridoma clones; however, no useful α-CLEC-2 antibody was developed (data not shown). Three additional attempts where rats were repeatedly immunized with native CLEC-2 protein immuno-precipitated from platelet lysate using INU1 also failed to produce another α-CLEC-2 antibody (data not shown). Thus, another fusion had to be performed using rats immunized with the mCLEC-2 Fc-fusion protein until the second α-murine CLEC-2 antibody, termed INU2, was successfully generated (Fig 3.16). This delicate proportion exemplifies the challenges underlying the generation of monoclonal antibodies. A reason why the antibody generation emerged to be difficult could be that the protein structure of mouse and rat CLEC-2 share a high homology of 90.0% (Fig 4.1) especially in the extracellular domain of the protein. Thus, native CLEC-2 protein present in murine platelet lysates or immunoprecipitations used for immunization may not be very antigenic in the rat.

```
CLEC2_rattus     MQDEDGYITLNIKPRKQALSSAEPASSWWRLTALILLISTMGLVAGLVALGIMSVTQQKY 60
CLEC2_mus        MQDEDGYITLNIKPRKQALSSAEPASSWWRVMALVLLISSMGLVVGLVALGIMSVTQQKY 60
                 ******************************: **:****:**** .**************


CLEC2_rattus     LLAEKENLSATLQQLAKKFCQELIRQSEIKTKSSFEHKCSPCATKWRYHGDSCYGFFRRN 120
CLEC2_mus        LLAEKENLSATLQQLAKKFCQELIRQSEIKTKSTFEHKCSPCATKWRYHGDSCYGFFRRN 120
                 *********************************:**************************


CLEC2_rattus     LTWEDSKLFCSEQNATLVKTASQSTLKYITDRITSVRWIGLSRQNSKKDWMWEDSSVLHN 180
CLEC2_mus        LTWEESKQYCTEQNATLVKTASQSTLDYIAERITSVRWIGLSRQNSKKDWMWEDSSVLRK 180
                 ****:** :*:***************.**::***************************::


CLEC2_rattus     NSIDLSRNTEENMNCAYLHNGKIHPASCTERHYLICERNAALTRVEQLL 229
CLEC2_mus        NGINLSGNTEENMNCAYLHNGKIHPASCKERHYLICERNAGMTRVDQLL 229
                 *.*:** ********************.***********.:***:***
```

Fig 4.1 Alignment of rat and mouse CLEC-2 protein. Rat (CLEC-2_rattus, accession no. GU357482) and mouse (CLEC2_mus, accession no. BC064054) CLEC-2 protein share 90.0% aa identity. Alignment starts with the intracellular domain and ends with the extracellular domain (from left to right).

4.2 The platelet activating receptor CLEC-2 is essential in the process of thrombus formation

4.2.1 Treatment with INU1 leads to down-regulation of CLEC-2 *in vivo*

In the present thesis it was demonstrated that treatment with INU1 led to loss of CLEC-2 on circulating platelets in mice. Also, it was shown that murine CLEC-2 can be specifically targeted and functionally inactivated by the antibody INU1 *in vivo*. Remarkably, this *in vivo* inhibition by far exceeded the inhibitory potential of the antibody *in vitro*, as it is not based only on blockade of the receptor. Rather, INU1 induced the irreversible loss of CLEC-2 from circulating platelets (Fig 3.6), a process previously reported only for GPVI in mouse and human platelets upon treatment of mice with the specific α-GPVI antibodies JAQ1, 2 and 3[66]. The complete loss of functional CLEC-2 in platelets of INU1-treated mice was confirmed by different approaches: Firstly, these platelets were completely refractory to activation with

rhodocytin (Fig 3.6, Fig 3.7, Fig 3.8), whereas Fab-fragments of the antibody (INU1-Fab) had only limited inhibitory potential *in vitro* (Fig 3.5). Secondly, flow cytometric analyses confirmed the complete loss of CLEC-2 from the surface of circulating platelets within 24 h after INU1 injection (Fig 3.6), and thirdly, immunoprecipitation confirmed a prolonged absence of the protein for at least 5 days (Fig 3.6).

The route of CLEC-2 down-regulation has not yet been identified, but mClec-2A expressed in human embryonic kidney 293T cells was shown to be proteolytically cleaved to produce a soluble extracellular fragment[27]. This indicates that the loss of CLEC-2 could occur through ectodomain shedding, but also internalization/degradation might contribute to this process. Studies from our laboratory have previously demonstrated that antibody-induced down-regulation of GPVI can occur through both of these routes, ectodomain shedding as well as internalization/degradation, and that these are regulated by diverging signaling pathways downstream of the receptor *in vivo*[85,89]. These are, however, difficult to assess as neither GPVI[66,78,101-102] nor CLEC-2 can be down-regulated in murine platelets by antibodies *in vitro*. This implies that additional signals or a certain environment may be required for this process to occur that is absent in the used *in vitro* assays such as possibly shear forces present in the blood stream. It seems likely, however, that the Fc-part of the antibody or receptor dimerization is not required for CLEC-2 down-regulation *in vivo*, as Fab-fragments of the first batch were equally efficient in receptor down-regulation compared with the intact IgG (see Fig 3.6).

Upon INU1 injection (8 µg/g body weight), CLEC-2 was not detectable in platelets for minimum 7 days, although the normal life span of mouse platelets is only approximately 4-5 days[116], indicating that the antibody may also affect megakaryocytes. Indeed, neither the antibody INU1 nor the receptor CLEC-2 itself was detectable on megakaryocytes in bone marrow 60 min after antibody injection (data not shown); suggesting that down-regulation of the receptor occurs also in megakaryocytes. Furthermore, preliminary data suggest that a second injection of INU1 on day 6 has no effect on circulating (CLEC-2–deficient) platelets but prolongs the absence of CLEC-2 (data not shown). Similar effects can be seen in JAQ1-treated mice where the "knock-out like" phenotype does, however, last for 2 weeks upon a single injection of 100 µg antibody per mouse[66,78,115]. This indicates that INU1 may affect only those megakaryocytes that produce the very next generation of platelets, but further studies will be required to test this hypothesis.

On the other hand, microparticle formation was observed (70% of gated events, David Stegner, personal communication; data not shown) in initial flow cytometric studies of platelets 30 min after INU1-treatment in mice (200 µg i.v.). This finding suggests that INU1-treatment could first induce microparticle formation in the treated animals and second elicit

receptor down-regulating mechanisms in megakaryocytes that produce the next generation of CLEC-2-deficient platelets.

To further analyze the down-regulation of CLEC-2, platelets were treated with monovalent INU1-Fab-fragments (INU1-Fab) prior to activation in aggregometry studies using several agonists. Here, it was observed that ADP-induced aggregation was slightly but significantly amplified (Fig 3.5), indicating that occupancy of the INU1 binding epitope on CLEC-2 by INU1-Fab induces subliminal signaling independently of receptor clustering. This notion may also be supported by the observation that INU1-Fab of the first batch induced transient thrombocytopenia to the same extent as the intact IgG in the first set of initial experiments. It is not clear whether the transient drop in platelet counts upon treatment with INU1 is mechanistically linked to the loss of CLEC-2, but it is tempting to speculate that INU1-opsonized platelets might become (partially) activated and transiently trapped in the reticulo-endothelial system where the actual loss of CLEC-2 could occur. In the case of JAQ-induced GPVI down-regulation, shedding of the receptor is associated with transient thrombo-cytopenia, whereas internalization/degradation can occur independently thereof[89].

To allow deeper analysis of the underlying mechanism of receptor down-regulation, a second α-CLEC-2 antibody, termed INU2, was recently generated. INU2 recognized a protein of an apparent molecular weight of ~35 kDa from platelet lysate, and the mCLEC-2 Fc-fusion protein on western blot and ELISA (Fig 3.16). However, it does not bind to native CLEC-2 protein on platelets as no signal was detected using flow cytometry (data not shown). This suggests that INU2 binds to a different epitope of CLEC-2 than INU1 which is free for binding of the antibody only under denaturing conditions. For studies on the mechanism of INU1-induced CLEC-2 down-regulation, INU2 will be used in experiments in the near future.

4.2.2 Thrombus instability in CLEC-2-depleted mice

Irrespective of the underlying mechanism, platelets from INU1-treated mice showed a specific loss of CLEC-2 activity that translated into a severe defect in thrombus growth and stabilization under flow conditions *in vitro* and *in vivo* (Fig 3.9, Fig 3.10 and Fig 3.12).

Similarly, impaired aggregate stabilization can also be seen in mice lacking functional stromal interaction molecule 1 (STIM1), an essential regulator of Ca^{2+} signaling in platelets[117-118]. These platelets display a selective defect in ITAM- and hemITAM-dependent activation, indicating that this signaling route is of importance not only for platelet activation on the ECM via GPVI but also for thrombus growth where the collagen/GPVI-interaction does not play a role[117-118]. In the light of the data reported in this thesis, it is tempting to speculate that the thrombus instability observed in the absence of STIM1 may be caused to a great extent by impaired CLEC-2 signaling. Similarly, the thrombus formation defects seen in mice lacking critical molecules of (hem)ITAM-signaling pathways, such as LAT[119] or PLCγ2[120], might also

be related to defective CLEC-2 signaling. This hypothesis is further strengthened by a study from our group demonstrating that mice carrying a hyperreactive mutant of PLCγ2 (*Plcg2*^{*Ali5/+*})

be related to defective CLEC-2 signaling. This hypothesis is further strengthened by a study from our group demonstrating that mice carrying a hyperreactive mutant of PLCγ2 (*Plcg2*$^{Ali5/+}$) showed markedly enhanced thrombus formation on collagen under flow *in vitro* and a prothrombotic phenotype *in vivo*[121].

Additionally, during the course of this thesis, several groups[59,62-63,122] published studies on CLEC-2 knock-out (*Clec-2*$^{-/-}$) mice concertedly reporting on lethality at the embryonic/ neonatal stages of development. To circumvent the lethality, Suzuki-Inoue *et al.*[63] studied the process of thrombus stabilization using fetal liver cell-chimeric *Clec-2*$^{-/-}$ (*Clec-2*$^{-/-BM}$) mice. Importantly, the authors' findings are consistent with the here presented results. In flow adhesion studies at a shear rate of 2,000 sec^{-1} single-cell adhesion of *Clec-2*$^{-/-BM}$ platelets on the surface of collagen was normal compared to WT, whereas thrombus formation and stable aggregate formation was significantly impaired *ex vivo*[63], thus strongly confirming our results. Furthermore, in a laser-induced injury model in mesenteric capillaries it was reported that in contrast to WT, *Clec-2*$^{-/-BM}$ platelets adhered to the vessel wall more loosely and were frequently washed away by the blood flow. Importantly, in *Clec-2*$^{-/-BM}$ mice the platelet aggregates/thrombi never occluded the capillaries[63]. In line with our findings, and by use of another *in vivo* thrombosis model, the authors therefore concluded that CLEC-2 is critically involved in the process of thrombus formation.

In contrast to these consistent findings, another study by Hughes *et al.* from the group of S.P. Watson -also using fetal liver cell-chimeric *Clec-2*$^{-/-BM}$ mice- did not confirm a requirement of CLEC-2 for platelet aggregation under shear flow on collagen[62]. However, an explanation for these contradictory results, as the authors themselves admit[62], is not easy to find. A low platelet count in the *Clec-2*$^{-/-BM}$ animals used by Suzuki-Inoue *et al.*[63] causing decreased platelet aggregation, as suggested by Hughes *et al.*[62], seems to be rather unlikely as platelet counts were measured by the authors and found to be unaltered. Rather, different experimental conditions or differences in generation of the *Clec-2*$^{-/-BM}$ mice used by Suzuki-Inoue *et al.*[63] and Hughes *et al.*[62] may be reasons for the discrepant results. Also, difficulties in the procedure of blood-sampling under conditions used by Hughes *et al.* could eventually have led to pre-activated platelets subsequently enhancing the process of thrombus formation thus leading to a false positive result.

Furthermore, Hughes *et al.* underlined their hypothesis that CLEC-2 signaling is not required for platelet aggregation under shear with the finding that tyrosine phosphorylation of CLEC-2 was not detectable in samples of lysed platelet aggregates derived from *ex vivo* flow adhesion studies[62]. However, as the samples were prepared after a perfusion period of 4 min, it is possible that CLEC-2 signaling was already switched off in the aggregated platelets. Thus, the tyrosine residue present in the intracellular hemITAM signaling motif of CLEC-2 could possibly be de-phosphorylated at this stage.

In summary, the findings presented in this thesis together with the study by Suzuki-Inoue *et al.* strongly point to a fundamental role of CLEC-2 in the process of thrombus formation and stabilization (see also Fig 4.2).

Additionally, in the current work the role of CLEC-2 in hemostasis was analyzed in mice by two different methods. The filter-paper method revealed that lack of CLEC-2 was associated with a significant but variable increase in tail bleeding times (Fig 3.11). However, compared with bleeding time prolongations induced by integrin $\alpha IIb\beta 3$- or GPIbα-inhibition[83] the effect was moderate. Importantly, in a second model of tail bleeding time analysis, where the wounded tail tip is located in saline (37°C), bleeding times of CLEC-2-deficient mice were unaltered compared to controls (Fig 3.21). In line with the latter result, the two groups mentioned above also reported on unaltered bleeding times in *Clec-2*[-/-BM] mice by use of the saline-method[62-63]. The discrepancy found in our own results could be due to the different experimental conditions present in the two models. It can be assumed that the high variability in bleeding times in the filter-paper model may reflect a rather mild hemostatic defect in CLEC-2-deficient mice that is caused by the described thrombus instability at the site of the tail wound. Based on this assumption, one may speculate that the lack of CLEC-2 signaling is to a certain extent compensated by signaling induced by other agonists present at the wound site (such as ADP, TxA$_2$, thrombin, etc.). Thus, slight differences in the injury may explain the variable results in experiments made with the filter-paper method. Additionally, these compensatory effects could have a stronger influence under the conditions of the saline-model, thus explaining the varying results between the two different models. In line with results in this study, a similar variability in tail bleeding times has previously been reported for other mouse lines with deficiencies in activatory platelet receptors, such as P2Y1[123] or the α2A adrenergic receptor[124]. Although bleeding times do not allow reliable prediction of a potential bleeding risk[125] one may speculate based on these results that anti-CLEC-2 therapy in human patients might be associated with a low risk of clinical hemorrhage.

So far, CLEC-2-deficient humans have not been reported and it is not clear whether mutations in the *CLEC-2* gene would have lethal effects on human development as it has been reported for mice. However, it can be anticipated that patients with an acquired CLEC-2 deficiency exist, caused by autoantibody-induced CLEC-2 clearing in platelets as it has previously been reported for GPVI-deficient patients[80,101]. The identification of such patients might help to further define the role of CLEC-2 in the physiology of human platelets.

In this study it was shown that CLEC-2 plays a fundamental role in thrombus formation in thrombosis and has an at least partial role in hemostasis. Despite the previously known activatory potential of the receptor[14,23] these results were unanticipated, as the only known endogenous ligand of the receptor, podoplanin, is expressed mainly in epithelial and tumor

cells and can therefore not account for CLEC-2 activation at sites of vascular injury[12,48]. An additional ligand of CLEC-2 that could -under physiological conditions- come into contact with CLEC-2 expressed on platelets has not been reported to date but is, however, eagerly awaited. In INU1-treated animals, thrombus formation under flow conditions *ex vivo* and also *in vivo* was severely defective in the antibody-induced absence of CLEC-2. This strongly suggests that the ligand(s) of the receptor is present in plasma or may be presented on the surface of or released by (activated) platelets (Fig 4.2).
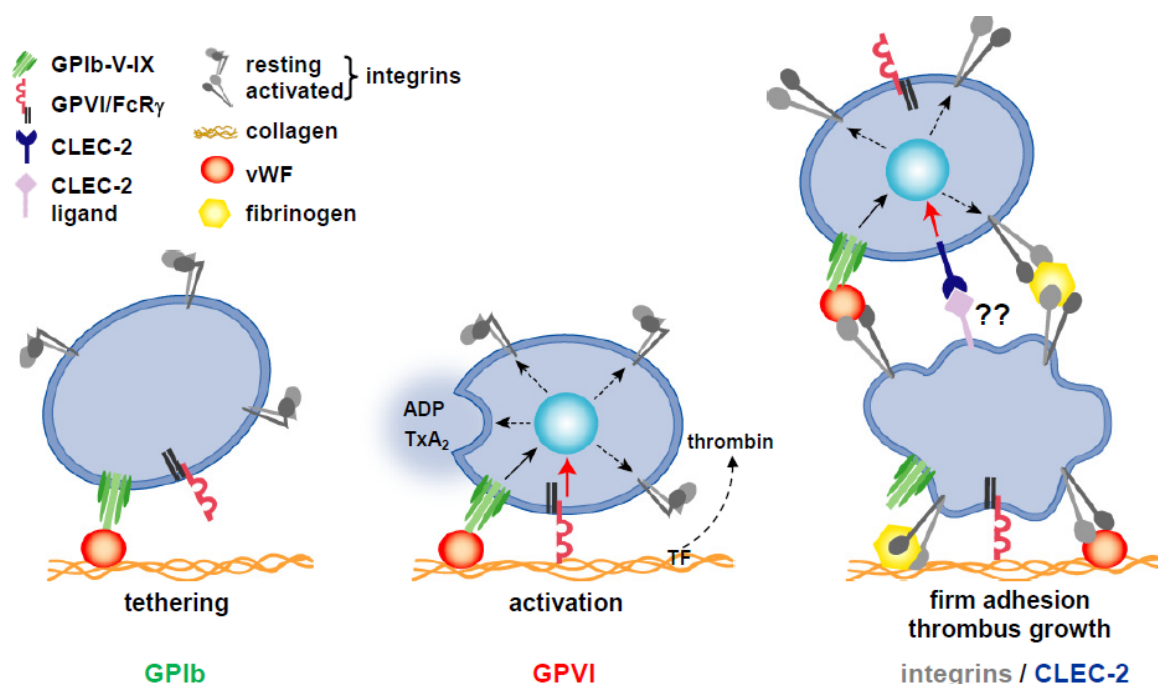

Fig 4.2 Adapted model of platelet adhesion to ECM at sites of vascular injury and subsequent thrombus formation. The forming thrombus is stabilized by signaling via CLEC-2, whose ligand/counter-receptor remains to be identified, and other receptors. Taken from: Nieswandt B, Pleines I and Bender M, Platelet adhesion and activation mechanisms in arterial thrombosis and ischemic stroke, 2011, in press.

Also it has been proposed that homophilic interactions of CLEC-2 itself could play a role in the process of thrombus formation[63] but this hypothesis has been questioned by others[62]. Furthermore, CLEC-2 ligand(s) could also be present on the injured vessel wall, but this may not be crucial for attachment of the first layer of platelets as indicated by unaltered formation of small aggregates at sites of injury in CLEC-2-deficient mice *in vivo* (Fig 3.12). This notion is also supported by the observation that CLEC-2-deficient platelets can attach normally to collagen under high shear flow conditions (Fig 3.9 and Fig 3.10), a process known to be driven mainly by GPIb, GPVI, and the integrins $\alpha2\beta1$ and $\alpha IIb\beta3$[7-8,126]. Rather, CLEC-2-dependent signaling appears to be required for establishing (activation-dependent) stable platelet-platelet contacts under flow conditions as revealed by the defective transition of newly recruited platelets to firm adhesion on the surface of collagen-adherent platelets *ex*

vivo. This process also appears to be crucial for stable thrombus formation *in vivo* as revealed by the constant release of individual platelets and frequent embolization of small aggregates from the surface of the developing thrombus in CLEC-2-deficient mice (Fig 3.12 and Fig 4.2). Therefore, not only CLEC-2[12,127] but also its possible ligand(s) could represent an interesting novel anti-thrombotic target. However, it is important to note that CLEC-2-deficient mice were not protected in another thrombosis model performed in our laboratory where injury of the aorta is mechanically induced by a single firm compression of the vessel (Fig 3.13), although a trend to a prolonged occlusion time was observed. This surprising result may be due to the lower shear rates present in a bigger vessel compared to small mesenteric arterioles. Here, other mechanisms could possibly compensate for the lack of CLEC-2 and thus mediate the process of thrombus stabilization, such as sufficient activation of platelets to the growing thrombus by "second wave" mediators like ADP and TxA_2 or locally produced thrombin. These mechanisms might be sufficient to stabilize the growing thrombus and the function of CLEC-2 might be circumvented under these conditions.

Additionally, in the present thesis CLEC-2-deficient mice were subjected to the tMCAO model as a standard model for ischemic stroke. While occlusive thrombus formation is the principal pathogenic event in myocardial infarction, the situation is more complex in ischemic stroke where infarct development often progresses despite sustained early reperfusion of previously occluded major intracranial arteries, a process referred to as "reperfusion injury"[128]. Increasing experimental evidence suggest that early platelet adhesion and activation events orchestrate a "thrombo-inflammatory" cascade in this setting, whereas the later phases of platelet aggregation and thrombus formation are not necessarily required (Nieswandt B, Pleines I and Bender M, Platelet adhesion and activation mechanisms in arterial thrombosis and ischemic stroke, 2011, in press). Based on this model, it may not be surprising that CLEC-2-deficient mice showed no reduction in infarct size and were not protected from stroke in the tMCAO model (Fig 3.14) as CLEC-2 is supposed to play a role in thrombus growth, which may not be a central pathomechanism in infarct progression. Therefore, CLEC-2 would probably not be suitable as a target for the treatment of cerebral ischemia.

4.3 CLEC-2 expression on immune cells

In the current study, the expression of CLEC-2 on murine immune cells was analyzed by staining with INU1 in flow cytometry. However, INU1 did not stain both $CD4^+$ and $CD8^+$ cells as well as B cells ($B220^+$ cells) isolated from lymph nodes and spleen. Furthermore, CLEC-2 was neither found on thymocytes ($CD4^+/CD8^+$ and $CD4^-/CD8^-$ cells) nor on peritoneal macrophages that were gated using the macrophage-specific marker F4/80 and stained with INU1 (Fig 3.4A).

Interestingly, CLEC-2 expression was clearly detectable by INU1-FITC on mouse peripheral CD11b$^+$/Gr1$^+$ double-positive blood neutrophils (Fig 3.4B, left) being in line with data shown by Kerrigan et al.[26]. However, the same population yielded positive MFI signals with the platelet-specific marker JON6-PE (α-integrin αIIbβ3) (Fig 3.4B, right), indicating that the CLEC-2 signal was not specifically derived from neutrophils but rather from platelets that were possibly captured by the immune cells. Furthermore, a compensation error was excluded. Also, the positive CLEC-2 signal detected on neutrophils was found to be decreased with reducing concentrations of platelets in the tested samples (data not shown). This led to the hypothesis that the gated neutrophil population was contaminated with platelets inducing the CLEC-2-positive signal.

This discrepancy between our results and Kerrigan et al.[26] is not easy to explain. However, it was further underlined by the finding that initially CLEC-2-negative splenic CD11b$^+$ cells (Fig 3.4A) showed an INU1-FITC-positive signal when co-incubated with platelets (Timo Vögtle, personal communication). An explanation for the observed differences could be that the polyclonal α-CLEC-2 antibody used by Kerrigan et al. bound to a different epitope from that targeted by INU1. Also, possibly a different isoform of the CLEC-2 protein could be expressed on immune cells that is not recognized by INU1. On the other hand, it could be hypothesized that CLEC-2 is not expressed on peripheral immune cells in mice but that the CLEC-2-positive signal on neutrophils observed by the authors as well as by us was derived from platelets. These platelets could have been either captured by immune cells in a direct interaction or were indirectly detected by the laser-beam of the FACS at the same time as neutrophils. This could also explain the finding by Kerrigan et al. that neutrophils from bone marrow and peritoneum showed only a very weak, if not unspecific, expression of CLEC-2[26] as those cells might not have been in contact with blood platelets during preparation of the samples. The authors concluded that CLEC-2 expression on neutrophils is up-regulated upon migration from the bone marrow to the blood, but then again down-regulated upon emigration into the peritoneum[26]. However, the authors could not confirm this mechanism in an in vitro assay included in their study. Furthermore, the authors concluded that CLEC-2 functions as an activatory receptor on neutrophils inducing phagocytosis using a stably CLEC-2-transfected NIH3T3 fibroblast cell line. Additionally it was reported that CLEC-2 promotes production of the pro-inflammatory cytokine tumor necrosis factor-α (TNF-α) in murine primary neutrophils stimulated with rhodocytin, but not the respiratory burst[26]. Recently, in line with the latter finding, another study by Chang et al. showed that rhodocytin elicited the release of the pro-inflammatory cytokines TNF-α and interleukin-6 (IL-6) in mouse RAW 264.7 macrophages and human THP-1 monocytic cells in vitro[129]. The authors thus proposed that rhodocytin may induce inflammatory responses via interacting with CLEC-2 on

monocytes and macrophages. However, the physiological relevance of this mechanism has to be determined.

4.4 INU1-Fab-fragment-induced lethality in mice

In the present thesis, the *in vivo* effects of Fab-fragments of the antibody INU1 (INU1-Fab) were assessed. It was expected that this treatment would have a minor effect on the immune system of challenged mice, because INU1-Fab lacks the Fc-fragment of the full IgG that is required for recognition of the antibody by immune cells and the complement system. In initial experiments, where a single batch of generated INU1-Fab was used, results were achieved that confirmed this hypothesis (Fig 3.6). Here, mice survived the treatment with the Fab-fragment.

Very unexpectedly, however, and in sharp contrast to these initial results, treatment with INU1-Fab generated in a second batch, led to 100% mortality in mice (Fig 3.15A). Also a third batch produced by the same method had an equivalent lethal effect in mice (data not shown). Therefore, another method of Fab-fragment preparation was utilized by uncoupled digestion using pepsin and DL-dithiothreitol and subsequent size separation after each digestion step via a Superdex (SD) column. Very surprisingly, such produced Fab-fragments (termed INU1-Fab^{SD}) were also lethal (Fig 3.15B). It seems that the lethal effect of INU1-Fab^{SD} is platelet- and CLEC-2-specific, as neither platelet-depleted nor CLEC-2-deficient mice died compared to control animals upon treatment with 50 µg INU1-Fab^{SD} (Fig 3.15C). Furthermore, even very low doses of 5 µg INU1-Fab^{SD} per mouse had a lethal effect (Fig 3.15C). This very surprising effect is in sharp contrast to treatment with the full IgG, which is very well tolerated by the animals and does not cause mortality.

A possible reason for the lethal effect could be that INU1-Fab treatment induced rapid platelet activation *in vivo* causing thrombotic events that ultimately led to stroke or lung embolism. Such activation would, however, be rather difficult to explain because none of the produced INU1-Fab batches elicited platelet aggregation *in vitro* under conditions of aggregometry (Fig 3.5 and data not shown). However, under *in vivo* conditions other factors could come into play that are not present in the *in vitro* assays, such as a possible interaction of platelets with immune- or endothelial cells. Also, neither integrin $\alpha2\beta1$- nor αIIb$\beta3$-blockage of platelets had a protective effect to treatment with INU1-Fab^{SD} (Fig 3.15D) further indicating that platelet aggregation did not cause the lethal effect.

It is interesting that treatment with the full IgG is less harmful to the animals compared to INU1-Fab. Possibly, binding of INU1-IgG to platelets could lead to agglutination of the cells. The opsonized platelets could then be removed from the blood stream in the reticulo-endothelial system of the spleen as they are easily detectable for immune cells via the Fc-portion of the full IgG. It could also be speculated that this mechanism is missing when mice

are treated with INU1-Fab, due to the lack of the Fc-portion of the full IgG. On the other hand, animals treated with Fab$_2$-fragments of INU1 survived this challenge (Fig 3.15B), arguing against this hypothesis. However, it remains difficult to explain why INU1-Fab treatment causes lethality. Possibly, upon binding of INU1-Fab to CLEC-2, maybe due to shear forces or other mechanisms minimal signaling of the platelets is induced *in vivo*. The activated INU1-Fab-bound platelets could then eventually release vasoactive substances causing vascular leakage and a severe anaphylactic shock reaction in the treated animals. Due to the very fast removal of INU1-IgG-bound platelets in the spleen, this effect does not occur upon treatment with INU1-IgG.

Indeed, some of the observations made, point to an anaphylactic shock reaction such as peripheral cyanosis observed on the tail veins of the treated animals. This finding could lead to a new hypothesis: Potentially, vascular integrity could be altered via CLEC-2 signaling in platelets. However, at this point it is unclear why a monovalent binding partner of CLEC-2, namely INU1-Fab, induces a more severe toxic reaction in the animals than the full IgG.

However, during the period of this thesis the underlying mechanism of INU1-Fab^{SD}-induced lethality and the reason for the discrepancy towards the initial experiments using INU1-Fab could not be fully solved and will have to be studied in more detail in the future. These findings were not only unanticipated but are also alarming taking into consideration that CLEC-2 has been proposed as a potential anti-thrombotic target in human patients. Although data obtained in mice cannot be directly extrapolated to the human system, these severe complications have to be considered for a potential future α-CLEC-2 treatment in patients.

4.5 Potential side effects of INU1-IgG treatment

In the present thesis, the role of CLEC-2 in hemostasis and thrombosis was analyzed by antibody-mediated "immunodepletion" and down-regulation of the receptor from circulating platelets. In general, in most studies a genetic knock-out mouse model is chosen to investigate the function of murine proteins *in vivo*. However, in contrast to a constitutive CLEC-2 deficiency, injection of INU1 allowed the temporally restricted depletion of the receptor and thus it can be assumed that compensatory mechanisms were not established in the treated animals. Therefore, the physiological role of CLEC-2 could be analyzed in a direct approach in the murine model in this study.

To circumvent the problem of embryonic lethality in the constitutive CLEC-2 knock-out model[59,62-63,122], the role of CLEC-2 in hemostasis and thrombosis has been analyzed in two different studies using fetal liver cell-chimeric *Clec-2$^{-/-BM}$* mice wherein knock-out of the receptor is restricted to the hematopoietic system. Here, a possible effect of CLEC-2 expressed in non-hematopoietic tissues could not be excluded. In contrast, the antibody treatment most probably also targeted other CLEC-2 expressing cells such as natural killer

cells. However, the "immunodepletion"-approach used in this study has been criticized[62-63], because it is unclear at present whether this treatment could also have potential side effects *in vivo* thus questioning whether the described phenotype could be directly related to the lack of CLEC-2. The most prominent effect of INU1-treatment was the subsequent transient thrombocytopenia observed in the animals (Fig 3.6A). However, platelet counts returned back to normal 3-4 days p.i.. Probably, other side effects caused by the antibody treatment are rather minor as indicated by several observations:

Interestingly, the phenotype of *Clec-2*[-/-BM] mice later published by Suzuki-Inoue *et al.*[63] impressively resembles that of INU1-treated CLEC-2-deficient mice described in the present thesis in terms of defective thrombus formation under flow *ex vivo* and in the thrombosis model *in vivo* (see also chapter 4.2.2).

Furthermore, in collaboration with a group working on lymphangiogenesis, it was found that treatment of murine embryos with INU1 similarly induces the "non-separating" phenotype of lymph- and blood vessels as described in CLEC-2 and podoplanin knock-out mice[63,130] (Ph.D. Lijun Xia, OMRF, Oklahoma City, USA, personal communication).

Additionally, comparison of JAQ1/INU1- and *Gp6*^{-/-}/INU1-treated GPVI/CLEC-2 double-deficient mice in this study revealed that the resulting *in vivo* phenotypes were mirroring each other (see also chapter 3.3). Thus, it was demonstrated that at least the antibody (JAQ1)-induced GPVI deficiency is comparable to the constitutive knock-out of GPVI in the background of INU1-induced CLEC-2 deficiency. This observation was further strengthened by the recent findings of Bender and co-workers from our group who compared the phenotypes of GPVI deficiency upon JAQ1-treatment and constitutive *Gp6*^{-/-} mice in different thrombosis models[106]. Here, it was found that JAQ1-treatment very well phenocopied the thrombo-protective effect of genetic GPVI deficiency as both resulting phenotypes were found to be similar.

Together, these findings strongly support the hypothesis that the described phenotype of INU1-treated CLEC-2-deficient mice in the present thesis is specifically caused by the CLEC-2 deficiency itself and most probably not by an antibody-mediated side effect on the treated animals. However, to completely exclude any possible side effects further studies have to be performed.

4.6 GPVI and CLEC-2 play redundant roles in hemostasis and thrombosis

In the second part of the present thesis experiments were performed in mice to address the questions i) whether *in vivo* trans-inhibition of the (hem)ITAM-bearing receptors GPVI and CLEC-2 occurs upon down-regulation of the respective other receptor and ii) whether this would affect receptor signaling. It was demonstrated that treatment with the specific α-GPVI antibody JAQ1 or the specific α-CLEC-2 antibody INU1 induced independent inactivation and

down-regulation of the targeted receptor on platelets without affecting expression or signaling of the respective other receptor *in vivo* (Fig 3.17). These results clearly indicate that trans-inhibition is not operating between GPVI and CLEC-2, at least in murine platelets.

Both receptors, GPVI and CLEC-2, have been proposed as novel anti-thrombotic targets and share several similarities in their intracellular signaling cascade[14,66] (see also chapter 1.5). Therefore, it was speculated that both glycoproteins could at least partially compensate for each other in platelet physiology[14]. To test whether GPVI and CLEC-2 have redundant functions, double-deficient mice were analyzed by combined treatment of JAQ1 and INU1. Here, on circulating platelets the specific loss of both receptors, GPVI and CLEC-2, was observed (Tab 3.2). Furthermore, it was found that signaling of both receptors was completely abolished whereas only moderate effects on other signaling pathways were detected. The described mild thrombin-defect found on d5 p.i. was observed to be further decreased on d6 after treatment and data obtained by aggregometry led to the assumption that this mild thrombin-defect has no major consequences to platelet activation *in vivo* (Fig 3.19 and Fig 3.20).

Very unexpectedly, tail bleeding time analysis of GPVI/CLEC-2 double-deficient mice displayed in two different models that these animals suffered from infinite bleeding times (Fig 3.21). Furthermore, GPVI/CLEC-2 double-deficient mice showed an acutely more pronounced phenotype compared to single-deficient animals in a model of arterial thrombosis in FeCl$_3$-injured mesenteric arterioles (Fig 3.22), clearly revealing redundant functions of the two receptors in hemostasis and thrombosis *in vivo*. Very interestingly, the hypothesis of a functional redundancy between GPVI and CLEC-2 was further strengthened by data obtained from newly generated $Gp6^{-/-}$ mice that were treated with INU1 to induce CLEC-2 deficiency ($Gp6^{-/-}$/INU1). The *in vivo* phenotype of these mice phenocopied the effect of antibody-induced double-deficiency of the two receptors (Fig 3.24). As the activation of platelets is indispensable for thrombus formation, a functional redundancy of the two receptors seems plausible. In this process, the early occurring collagen/GPVI-interaction is known to be crucial for platelet activation[5], whereas the further thrombus growth is induced by recruitment and activation of additional platelets from the blood stream by the released "second wave" mediators ADP and TxA$_2$ for the subsequent clustering of platelets[8,17]. As these signals might not be sufficient for firm thrombus stability, we and others have postulated that CLEC-2 plays an essential role during this later phase[63,104]. Thus, the hypothesized functional redundancy of the two receptors GPVI and CLEC-2 *in vivo* appears to be reasonable.

Although it is not always possible to transfer data obtained in mice to the human system, these findings indicate that a future α-GPVI or α-CLEC-2 treatment of human patients might bear the risk of uncontrolled bleeding in those patients exhibiting defects in the respective

other (hem)ITAM signaling pathway. These findings may therefore have important implications for the development of α-GPVI or α-CLEC-2 based anti-thrombotic therapeutics in human patients.

4.7   CLEC-2 as a novel therapeutic target

The platelet membrane receptor CLEC-2 has intensively been discussed by us and others as a potential novel anti-thrombotic target[12,14,104]. This seems reasonable due to the relatively restricted expression of CLEC-2[63]. In human patients an ideal anti-thrombotic treatment would protect from thrombotic disorders while at the same time not affecting hemostasis. Interestingly, we and others have reported on not or only mildly increased tail bleeding times in CLEC-2-deficient mice[62-63,104] (Fig 3.11 and Fig 3.21). This was accompanied by protection from pathological thrombus formation in thrombosis models such as in our study the $FeCl_3$-induced injury of mesenteric arterioles (Fig 3.12) or in a laser-induced injury model of mesenteric capillaries[63]. In contrast, Hughes and co-workers reported that performance of the $FeCl_3$-driven thrombosis model in mesenteric arterioles failed due to extensive bleeding in CLEC-2-deficient mice; that was probably caused by the blood- and lymphatic vessel misconnecting phenotype of the animals[62]. However, an explanation for the discrepancy towards the study by Suzuki-Inoue *et al.*[63] was not given by the authors.

Additionally to its proposed function in platelet-driven hemostasis and thrombosis, CLEC-2 on platelets also serves as a target-structure for podoplanin expressed on several tumor cells including squamous cell carcinoma, mesothelioma, testicular seminoma, and brain tumors[48,131]. This podoplanin/CLEC-2 interaction has been described to be important for hematogenous tumor metastasis via platelets[48,131] and could therefore represent an interesting target to inhibit tumor cell spreading in cancer patients. Indeed, an interesting study has shown that by blockade of the podoplanin/CLEC-2 interaction with an α-podoplanin antibody pulmonary metastasis in a mouse model was significantly reduced[131]. Also, tumor cell growth requires extensive formation of new vessels to supply the cells with nutrients. It would thus be interesting to investigate whether blockage of the podoplanin/CLEC-2 interaction could potentially abrogate this process. In contrast, possible α-CLEC-2 drugs are not expected to interfere with the existing blood- and lymph vessels in adult patients[63].

Furthermore, CLEC-2 was identified as an attachment factor for human immunodeficiency virus type 1 (HIV-1) on platelets[46]. Thus, targeting or blockage of the receptor could potentially lead to inhibition of HI-virus spread in infected patients. In consequence of these results, it is interesting to further investigate possibilities to target CLEC-2 in human patients.

On the other hand, during the course of this study, it was demonstrated that CLEC-2 deficiency does not protect from ischemic brain infarction in the murine tMCAO model (Fig

3.14) or from occlusive thrombus formation upon mechanically induced injury of the aorta (Fig 3.13). Furthermore, in this study, treatment with INU1-Fab-fragments was shown to have a lethal effect in mice.

However, despite these controversial results obtained in studies from mice, human CLEC-2 could still potentially represent an interesting therapeutic target. CLEC-2 in human platelets could for example be functionally inactivated *in vivo* by anti-human CLEC-2 antibodies or other inhibitory agents. Therefore, it would be of high interest to analyze the potential of α-CLEC-2 treatment in mice using blocking compounds or inhibitors of the receptor. Would such a compound also induce intra-cellular signaling and down-regulation of the receptor or have even such tremendous consequences as the described INU1-Fab treatment?

4.8   Concluding remarks and future plans

Taken together, the results presented in the current study demonstrated for the first time that CLEC-2 is an essential mediator of platelet activation *in vitro* and *in vivo*. Additionally, it was shown that the receptor can be targeted and functionally inactivated *in vivo* using the α-CLEC-2 antibody INU1. By the used "immunodepletion"-approach of CLEC-2 the otherwise lethal constitutive knock-out of the receptor could be circumvented bearing the advantage to analyze the role of CLEC-2 in platelet function *in vivo*. Furthermore, it was demonstrated that the platelet receptors GPVI and CLEC-2 have unexpected redundant functions in platelet physiology. These findings may serve as a basis for the development of a new generation of safe agents for prophylaxis and treatment of ischemic cardiovascular events in human patients.

Further studies are planned in our laboratory to investigate the function of CLEC-2 in murine models of arterial thrombosis and the combined knock-out of GPVI and CLEC-2 using conditional CLEC-2 knock-out mice in collaboration with S.P. Watson, University of Birmingham, UK. Additionally, the mechanism of receptor down-regulation upon INU1 antibody treatment will be further investigated using the newly generated antibody INU2 and thoroughly analysis of the surprisingly lethal effect of INU1-Fab-fragments will be performed. These studies will provide new insights in the role of GPVI and CLEC-2 as potential novel anti-thrombotic targets.

5 References

1.	Ruggeri ZM. Platelets in atherothrombosis. Nature medicine. 2002;8:1227-1234.

2.	Savage B, Almus-Jacobs F, Ruggeri ZM. Specific synergy of multiple substrate-receptor interactions in platelet thrombus formation under flow. Cell. 1998;94:657-666.

3.	Nieswandt B, Brakebusch C, Bergmeier W, et al. Glycoprotein VI but not alpha2beta1 integrin is essential for platelet interaction with collagen. The EMBO journal. 2001;20:2120-2130.

4.	Furie BC, Furie B. Tissue factor pathway vs. collagen pathway for in vivo platelet activation. Blood cells, molecules & diseases. 2006;36:135-138.

5.	Nieswandt B, Watson SP. Platelet-collagen interaction: is GPVI the central receptor? Blood. 2003;102:449-461.

6.	Offermanns S. Activation of platelet function through G protein-coupled receptors. Circulation research. 2006;99:1293-1304.

7.	Jackson SP, Nesbitt WS, Kulkarni S. Signaling events underlying thrombus formation. Journal of thrombosis and haemostasis : JTH. 2003;1:1602-1612.

8.	Varga-Szabo D, Pleines I, Nieswandt B. Cell adhesion mechanisms in platelets. Arteriosclerosis, thrombosis, and vascular biology. 2008;28:403-412.

9.	Clemetson KJ. Platelet activation: signal transduction via membrane receptors. Thrombosis and haemostasis. 1995;74:111-116.

10.	Jung SM, Moroi M. Platelets interact with soluble and insoluble collagens through characteristically different reactions. The Journal of biological chemistry. 1998;273:14827-14837.

11.	Brass LF, Zhu L, Stalker TJ. Minding the gaps to promote thrombus growth and stability. The Journal of clinical investigation. 2005;115:3385-3392.

12.	O'Callaghan CA. Thrombomodulation via CLEC-2 targeting. Current opinion in pharmacology. 2009;9:90-95.

13.	Watson SP, Asazuma N, Atkinson B, et al. The role of ITAM- and ITIM-coupled receptors in platelet activation by collagen. Thrombosis and haemostasis. 2001;86:276-288.

14.	Suzuki-Inoue K, Fuller GL, Garcia A, et al. A novel Syk-dependent mechanism of platelet activation by the C-type lectin receptor CLEC-2. Blood. 2006;107:542-549.

15.	Berridge MJ, Bootman MD, Roderick HL. Calcium signalling: dynamics, homeostasis and remodelling. Nature reviews Molecular cell biology. 2003;4:517-529.

16.	Bird GS, Aziz O, Lievremont JP, et al. Mechanisms of phospholipase C-regulated calcium entry. Current molecular medicine. 2004;4:291-301.

17.	Stegner D, Nieswandt B. Platelet receptor signaling in thrombus formation. Journal of molecular medicine. 2011;89:109-121.

18. Colonna M, Samaridis J, Angman L. Molecular characterization of two novel C-type lectin-like receptors, one of which is selectively expressed in human dendritic cells. European journal of immunology. 2000;30:697-704.

19. Sobanov Y, Bernreiter A, Derdak S, et al. A novel cluster of lectin-like receptor genes expressed in monocytic, dendritic and endothelial cells maps close to the NK receptor genes in the human NK gene complex. European journal of immunology. 2001;31:3493-3503.

20. Chung CH, Peng HC, Huang TF. Aggretin, a C-type lectin protein, induces platelet aggregation via integrin alpha(2)beta(1) and GPIb in a phosphatidylinositol 3-kinase independent pathway. Biochemical and biophysical research communications. 2001;285:689-695.

21. Navdaev A, Clemetson JM, Polgar J, et al. Aggretin, a heterodimeric C-type lectin from Calloselasma rhodostoma (malayan pit viper), stimulates platelets by binding to alpha 2beta 1 integrin and glycoprotein Ib, activating Syk and phospholipase Cgamma 2, but does not involve the glycoprotein VI/Fc receptor gamma chain collagen receptor. The Journal of biological chemistry. 2001;276:20882-20889.

22. Suzuki-Inoue K, Ozaki Y, Kainoh M, et al. Rhodocytin induces platelet aggregation by interacting with glycoprotein Ia/IIa (GPIa/IIa, Integrin alpha 2beta 1). Involvement of GPIa/IIa-associated src and protein tyrosine phosphorylation. The Journal of biological chemistry. 2001;276:1643-1652.

23. Bergmeier W, Bouvard D, Eble JA, et al. Rhodocytin (aggretin) activates platelets lacking alpha(2)beta(1) integrin, glycoprotein VI, and the ligand-binding domain of glycoprotein Ibalpha. The Journal of biological chemistry. 2001;276:25121-25126.

24. Yokoyama WM, Plougastel BF. Immune functions encoded by the natural killer gene complex. Nature reviews Immunology. 2003;3:304-316.

25. Senis YA, Tomlinson MG, Garcia A, et al. A comprehensive proteomics and genomics analysis reveals novel transmembrane proteins in human platelets and mouse megakaryocytes including G6b-B, a novel immunoreceptor tyrosine-based inhibitory motif protein. Molecular & cellular proteomics : MCP. 2007;6:548-564.

26. Kerrigan AM, Dennehy KM, Mourao-Sa D, et al. CLEC-2 is a phagocytic activation receptor expressed on murine peripheral blood neutrophils. Journal of immunology. 2009;182:4150-4157.

27. Xie J, Wu T, Guo L, et al. Molecular characterization of two novel isoforms and a soluble form of mouse CLEC-2. Biochemical and biophysical research communications. 2008;371:180-184.

28. Drickamer K. C-type lectin-like domains. Current opinion in structural biology. 1999;9:585-590.

29. Pyz E, Marshall AS, Gordon S, Brown GD. C-type lectin-like receptors on myeloid cells. Annals of medicine. 2006;38:242-251.

30. Weis WI, Taylor ME, Drickamer K. The C-type lectin superfamily in the immune system. Immunological reviews. 1998;163:19-34.

31. Drickamer K, Taylor ME. Biology of animal lectins. Annual review of cell biology. 1993;9:237-264.

32. Fuller GL, Williams JA, Tomlinson MG, et al. The C-type lectin receptors CLEC-2 and Dectin-1, but not DC-SIGN, signal via a novel YXXL-dependent signaling cascade. The Journal of biological chemistry. 2007;282:12397-12409.

33. May F. Generation of a targeting vector for the creation of C-type lectin-like receptor 2 (CLEC-2) deficient mice. Institute of Zoology. Vol. Diploma. Darmstadt: Technical University of Darmstadt; 2007:62.

34. Watson AA, Brown J, Harlos K, Eble JA, Walter TS, O'Callaghan CA. The crystal structure and mutational binding analysis of the extracellular domain of the platelet-activating receptor CLEC-2. The Journal of biological chemistry. 2007;282:3165-3172.

35. Watson AA, O'Callaghan CA. Crystallization and X-ray diffraction analysis of human CLEC-2. Acta crystallographica Section F, Structural biology and crystallization communications. 2005;61:1094-1096.

36. Watson SP, Herbert JM, Pollitt AY. GPVI and CLEC-2 in hemostasis and vascular integrity. Journal of thrombosis and haemostasis : JTH. 2010;8:1456-1467.

37. Hughes CE, Pollitt AY, Mori J, et al. CLEC-2 activates Syk through dimerization. Blood. 2010;115:2947-2955.

38. Watson AA, Christou CM, James JR, et al. The platelet receptor CLEC-2 is active as a dimer. Biochemistry. 2009;48:10988-10996.

39. Hughes CE, Auger JM, McGlade J, Eble JA, Pearce AC, Watson SP. Differential roles for the adapters Gads and LAT in platelet activation by GPVI and CLEC-2. Journal of thrombosis and haemostasis : JTH. 2008;6:2152-2159.

40. Clements JL, Lee JR, Gross B, et al. Fetal hemorrhage and platelet dysfunction in SLP-76-deficient mice. The Journal of clinical investigation. 1999;103:19-25.

41. Dhanjal TS, Ross EA, Auger JM, et al. Minimal regulation of platelet activity by PECAM-1. Platelets. 2007;18:56-67.

42. Mori J, Pearce AC, Spalton JC, et al. G6b-B inhibits constitutive and agonist-induced signaling by glycoprotein VI and CLEC-2. The Journal of biological chemistry. 2008;283:35419-35427.

43. Pollitt AY, Grygielska B, Leblond B, Desire L, Eble JA, Watson SP. Phosphorylation of CLEC-2 is dependent on lipid rafts, actin polymerization, secondary mediators, and Rac. Blood. 2010;115:2938-2946.

44. Pleines I, Elvers M, Strehl A, et al. Rac1 is essential for phospholipase C-gamma2 activation in platelets. Pflugers Archiv : European journal of physiology. 2009;457:1173-1185.

45. Shin Y, Morita T. Rhodocytin, a functional novel platelet agonist belonging to the heterodimeric C-type lectin family, induces platelet aggregation independently of glycoprotein Ib. Biochemical and biophysical research communications. 1998;245:741-745.

46. Chaipan C, Soilleux EJ, Simpson P, et al. DC-SIGN and CLEC-2 mediate human immunodeficiency virus type 1 capture by platelets. Journal of virology. 2006;80:8951-8960.

47. Christou CM, Pearce AC, Watson AA, et al. Renal cells activate the platelet receptor CLEC-2 through podoplanin. The Biochemical journal. 2008;411:133-140.

48. Suzuki-Inoue K, Kato Y, Inoue O, et al. Involvement of the snake toxin receptor CLEC-2, in podoplanin-mediated platelet activation, by cancer cells. The Journal of biological chemistry. 2007;282:25993-26001.

49. Wicki A, Christofori G. The potential role of podoplanin in tumour invasion. British journal of cancer. 2007;96:1-5.

50. Chaipan C, Steffen I, Tsegaye TS, et al. Incorporation of podoplanin into HIV released from HEK-293T cells, but not PBMC, is required for efficient binding to the attachment factor CLEC-2. Retrovirology. 2010;7:47.

51. Honn KV, Tang DG, Crissman JD. Platelets and cancer metastasis: a causal relationship? Cancer metastasis reviews. 1992;11:325-351.

52. Nieswandt B, Hafner M, Echtenacher B, Mannel DN. Lysis of tumor cells by natural killer cells in mice is impeded by platelets. Cancer research. 1999;59:1295-1300.

53. Abtahian F, Guerriero A, Sebzda E, et al. Regulation of blood and lymphatic vascular separation by signaling proteins SLP-76 and Syk. Science. 2003;299:247-251.

54. D'Amico G, Alitalo K. Inside bloody lymphatics. Blood. 2010;116:512-513.

55. Rafii S, Skobe M. Splitting vessels: keeping lymph apart from blood. Nature medicine. 2003;9:166-168.

56. Uhrin P, Zaujec J, Breuss JM, et al. Novel function for blood platelets and podoplanin in developmental separation of blood and lymphatic circulation. Blood. 2010;115:3997-4005.

57. Sebzda E, Hibbard C, Sweeney S, et al. Syk and Slp-76 mutant mice reveal a cell-autonomous hematopoietic cell contribution to vascular development. Developmental cell. 2006;11:349-361.

58. Wang D, Feng J, Wen R, et al. Phospholipase Cgamma2 is essential in the functions of B cell and several Fc receptors. Immunity. 2000;13:25-35.

59. Bertozzi CC, Schmaier AA, Mericko P, et al. Platelets regulate lymphatic vascular development through CLEC-2-SLP-76 signaling. Blood. 2010;116:661-670.

60. Fu J, Gerhardt H, McDaniel JM, et al. Endothelial cell O-glycan deficiency causes blood/lymphatic misconnections and consequent fatty liver disease in mice. The Journal of clinical investigation. 2008;118:3725-3737.

61. Carramolino L, Fuentes J, Garcia-Andres C, Azcoitia V, Riethmacher D, Torres M. Platelets play an essential role in separating the blood and lymphatic vasculatures during embryonic angiogenesis. Circulation research. 2010;106:1197-1201.

62. Hughes CE, Navarro-Nunez L, Finney BA, Mourao-Sa D, Pollitt AY, Watson SP. CLEC-2 is not required for platelet aggregation at arteriolar shear. Journal of thrombosis and haemostasis : JTH. 2010;8:2328-2332.

63. Suzuki-Inoue K, Inoue O, Ding G, et al. Essential in vivo roles of the C-type lectin receptor CLEC-2: embryonic/neonatal lethality of CLEC-2-deficient mice by

blood/lymphatic misconnections and impaired thrombus formation of CLEC-2-deficient platelets. The Journal of biological chemistry. 2010;285:24494-24507.

64. Clemetson JM, Polgar J, Magnenat E, Wells TN, Clemetson KJ. The platelet collagen receptor glycoprotein VI is a member of the immunoglobulin superfamily closely related to FcalphaR and the natural killer receptors. The Journal of biological chemistry. 1999;274:29019-29024.

65. Jandrot-Perrus M, Busfield S, Lagrue AH, et al. Cloning, characterization, and functional studies of human and mouse glycoprotein VI: a platelet-specific collagen receptor from the immunoglobulin superfamily. Blood. 2000;96:1798-1807.

66. Nieswandt B, Schulte V, Bergmeier W, et al. Long-term antithrombotic protection by in vivo depletion of platelet glycoprotein VI in mice. The Journal of experimental medicine. 2001;193:459-469.

67. Nieswandt B, Bergmeier W, Schulte V, Rackebrandt K, Gessner JE, Zirngibl H. Expression and function of the mouse collagen receptor glycoprotein VI is strictly dependent on its association with the FcRgamma chain. The Journal of biological chemistry. 2000;275:23998-24002.

68. Berlanga O, Tulasne D, Bori T, et al. The Fc receptor gamma-chain is necessary and sufficient to initiate signalling through glycoprotein VI in transfected cells by the snake C-type lectin, convulxin. European journal of biochemistry / FEBS. 2002;269:2951-2960.

69. Gibbins JM, Okuma M, Farndale R, Barnes M, Watson SP. Glycoprotein VI is the collagen receptor in platelets which underlies tyrosine phosphorylation of the Fc receptor gamma-chain. FEBS letters. 1997;413:255-259.

70. Gibbins J, Asselin J, Farndale R, Barnes M, Law CL, Watson SP. Tyrosine phosphorylation of the Fc receptor gamma-chain in collagen-stimulated platelets. The Journal of biological chemistry. 1996;271:18095-18099.

71. Gibbins JM. Platelet adhesion signalling and the regulation of thrombus formation. Journal of cell science. 2004;117:3415-3425.

72. Briddon SJ, Watson SP. Evidence for the involvement of p59fyn and p53/56lyn in collagen receptor signalling in human platelets. The Biochemical journal. 1999;338 (Pt 1):203-209.

73. Ezumi Y, Shindoh K, Tsuji M, Takayama H. Physical and functional association of the Src family kinases Fyn and Lyn with the collagen receptor glycoprotein VI-Fc receptor gamma chain complex on human platelets. The Journal of experimental medicine. 1998;188:267-276.

74. Fujii C, Yanagi S, Sada K, Nagai K, Taniguchi T, Yamamura H. Involvement of protein-tyrosine kinase p72syk in collagen-induced signal transduction in platelets. European journal of biochemistry / FEBS. 1994;226:243-248.

75. Yanaga F, Poole A, Asselin J, et al. Syk interacts with tyrosine-phosphorylated proteins in human platelets activated by collagen and cross-linking of the Fc gamma-IIA receptor. The Biochemical journal. 1995;311 (Pt 2):471-478.

76. Zhang W, Trible RP, Samelson LE. LAT palmitoylation: its essential role in membrane microdomain targeting and tyrosine phosphorylation during T cell activation. Immunity. 1998;9:239-246.

77. Gross BS, Lee JR, Clements JL, et al. Tyrosine phosphorylation of SLP-76 is downstream of Syk following stimulation of the collagen receptor in platelets. The Journal of biological chemistry. 1999;274:5963-5971.

78. Schulte V, Rabie T, Prostredna M, Aktas B, Gruner S, Nieswandt B. Targeting of the collagen-binding site on glycoprotein VI is not essential for in vivo depletion of the receptor. Blood. 2003;101:3948-3952.

79. Schulte V, Snell D, Bergmeier W, Zirngibl H, Watson SP, Nieswandt B. Evidence for two distinct epitopes within collagen for activation of murine platelets. The Journal of biological chemistry. 2001;276:364-368.

80. Moroi M, Jung SM, Okuma M, Shinmyozu K. A patient with platelets deficient in glycoprotein VI that lack both collagen-induced aggregation and adhesion. The Journal of clinical investigation. 1989;84:1440-1445.

81. Sugiyama T, Okuma M, Ushikubi F, Sensaki S, Kanaji K, Uchino H. A novel platelet aggregating factor found in a patient with defective collagen-induced platelet aggregation and autoimmune thrombocytopenia. Blood. 1987;69:1712-1720.

82. Gruner S, Prostredna M, Koch M, et al. Relative antithrombotic effect of soluble GPVI dimer compared with anti-GPVI antibodies in mice. Blood. 2005;105:1492-1499.

83. Kleinschnitz C, Pozgajova M, Pham M, Bendszus M, Nieswandt B, Stoll G. Targeting platelets in acute experimental stroke: impact of glycoprotein Ib, VI, and IIb/IIIa blockade on infarct size, functional outcome, and intracranial bleeding. Circulation. 2007;115:2323-2330.

84. Massberg S, Gawaz M, Gruner S, et al. A crucial role of glycoprotein VI for platelet recruitment to the injured arterial wall in vivo. The Journal of experimental medicine. 2003;197:41-49.

85. Bender M, Hofmann S, Stegner D, et al. Differentially regulated GPVI ectodomain shedding by multiple platelet-expressed proteinases. Blood. 2010;116:3347-3355.

86. Gruner S, Prostredna M, Aktas B, et al. Anti-glycoprotein VI treatment severely compromises hemostasis in mice with reduced alpha2beta1 levels or concomitant aspirin therapy. Circulation. 2004;110:2946-2951.

87. Bergmeier W, Rabie T, Strehl A, et al. GPVI down-regulation in murine platelets through metalloproteinase-dependent shedding. Thrombosis and haemostasis. 2004;91:951-958.

88. Gardiner EE, Arthur JF, Kahn ML, Berndt MC, Andrews RK. Regulation of platelet membrane levels of glycoprotein VI by a platelet-derived metalloproteinase. Blood. 2004;104:3611-3617.

89. Rabie T, Varga-Szabo D, Bender M, et al. Diverging signaling events control the pathway of GPVI down-regulation in vivo. Blood. 2007;110:529-535.

90. Andrews RK, Suzuki-Inoue K, Shen Y, Tulasne D, Watson SP, Berndt MC. Interaction of calmodulin with the cytoplasmic domain of platelet glycoprotein VI. Blood. 2002;99:4219-4221.

91. Gardiner EE, Al-Tamimi M, Mu FT, et al. Compromised ITAM-based platelet receptor function in a patient with immune thrombocytopenic purpura. Journal of thrombosis and haemostasis : JTH. 2008;6:1175-1182.

92. Hibbs ML, Bonadonna L, Scott BM, McKenzie IF, Hogarth PM. Molecular cloning of a human immunoglobulin G Fc receptor. Proceedings of the National Academy of Sciences of the United States of America. 1988;85:2240-2244.

93. Huang MM, Indik Z, Brass LF, Hoxie JA, Schreiber AD, Brugge JS. Activation of Fc gamma RII induces tyrosine phosphorylation of multiple proteins including Fc gamma RII. The Journal of biological chemistry. 1992;267:5467-5473.

94. Gardiner EE, Karunakaran D, Arthur JF, et al. Dual ITAM-mediated proteolytic pathways for irreversible inactivation of platelet receptors: de-ITAM-izing FcgammaRIIa. Blood. 2008;111:165-174.

95. Spalton JC, Mori J, Pollitt AY, Hughes CE, Eble JA, Watson SP. The novel Syk inhibitor R406 reveals mechanistic differences in the initiation of GPVI and CLEC-2 signaling in platelets. Journal of thrombosis and haemostasis : JTH. 2009;7:1192-1199.

96. Ozaki Y, Suzuki-Inoue K, Inoue O. Novel interactions in platelet biology: CLEC-2/podoplanin and laminin/GPVI. Journal of thrombosis and haemostasis : JTH. 2009;7 Suppl 1:191-194.

97. Meadows TA, Bhatt DL. Clinical aspects of platelet inhibitors and thrombus formation. Circulation research. 2007;100:1261-1275.

98. Holmes DR, Jr., Kereiakes DJ, Kleiman NS, Moliterno DJ, Patti G, Grines CL. Combining antiplatelet and anticoagulant therapies. Journal of the American College of Cardiology. 2009;54:95-109.

99. Elbakri A, Nelson PN, Abu Odeh RO. The state of antibody therapy. Human immunology. 2010;71:1243-1250.

100. Use of a monoclonal antibody directed against the platelet glycoprotein IIb/IIIa receptor in high-risk coronary angioplasty. The EPIC Investigation. The New England journal of medicine. 1994;330:956-961.

101. Boylan B, Chen H, Rathore V, et al. Anti-GPVI-associated ITP: an acquired platelet disorder caused by autoantibody-mediated clearance of the GPVI/FcRgamma-chain complex from the human platelet surface. Blood. 2004;104:1350-1355.

102. Boylan B, Berndt MC, Kahn ML, Newman PJ. Activation-independent, antibody-mediated removal of GPVI from circulating human platelets: development of a novel NOD/SCID mouse model to evaluate the in vivo effectiveness of anti-human platelet agents. Blood. 2006;108:908-914.

103. Nieswandt B, Bergmeier W, Rackebrandt K, Gessner JE, Zirngibl H. Identification of critical antigen-specific mechanisms in the development of immune thrombocytopenic purpura in mice. Blood. 2000;96:2520-2527.

104. May F, Hagedorn I, Pleines I, et al. CLEC-2 is an essential platelet-activating receptor in hemostasis and thrombosis. Blood. 2009;114:3464-3472.

105. Bergmeier W, Schulte V, Brockhoff G, Bier U, Zirngibl H, Nieswandt B. Flow cytometric detection of activated mouse integrin alphaIIbbeta3 with a novel monoclonal antibody. Cytometry. 2002;48:80-86.

106. Bender M, Hagedorn I, Nieswandt B. Genetic and antibody-induced GPVI deficiency equally protect mice from mechanically and FeCl(3) -induced thrombosis. Journal of thrombosis and haemostasis : JTH. 2011.

107. Dirnagl U. Bench to bedside: the quest for quality in experimental stroke research. Journal of cerebral blood flow and metabolism : official journal of the International Society of Cerebral Blood Flow and Metabolism. 2006;26:1465-1478.

108. Murray CJ, Lopez AD. Mortality by cause for eight regions of the world: Global Burden of Disease Study. Lancet. 1997;349:1269-1276.

109. Zhang ZG, Zhang L, Tsang W, et al. Dynamic platelet accumulation at the site of the occluded middle cerebral artery and in downstream microvessels is associated with loss of microvascular integrity after embolic middle cerebral artery occlusion. Brain research. 2001;912:181-194.

110. Choudhri TF, Hoh BL, Zerwes HG, et al. Reduced microvascular thrombosis and improved outcome in acute murine stroke by inhibiting GP IIb/IIIa receptor-mediated platelet aggregation. The Journal of clinical investigation. 1998;102:1301-1310.

111. Kiefer TL, Becker RC. Inhibitors of platelet adhesion. Circulation. 2009;120:2488-2495.

112. Arai M, Yamamoto N, Moroi M, Akamatsu N, Fukutake K, Tanoue K. Platelets with 10% of the normal amount of glycoprotein VI have an impaired response to collagen that results in a mild bleeding tendency. British journal of haematology. 1995;89:124-130.

113. Kato K, Kanaji T, Russell S, et al. The contribution of glycoprotein VI to stable platelet adhesion and thrombus formation illustrated by targeted gene deletion. Blood. 2003;102:1701-1707.

114. Lockyer S, Okuyama K, Begum S, et al. GPVI-deficient mice lack collagen responses and are protected against experimentally induced pulmonary thromboembolism. Thrombosis research. 2006;118:371-380.

115. Schulte V, Reusch HP, Pozgajova M, Varga-Szabo D, Gachet C, Nieswandt B. Two-phase antithrombotic protection after anti-glycoprotein VI treatment in mice. Arteriosclerosis, thrombosis, and vascular biology. 2006;26:1640-1647.

116. Ault KA, Knowles C. In vivo biotinylation demonstrates that reticulated platelets are the youngest platelets in circulation. Experimental hematology. 1995;23:996-1001.

117. Grosse J, Braun A, Varga-Szabo D, et al. An EF hand mutation in Stim1 causes premature platelet activation and bleeding in mice. The Journal of clinical investigation. 2007;117:3540-3550.

118. Varga-Szabo D, Braun A, Kleinschnitz C, et al. The calcium sensor STIM1 is an essential mediator of arterial thrombosis and ischemic brain infarction. The Journal of experimental medicine. 2008;205:1583-1591.

119. Judd BA, Myung PS, Obergfell A, et al. Differential requirement for LAT and SLP-76 in GPVI versus T cell receptor signaling. The Journal of experimental medicine. 2002;195:705-717.

120. Mangin P, Nonne C, Eckly A, et al. A PLC gamma 2-independent platelet collagen aggregation requiring functional association of GPVI and integrin alpha2beta1. FEBS letters. 2003;542:53-59.

121. Elvers M, Pozgaj R, Pleines I, et al. Platelet hyperreactivity and a prothrombotic phenotype in mice with a gain-of-function mutation in phospholipase Cgamma2. Journal of thrombosis and haemostasis : JTH. 2010;8:1353-1363.

122. Tang T, Li L, Tang J, et al. A mouse knockout library for secreted and transmembrane proteins. Nature biotechnology. 2010;28:749-755.

123. Leon C, Hechler B, Freund M, et al. Defective platelet aggregation and increased resistance to thrombosis in purinergic P2Y(1) receptor-null mice. The Journal of clinical investigation. 1999;104:1731-1737.

124. Pozgajova M, Sachs UJ, Hein L, Nieswandt B. Reduced thrombus stability in mice lacking the alpha2A-adrenergic receptor. Blood. 2006;108:510-514.

125. Rodgers RP, Levin J. A critical reappraisal of the bleeding time. Seminars in thrombosis and hemostasis. 1990;16:1-20.

126. Ruggeri ZM, Mendolicchio GL. Adhesion mechanisms in platelet function. Circulation research. 2007;100:1673-1685.

127. Kunicki TJ. CLEC ... too! Blood. 2009;114:3364-3365.

128. Stoll G, Kleinschnitz C, Nieswandt B. Combating innate inflammation: a new paradigm for acute treatment of stroke? Annals of the New York Academy of Sciences. 2010;1207:149-154.

129. Chang CH, Chung CH, Hsu CC, Huang TY, Huang TF. A novel mechanism of cytokine release in phagocytes induced by aggretin, a snake venom C-type lectin protein, through CLEC-2 ligation. Journal of thrombosis and haemostasis : JTH. 2010;8:2563-2570.

130. Bertozzi CC, Hess PR, Kahn ML. Platelets: covert regulators of lymphatic development. Arteriosclerosis, thrombosis, and vascular biology. 2010;30:2368-2371.

131. Kato Y, Kaneko MK, Kunita A, et al. Molecular analysis of the pathophysiological binding of the platelet aggregation-inducing factor podoplanin to the C-type lectin-like receptor CLEC-2. Cancer science. 2008;99:54-61.

6 Appendix

Abbreviations

aa	amino acid
ADP	adenosine diphosphate
APS	ammonium peroxodisulphat
ATP	adenosine trisphosphate
BLNK	B-cell linker protein
BSA	bovine serum albumin
Btk	Bruton agammaglobulinemia tyrosine kinase
°C	Degree Celsius
CLEC-2	C-type lectin-like receptor 2
$[Ca^{2+}]_i$	intracellular calcium concentration
cm²	square centimeter
CRD	carbohydrate recognition domain
CRP	collagen-related peptide
CTLD	C-type lectin-like domain
CVX	convulxin
DAG	diacylglycerol
ddH_2O	double-distilled water
DIC	differential interference contrast
DMEM	Dulbecco/Vogt Modified Eagle's Minimal Essential Medium
E	embryonic day
ECL	enhanced chemiluminescence
ECM	extracellular matrix
EDTA	ethylenediaminetetraacetic acid
ELISA	enzyme-linked immuno absorbance assay
et al.	*et alteri*
Fab	fragment antigen-binding
f.c.	final concentration
Fc	fragment crystallisable
FcR	Fc receptor
FCS	fetal calf (bovine) serum
Fig.	figure
FITC	fluorescein isothiocyanate
FSC	foreward scatter

Appendix

g	gramme
GP	glycoprotein
GPCR	G protein-coupled receptor
GTP	guanosine triphosphate
h	hour(s)
HAT	hypoxanthine-aminopterin-thymidine
HCl	hydrogen chloride
HIV-1	human immunodeficiency virus type 1
HRP	horseradish peroxidase
H_2O	water
IFI	integrated fluorescence intensity
Ig	immunoglobulin
IL-6	interleukin-6
IP	immunoprecipitation
IP_3	inositol 1,4,5-triphosphate
ITAM	immunoreceptor tyrosine-based activation motif
ITIM	immunoreceptor tyrosine-based inhibitory motif
kb	kilo base pair
kDa	kilo Dalton
l	liter
LAT	linker for activation of T-cells
M	molar
MFI	mean fluorescence intensity
min	minute(s)
MK	megakaryocyte
ml	milliliter
mm	millimeter
μ	micro
NaCl	sodium chloride
NaOH	sodium hydroxide
OD	optical density
o/n	overnight
PAA	polyacrylamide
PBS	phosphate buffered saline
PCR	polymerase chain reaction
PE	phycoerythrin
PECAM-1	Platelet Endothelial Cell Adhesion Molecule

PF4	platelet factor 4
PIP_2	phosphatidylinositol-4,5-bisphosphate
PI-3-K	phosphoinositide-3-kinase
PKC	proteinkinase C
PL (C)	phospholipase (C)
prp	platelet-rich plasma
PVDF	polyvinylidene difluoride
RC	rhodocytin
rpm	rounds per minute
RT	room temperature
SD	standard deviation
SDS	sodium dodecyl sulfate
SDS-PAGE	sodium dodecyl sulfate polyacrylamide gel electrophoresis
sec	second
Seq	Sequence
SH2	Src homology 2 domains
SLP-76	Src-homology 2 domain-containing leukocyte-specific phosphoprotein of 76 kDa
SOCE	store-operated Ca^{2+} entry
SSC	sideward scatter
TAE	TRIS acetate EDTA buffer
TE	TRIS EDTA buffer
TEM	transmission electron microscopy
TF	tissue factor
TNF-α	tumor necrosis factor-α
TRIS	trishydroxymethylaminomethane
TxA_2	thromboxane A_2
U	units
Vav3	Guanine nucleotide exchange factor Vav3
vWF	von Willebrand factor
wt	wild-type
x g	acceleration of gravity (9.81 m/ sec²)

Acknowledgements

The work presented here was accomplished at the Department of Experimental Biomedicine, University Hospital of Würzburg and the Rudolf Virchow Center, DFG Research Center for Experimental Biomedicine, University of Würzburg, in the group of Prof. Dr. Bernhard Nieswandt.

During the period of my PhD project (July 2007 – June 2011) many people helped and supported me and without this help this thesis would not have been possible.

Therefore, I would like to express my thanks to the following people:

- My supervisor, Prof. Dr. Bernhard Nieswandt, for giving me the opportunity to work in his laboratory, for his constant support and outstanding scientific ideas. Especially, I would like to thank him for allowing me to travel to and/or participate in several international conferences and meetings, amongst others the very impressing XXIInd Congress of the ISTH 2009 in Boston, USA.

- Prof. Dr. Ulrich Walter for helpful discussions and for reviewing my thesis.

- PD Dr. Heike Hermanns for pleasant scientific discussions and for reviewing my thesis.

- My colleagues who have become friends: Dr. Lidija Chakarova, Ina Hagedorn and Dr. Irina Pleines for their support and encouragement in lab, for listening to me in and out of office and for spending their time on carefully proofreading my thesis.

- My colleague Dr. Markus Bender for sharing his GPVI knock-out mouse with me, the enjoyable team work and proofreading my thesis.

- My former colleague and friend Sandra Niklasch for great help with the administrative stuff and the enjoyable non-scientific talks.

- Steffi Hartmann, the Queen of Hybridomas, for her excellent assistance and outstanding help in the cell-culture lab.

- My colleague Timo Vögtle for his kind help and advice with the FACS measurements of immune cells.

- Our technical assistants Sylvia Hengst, Juliana Goldmann, Birgit Midloch and Jonas Müller for their everyday support and nice music in the molecular biology lab.

- All past and present members of the Nieswandt group that have not been mentioned here by name for the great working atmosphere, the numerous help in lab and the fun at work and after-hours (which is not just a saying).

- And last, but most importantly, I wish to thank my family: My parents Monika and Günter May and my sister Katja May who have always encouraged and constantly supported me in my professional and private life. Thank you!

Publications

Bender M[§], **May F**[§], Hagedorn I, Braun A, Nieswandt B. Severely defective hemostasis and arterial thrombus formation in GPVI/CLEC-2 double-depleted mice. *Manuscript in revision.* [§]*Authors contributed equally.*

May F, Hagedorn I, Pleines I, Bender M, Vögtle T, Eble J, Elvers M, Nieswandt B. CLEC-2 is an essential platelet-activating receptor in hemostasis and thrombosis. *Blood.* 2009;114(16):3464-72

Elvers M, Pozgaj R, Pleines I, **May F**, Kuijpers MJ, Heemskerk JM, Yu P, Nieswandt B. Platelet hyperreactivity and a prothrombotic phenotype in mice with a gain-of-function mutation in phospholipase Cγ2. *J Thromb Haemost*. 2010;8(6):1353-63.

Pleines I, Elvers M, Strehl A, Pozgajova M, Varga-Szabo D, **May F**, Chrostek-Grashoff A, Brakebusch C, Nieswandt B. Rac1 is essential for phospholipase Cγ2 activation in platelets. *Pflugers Arch*. 2009;457(5):1173-85.

Oral presentations

Severely defective hemostasis and arterial thrombus formation in GPVI/CLEC-2 double-depleted mice. XXIIIrd Congress of the International Society on Thrombosis and Haemostasis (ISTH), July 2011, Kyoto (Japan). **Accepted for oral presentation.**
Winner of **Young Investigator's Award** (prize money: 500 US$).

Proteolytic regulation of platelet membrane glycoproteins. SFB 688 Mini-Symposium, March 2011, Würzburg (Germany). Presentation was shared with Markus Bender.

CLEC-2 is an essential platelet activating receptor in hemostasis and thrombosis. First Joint Meeting GTH & NVTH, February 2010, Nürnberg (Germany).
Winner of **Best Abstract Award** (prize money: 500 €).

CLEC-2 is an essential platelet activating receptor in hemostasis and thrombosis. First French-UK Platelet Meeting, October 2009, Toulouse (France).

Poster

Down-regulation of the platelet receptors GPVI and CLEC-2 results in an infinite bleeding phenotype. CHIASMA 5th International Symposium, GSLS, October 2010, Würzburg (Germany).

Proteolytic regulation of platelet membrane glycoproteins. Joint Symposium of SFB 612 and SFB 688, October 2010, Bad Brückenau (Germany). Presentation was shared with Markus Bender.
Winner of **Best Poster Award** (prize money: 400 €).

Generation of CLEC-2 deficient mice and monoclonal α-mCLEC-2 antibodies. Meeting of the Graduate School of Life Sciences (GSLS), September 2008, Würzburg (Germany).

Affidavit

I hereby confirm that my thesis entitled
"The role of the (hem)ITAM-coupled receptors C-type lectin-like receptor 2 (CLEC-2) and Glycoprotein (GP) VI for platelet function: *in vitro* and *in vivo* studies in mice"
is the result of my own work. I did not receive any help or support from commercial consultants. All sources and/or materials applied are listed and specified in the thesis.

Furthermore, I confirm that this thesis has not yet been submitted as part of another examination process neither in identical nor in similar form.

Würzburg …………………………………………………………………………………

Date   Signature

Eidesstattliche Erklärung

Hiermit erkläre ich an Eides statt, die Dissertation
„Die Rolle der (hem)ITAM-gekoppelten Rezeptoren *C-type lectin-like receptor 2 (CLEC-2)* und Glycoprotein (GP) VI in der Thrombozytenfunktion: *in vitro*- und *in vivo*-Studien in Mäusen"
eigenständig, d.h. insbesondere selbständig und ohne Hilfe eines kommerziellen Promotionsberaters, angefertigt und keine anderen als die von mir angegebenen Quellen und Hilfsmittel verwendet zu haben.

Ich erkläre außerdem, dass die Dissertation weder in gleicher noch in ähnlicher Form bereits in einem anderen Prüfungsverfahren vorgelegen hat.

Würzburg …………………………………………………………………………………

Datum   Unterschrift